DEPARTMENT OF MECHANICAL ENGINEERING

STUDY OF PRESSURE LOSSES IN TUBING AND FITTINGS

FINAL REPORT

JUNE 1, 1964 - JUNE 1, 1966

CONTRACT NAS8-11297

ENGINEERING AND INDUSTRIAL RESEARCH STATION

MISSISSIPPI STATE UNIVERSITY

STATE COLLEGE, MISSISSIPPI

STUDY OF PRESSURE LOSSES IN TUBING AND FITTINGS

FINAL REPORT

June 1, 1964 - June 1, 1966

Authors:

Dr. C. W. Bouchillon
Dr. C. T. Carley, Jr.

Contributors:

Professor W. T. McKie, Jr.
Mr. J. E. Corley
Mr. R. C. Hearon
Mr. J. H. McDermit
Mr. A. K. Rosenhan

Approved:

C. W. Bouchillon
Principal Investigator

A. G. Holmes, Head
Department of Mechanical Engineering
Mississippi State University

This report was prepared by Mississippi State University under Contract NAS8-11297, Study of Pressure Losses in Tubing and Fittings, for the George C. Marshall Space Flight Center of the National Aeronautics and Space Administration. The work was administered under the technical direction of the Propulsion and Vehicle Engineering Laboratory of the George C. Marshall Space Flight Center with Mr. W. E. Wilkinson acting as project manager.

TABLE OF CONTENTS

page

Nomenclature iv

List of Figures viii

Abstract. x

I. Introduction

A. Objectives 1

B. Method of Attack 1

II. Analytical

A. Development of Empirical Equations for Existing Data 4

B. Theoretical Considerations

(1) Flow Through Convoluted Tubing 12

(2) Flow Through Arbitrary Systems 27

III. Experimental

A. Selection of Equipment 39

B. Description of Experimental Facility 39

C. Procedures for Data Acquisition and Processing

(1) Flexible Tubing 40

(2) Arbitrary Flow System 43

IV. Results

A. Empirical Equation 47

B. Experimental Results 47

(1) Flow Through Convoluted Tubing 47

(2) Flow Through Arbitrary Systems 49

TABLE OF CONTENTS (continued)

page

V. Conclusions and Recommendations

A. Conclusions 52

B. Recommendations 52

VI. List of References Cited 53

VII. List of Other References 56

VIII. Appendices

A. Friction Factors 92

B. Computer Program for Pressure Drop in Flow System 94

C. Derivation of Supply Tank Blowdown Equation 107

NOMENCLATURE

SYMBOL	DESCRIPTION	UNITS
a, b, c, d,	arbitrary constants	---
A	arbitrary constant	---
B_1, B_2	arbitrary constant	---
C	arbitrary constant	---
c_f	local skin friction coefficient	---
C1, C2, C3, C4, C5, C6, C7	arbitrary constants	---
D	nominal tube diameter	ft
D1	arbitrary constant	---
e	inverse of ln	---
E	convolution depth	ft
f	Darcy-Weisbach friction factor	---
f'	alternate friction factor formulation	---
F	sum of the square of errors	---
FN1	FN1 = ER/D^2	---
FN2	FN2 = ER/SD	---
H	arbitrary constant	---
k	arbitrary constant	---
K	arbitrary constant	---
L	length	ft
ln	natural logarithm	---
$\dot{m}$	mass rate of flow	lbm/sec
M	mass of gas in tank	lbm

NOMENCLATURE (continued)

SYMBOL	DESCRIPTION	UNITS
P	fluid pressure	lbf/ft^2
r	radial position	ft
R	radius of curvature of convolution	ft
$\tilde{R}$	gas constant in $P = \rho\tilde{R}T$	$\frac{ft\text{-}lbf\text{-}^oR}{lbm}$
Re	Reynolds number -- diameter	---
S	convolution axial spacing	ft
T	temperature	degrees rankine
U	axial velocity	ft/sec
U*	shear velocity = $\sqrt{T_w/\rho}$	ft/sec
V	time mean spatially averaged velocity	ft/sec
$\tilde{V}$	tank volume	ft^3
x	axial position	ft
y	distance from wall	ft
	GREEK CHARACTERS	
β	ratio of upstream to downstream diameter	---
δ	boundary layer thickness	ft
ε	roughness height	ft
μ	fluid viscosity	lbm/ft sec
ν	kinematic viscosity	ft^2/sec
Φ	functional representation	---
ϕ	angular position	radian
ρ	fluid density	lbm/ft^3
τ	shearing stress	lbf/ft^2
θ	angle of bend	radians

NOMENCLATURE (Continued)

SYMBOL	DESCRIPTION	UNITS
	SUBSCRIPTS	
0	original value	---
2	downstream	---
i	iteration number	
n	number	
N	new predicted value	
o	evaluated at the maximum value	
w	evaluated at the wall	
	SUPERSCRIPTS	
1	denotes value one increment removed	---
'	denotes value with one variable changed	
''	denotes value with two variables changed	
$\overline{\quad}$	overbar denotes time mean	
n	polytropic constant in $P(\tilde{V})^n = C$	---

NOMENCLATURE FOR GEOMETRY OF FLEXIBLE METAL HOSE

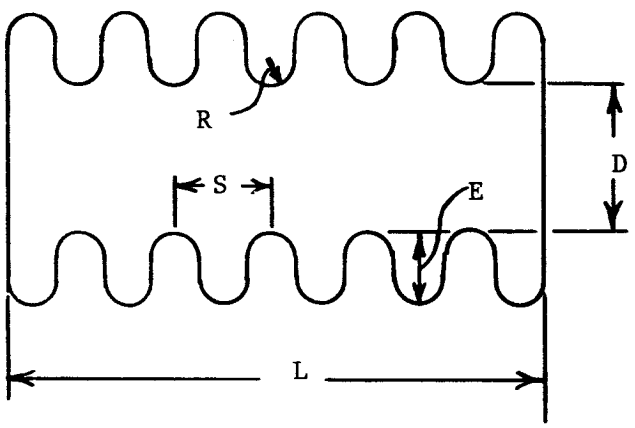

D = Internal Diameter

E = Convolution Height

L = Length

S = Pitch of Convolutions

R = Convolution Radius

LIST OF FIGURES

Figure		page
1.	Friction Factors for Flow in Flexible Metal Hose According to Pepersack	58
2.	Comparison of Correlation Equations with Experimental Data	59
3.	Comparison of Correlation Equations with Experimental Data	60
4.	Comparison of Correlation Equations with Experimental Data	61
5.	Comparison of Correlation Equations with Experimental Data	62
6.	Comparison of Correlation Equations with Experimental Data	63
7.	Comparison of Correlation Equations with Experimental Results	64
8.	Comparison of Correlation Equation with Experimental Results	65
9.	Supply Section	66
10.	Supply Section Details	67
11.	Measurement Section	68
12.	Measurement Section Details	69
13.	Pressure Measurement Connections	70
14.	Schematic Diagram of Test Section for Entrance Effects	71
15.	Schematic Diagram of Test Apparatus for Entrance Effects	72
16.	Schematic of Test Apparatus for Arbitrary Flow System	73
17.	Friction Factor vs Reynolds Number for 1/4" Dia. Hose	74
18.	Friction Factor vs Reynolds Number for 3/8" Dia. Hose	75
19.	Friction Factor vs Reynolds Number for 3/4" Dia. Hose	76

Figure

page

20. Friction Factor vs Reynolds Number for 1" Dia. Hose 77

21. Friction Factor vs Reynolds Number for 1-1/2" Dia. Hose . . . 78

22. Friction Factor vs Reynolds Number for 2" Dia. Hose 79

23. Comparison of Data 80

24. Comparison of Data 81

25. Comparison of Data 82

26. Longitudinal Temperature Distribution (Temperatures given in ^{o}F) 83

27. Longitudinal Temperature Distribution (Temperatures in ^{o}F) 84

28. Longitudinal Temperature Distribution (Temperatures in ^{o}F) 85

29. Longitudinal Temperature Distribution (Temperatures in ^{o}F) 86

30. Variation of Midpoint Temperature with Reynolds Number 87

31. Loss Coefficient vs. Reynolds Number for Pressure Regulator 88

32. Comparison of Predicted Pressure Drop and Actual Pressure Drop 89

33. Comparison of Predicted Pressure History and Actual Pressure History 90

34. Entrance Effects Study on Flexonics 1 inch Diameter Hose 91

ABSTRACT

The objectives of the research study were to develop means of predicting the performance of tubing and fitting systems for steady state and transient fluid flows.

One of the major results is an empirical equation which predicts the friction factor for flow through flexible metal hoses of various geometric configurations.

Another result is a computer program for prediction of the performance of a generalized system for steady state and slow transient, i. e., quasi-steady state phenomena which may be applied to many configurations, including systems with flexible corrugated metal hoses in them.

Work is continuing in the development of analyses for the improvement of the prediction equation for the corrugated flexible metal hose as a function of the geometry of the hose convolutions. The prediction of transient phenomena in tubing and fitting systems will require additional research in arriving at a satisfactory technique for solving the resultant partial differential equations.

I. Analytical

Recent investigations of the flow over rough walls reflect a substantial increase in friction factor at a given Reynolds number over that predicted by an equivalent roughness used in the Colebrook equation.

Visual flow studies reflect that vortices are generated in the cavities for certain conditions of flow. This condition has been used in the development of an empirical correlation equation for corrugated flexible metal hoses of various geometrical configuration. The argument in the development of the correlation equation evolved as follows.

The physical variables involved were the fluid density,ρ, the fluid viscosity,μ, the time mean spatially averaged velocity, V, the nominal tube diameter, D, the convolution axial spacing, S, the convolution depth, E, the convolution radius of curvature, R, the length of the hose, L, and the pressure drop, $(P_0 - P_2)$, thereby representing nine physical variables. According to Buckingham's Pi theorem, there should be six independent non-dimensional groupings of the nine physical variables. Taking the fully developed flow friction factor for smooth tubes as one combination of two of the independent groupings which has successfully been used, this reduced the number to five.

The argument was then made that a pseudo relative roughness term might be formulated from ER/D^2 and that the energy losses because of the existance of a vortex in the cavity would be a function of $\frac{ER}{SD}$. The former was thought to be a reasonable estimate at some equivalent roughness and the latter was formulated because of the energy losses

being a function of the area circumscribing the vortex, this area being proportional to $\frac{E}{S}$, and the intensity of turbulence which would be a function of R/D.

Considerable trial and error fitting resulted in the equation

$$\frac{1}{\sqrt{f}} = 1.74 - B1 \ln\left[\frac{C^{B2}}{1 + \frac{D1}{Re^4}} + \frac{H}{Re \sqrt{f}}\right]$$

where:

$$C = (17.0 \times FN2) \,.\, - 0.3$$

$$B1 = 100.0 \times FN1$$

$$B2 = 0.868/B1$$

$$D1 = (3.63 \times 10^{13}) \, (FN1)^{-3.71}$$

$$H = 0.283(1000 \, FN1)^{3.5}$$

$$FN1 = \frac{ER}{D^2}$$

$$FN2 = \frac{ER}{SD}$$

$$Re = \frac{\rho \,.\, V \,.\, D,}{\mu}$$ based on upstream conditions

This equation makes reasonable approximations for hoses greater than 3/4 inch diameter with conventional convolution configuration.

Further work is being undertaken to arrive at the values of the coefficients in an equation of the form

$$\frac{1}{\sqrt{f}} = C1 - C2 \ln\left[\frac{C3}{1 + \frac{C4}{Re^{C5}}} + \frac{C6}{Re^{C7} \sqrt{f}}\right]$$

such that the error is a minimum in a least squares sense. In that this equation is transcendential in nature, an iterative process is necessary to arrive at the values of the coefficients for each of the sets of test

data which are available from the results of the experimental portion of the research study.

II. Test Results

In order to substantiate the data appearing in the literature and to test the general validity of the prediction equation, a complete set of data was taken on ten sections of annularly convoluted flexible metal hose. The experimental system was also used to provide data on the pressure drop characteristics of flow through systems including valves, bends, tees, flexible hose, sudden contractions and expansions, etc. Data was also taken to investigate the entrance effects of turbulent flow in flexible metal hose. Dry air was used as a working fluid in all cases.

The first test results yielded data for each of the ten test sections (1/4 to 2 inch diameter and 10 feet long) which was reduced to friction factor versus Reynolds number form.

Additional data were taken to investigate the nature of the formation of a turbulent velocity profile upon entering a flexible tube. The turbulent entrance problem in flexible hose is undergoing further study.

III. Conclusions

The predictive program for system analysis has been demonstrated to give quantitative predictions for the steady state and quasi-steady state flow through a system composed of several components.

The correlation equation which has been developed for the friction factor for flow through flexible metal hoses will yield reasonable approximations over the range of variables considered.

The data presented were for a fitting to fitting measurement on a ten foot length of hose. Preliminary observations indicate that there are significant inlet and exit effects which should be separated from the "fully developed" region of flow in the convoluted flexible metal hoses.

I. INTRODUCTION

A. Objectives

The objectives of this research program were to develop an analytical method for predicting the behavior of the flow through tubing-fitting systems (for steady-state and transient flow conditions); to obtain experimental evaluation of the pressure losses in systems such as those encountered in missiles, (to include flexible connectors primarily); and to correlate the results of the analytical predictions and the experimental observations. The accomplishment of these objectives have resulted in design criteria for the behavioral characteristics of flexible connectors in tubing systems, and for tubing-fitting systems.

B. Method of Attack

The objectives of this research program were realized by implementation of the research in four phases. The phases of the program are described below.

Phase One

This phase of the program was comprised of the following:

1. A literature survey was made to establish the present state of the art in theoretical prediction, experimental evaluation, and correlation of experimental results relating to pressure losses in fittings for tubing systems.

2. Design of the experimental evaluation program according to statistical methods of experimental design was accomplished in order to optimize the usefulness of the experimental results in the range of variables to be considered.

3. The geometries for consideration in the development of the

analytical method of pressure loss prediction and for the experimental evaluation were established. Flexible connectors were given primary consideration and collaboration with representatives of NASA-MSFC established the types of connectors of most interest to NASA.

Phase Two

This phase consisted of theoretical considerations relating to the prediction of pressure losses in the flow of a fluid through flexible connectors in steady-state and transient flow conditions for various installations in tubing systems. Major attention was initially given to purely theoretical methods of prediction of pressure losses; however, difficulties arose in this method, and development of an analytical (theoretical-empirical) method for the prediction of the pressure losses in steady and unsteady flow through tubing systems was pursued. Empirical relations were introduced in this phase for those components for which steady-state data are available and the flexible connectors were evaluated experimentally in Phase Three.

Phase Three

The experimental evaluation of the pressure losses in tubing systems with flexible connectors constituted this phase of the proposed research program.

The experimental apparatus for this study is presented schematically in Figures 9 through 13. The essential components consist of the 350 scfm, 115 psi air compressor source for high pressure air, the 2000 cubic foot storage and the smaller surge tanks flow control valves, a turbine type flow meter installation, an entrance plenum chamber, the test section, the exit plenum chamber, downstream valve system for back pressure control, three differential pressure transducers, manometers, a system of pressure sensing leads, and four channels of recording for the differential and

static pressure data collection. A digital voltmeter has been employed for analog-digital conversion for the steady-state case, thereby making possible recordings which expedite data collection.

The fabrication of the proposed experimental apparatus as modified after collaboration with representatives of NASA-MSFC to accommodate any special requirements for the collection of data of special interest to NASA was accomplished during the first stage of this phase of the program.

Major emphasis was placed on the testing of flexible connectors of the type currently used in missile systems of special interest to NASA.

Phase Four

This phase was constituted of correlation of the analytical predictions and the experimental evaluation program, preparation of tabular, graphical, and analytical representation of the results, and preparation of a final report.

II. ANALYTICAL

A. Development of Empirical Equations for Existing Data.

Most of the available data on flow through flexible metal hose were listed by Belcher (1). A continuing search of the literature has yielded no further significant data on flow through convoluted metal hose. With the exception of the experimental work of Pepersack (2), most of the data is incomplete.

Thus, Pepersack's data was taken as a starting point for both the development of a predictive correlation equation and a search for the flow phenomena which produced the sudden pressure loss increase. This data was presented in the standard form for flow through pipes as the variation of friction factor with Reynolds number as shown in Figure 1.

In that the flow in flexible connectors at large Reynolds numbers is definitely in the turbulent regime, it was suspected that some sort of equivalent roughness could be determined and use of the generally accepted Moody diagram could be made for the determination of pressure losses therein. However, the presence of a transitional phenomena at a Reynolds number of approximately 10^5 precluded this approach.

Several attempts to fit polynomial curves to the data on hand resulted in a set of equations with variable coefficients. These variable coefficients were then considered a function of the various parameters of the design of the couplings. No effective method was evolved to correlate the results and the coefficients. This approach was then abandoned.

It was noted that the curves had the general characteristics of the rough pipe curves presented in Schlichting (3) according to Nikuradse

and therefore, it was believed that some sort of modification of the equations for smooth pipe friction factors and the regime of complete turbulence would yield fruitful results. The first equation of this form to be used was a simple modification of the equation presented in Schlichting (3) as representing the friction factor as a function of Reynolds number and relative roughness. Difficulties arose in achieving a good fit and investigation of the behavior of the equation by obtaining the derivative with respect to Reynolds number showed the function to be monotonically increasing with decreasing Reynolds number.

The second attempt was then to adjust the equation so that the significance of the term replacing the relative roughness term, i. e., RxE/SxD, arrived at by considering that the energy losses at high Reynolds numbers would be proportional to the area over which a standing vortex in the annular region acted.

Assuming that some friction factor would prevail with the concept of slip flow around the annulus, the energy losses would then be proportional to the area and the level of turbulence intensity which was assumed to be proportional to R.

The area of the annuli are proportional to E/S and the intensity of the turbulence in this region was assumed to be related to the radius of curvature of the convolution, R. This was non-dimensionalized by dividing by the mean diameter to give as the parameter for very high Reynolds numbers,

$$\frac{R \times E}{S \times D} \qquad (1)$$

A sub-objective was to determine the correlation of this parameter with the maximum values of friction factor obtained at high Reynolds numbers.

This resulted in

$$1/\sqrt{f} = 1.74 - 0.868 \ln((17.0 \frac{RE}{SD}) - 0.3) \quad (2)$$

which had a distinct similarity to the equation presented for the completely turbulent pipe flow regime in Schlichting (2) which, for large Reynolds numbers is

$$1/\sqrt{f} = 1.74 - 0.868 \ln(K_s/R) \quad (3)$$

Next the consideration that the completely rough regime of flow at low Reynolds number was influenced by the magnitude of the turbulence intensity which might be related through the non-dimensional parameters of

$$\frac{S \times E}{D^2} \quad \text{and} \quad \frac{R \times E}{D^2} \quad (4)$$

These parameters were inserted arbitrarily into a tentative correlation equation to yield:

$$\frac{1}{\sqrt{f}} = 1.74 - B1 \ln \left[\frac{C^{B2}}{1 + \frac{D1}{Re^3}} + \frac{H}{Re \sqrt{f}} \right] \quad (5)$$

where:

$$C = \frac{17RE}{SD} - 0.3 \qquad D1 = \frac{2 \times 10^{14} D^2}{RE}$$

$$B1 = \frac{30SE}{D^2} \qquad H = \frac{0.75 \times 10^4 SE}{D^2}$$

$$B2 = \frac{0.868}{B1}$$

Equation 5 was used to calculate the friction factor versus Reynolds number variation for six different connectors and the results are presented with the Pepersack's data (2) for comparison in Figures 2 through 7.

This equation is similar in form to an equation presented by Colebrook (4). His equation did not, or course, predict the sudden increase in the friction factor in the neighborhood of a Reynolds number of 10^5. However, equation 5 did not agree closely with Pepersack's data for the three-quarter inch diameter connector. In view of this, considerable study was afforded the form of the equation and the parameters involved. It was found that the use of two parameters;

$$FN1 = \frac{RE}{D^2} \qquad \text{and} \quad FN2 = \frac{RE}{SD}$$

yielded:

$$\frac{1}{\sqrt{f}} = 1.74 - B1 \ln \left[\frac{C^{B2}}{1 + D1/Re^4} + \frac{H}{Re\ \sqrt{f}} \right] \qquad (6)$$

where:

$$C = 17.0\ (ER/SD) - 0.3$$

$$D1 = (3.63 \times 10^{13})(ER/D^2)^{-3.71}$$

$$B1 = 100.0\ (ER/D^2)$$

$$B2 = 0.868/B1$$

$$H = 0.283 \left[(1000.0)(ER/D^2) \right]^{3.5}$$

It should be noted that the use of Reynolds number to the fourth power in equation (6) instead of the third power in equation (5) proved to give better results.

Equation (6) yields predictions of friction factor vs. Reynolds number variation as shown in Figures 2-8. The improvement obtained through the use of this equation over the first one is obvious. Of particular note is the agreement obtained for the three quarter inch diameter connector as shown in Figure 8. It was previously noted that the first equation failed to predict this data.

The evolution of equation (6) from physical reasoning through trial and error to its present form suggested that standard numerical methods of curve fitting might yield an equation which agreed as well with the data as this equation but have a form which would be easier to apply. The appearance of $\sqrt{f}$ on both sides of equation (6) makes its use awkard.

An effort was therefore begun to develop a computer program to correlate the data of Pepersack using standard mathematical techniques for curve fitting.

This effort began with a computer program to evaluate the coefficients, using Pepersack's data, in an equation of the form;

$$f = \frac{a_1 + \emptyset_1 (Re) + a_2 FN1 + a_3 FN2}{1 + a_4 \emptyset 2(Re) + a_5 FN1 + a_6 FN2} \qquad (7)$$

where $\emptyset_1(Re)$ and $\emptyset_2(Re)$ are some arbitrary function of Reynolds number. Several different functions were used in an attempt to fit Pepersack's data. Some of these were Re, Re^2, 1/Re, ln Re, ln(1/Re), and ln(lnRe). All attempts at correlating the data satisfactorily failed and it was concluded that the ratio of polynomials model as used herein was not sufficiently flexible to meet the demands of this particular set of data. In the attempts, equation (7) was modified by deleting the unity factor in the denominator.

The next approach was a brief return to the form of equation (6) in an attempt to have it yield a better correlation by a new method of coefficient determination. Repeated trials failed to produce significant improvement and, since the same unwieldy algebraic form was present, the attempt was abandoned.

A subsequent approach consisted of fitting each curve for the seven individual sections tested by Pepersack by an equation of the form;

$$f = a_n + b_n \phi(Re) + c_n \phi(Re)^2 + d_n \phi(Re)^3, \ (n = 1, 2, 3 \ldots 7) \quad (8)$$

Where $\phi(Re)$ represents an arbitrary function of Reynolds number. It is then postulated that the coefficients in each of the seven equations are functions of the geometrical parameters FN1 and FN2. The particular form of this functional relationship is sought through computer evaluation of the coefficients in an equation of the form,

$$a_n = k_o + k_1 FN1 + k_2 FN2 + k_3 FN1/FN2 + k_4 FN2/FN1 + k_5(FN1)^2 + k_6(FN2/FN1)^2 \quad (9)$$

and similar equations for b_n, c_n, and d_n. Once this has been done, a cross-correlation of the original seven equations might be accomplished to yield a single correlation equation. Several functional forms for $\phi(Re)$ were used including Re, 1/Re, lnRe, ln(Re), and ln(ln(Re)) with fair results in correlating individual curves. Similarily, the coefficients, k_n, were evaluated giving a functional form of equations (9) which correctly predict the coefficients for equations (8). The cross-correlation of these seven equations was not possible and the approach was abandoned. Two different curve fitting techniques were used in order to seek the best fit of the data. The first of these is that presented in Regression and Correlation Programs for the IBM 1620 Computer by F. H. Tyner, Jr.* The second is the method of Multiple

* Research Assistant, Department of Agricultural Economics, Mississippi Agricultural Experiment Station, State College, Mississippi.

Regression of Polynomials for 18 Variables by O. Dykstra, Jr.**

In view of the difficulties encountered in generating the coefficients to be used in the correlation equations for various flexible hoses, two methods of statistical analysis based on minimization of the sum of the squares of the error between the actual friction factor and the predicted friction factor have been attempted.

The equation in the general form of

$$\frac{1}{\sqrt{f}} = D_1 - C_2 \ln\left[\frac{C_3}{1 + \frac{C_4}{Re^{C5}}} + \frac{C_6}{Re^{C7}\sqrt{f}}\right]$$

is the mathematical model which has been selected to attempt to fit the experimental data.

The first method was essentially an iterative procedure in which an initial estimate of C_1 was made based on the predictions presented as equations 6, et.seq. The procedure was to vary C_1, determine if the sum of the squares of the error was reduced, if so, then continue to vary C_1 until there was a reversal in the change of the sum of the squares of the error. This in effect would obtain the best value of C_1 for the other C_i's. This procedure would then be repeated for each of the remaining C_i's and then the entire procedure would be repeated with the expectation that optimum values of C_i's would be found through the iterative process.

The second method is a bit more sophisticated and depends on the hypothesis that according to the chain rule of differentiation of a function of several variables.

$$dE = \frac{\partial F}{\partial C_1} dC_1, + \frac{\partial F}{\partial C_2} dC_2 + \frac{\partial F}{\partial C_3} dC_3 + \ldots \frac{\partial F}{\partial C_n} dC_n$$

**General Foods Research Center, 555 S. Broadway, Tarrytown, New York.

where $dF = F_N - F_O$ and $F = \sum (f_{cal} - f_{act})^2$ (1)

$dC_i = C_{iN} - C_{iO}$

E_{new} should be a minimum in order to establish an optimum value for the C_i's in a least squares sense.

Observing that the C_i's are independent, then in order for F_N to be a minimum, then all of the $\frac{\partial F}{\partial C_i}$'s are also a function of all of the C_i's, there are the seven requirements that

$$\sum_{j=1}^{7} \frac{\partial}{\partial C_j}\left(\frac{\partial F}{\partial C_i}\right) dC_j = \left(\frac{\partial F}{\partial C_i}\right)_0$$

This latter may be expressed in finite difference form as

$$\left(\frac{F' - F}{C_i^1 - C_i}\right) = \sum_{j=1}^{7}\left[\frac{\left(\frac{F'' - F}{C_i^1 - C_i}\right)_{C_j^1, C_m} - \left(\frac{F' - F}{C_i^1 - C_i}\right)_{C_j, C_m}}{\left(C_j^1 - C_j\right)}\right]\left(C_{jN} - C_{jO}\right)$$

This results in a system of linear algebraic equations which may be solved for the dC_j's and subsequently for the C_{jN}'s. Several iterations may be necessary in order to arrive at the optimum values because of the errors introduced by the finite difference approximations to the cross partials.

Work is continuing on these methods and additional information will be presented as it is generated.

B. Theoretical Considerations

(1) Flow Through Convoluted Tubing

The characteristics of flow through straight tubes are reasonably well-known. Laminar flow in long tubes has exact mathematical representation as well as experimental verification. Only the case of an incompressible fluid has an exact solution in the case of short tubes (5). There do not exist, however, any closed-form mathematical solutions for the general problem of flow in short tubes, although numerical solutions are available (6). It has been noted that flow through tubes and ducts with corrugations in the walls normal to the flow direction experiences a radically increased resistance compared with a similar flow through a smooth tube or duct (2,10). The frequent use of corrugated-type flexible connectors in present missile designs makes it imperative that an understanding of the phenomena producing this increased friction be sought and a reliable method of predicting the resulting pressure loss be developed.

The flow resistance through ducts is usually expressed in non-dimensional form either as:

$$f = - \frac{dp}{(\rho\ V^2/2)\ d(x/D)}$$

or

$$f' = \frac{\tau_w}{\rho V^2/2}$$

Where the pressure force, in the first case, and the wall shear stress, in the second case, are normalized by the dynamic pressure of the fluid stream. It is shown in Appendix A, that these two factors are related by $f = 4f'$ for steady flow of an incompressible fluid. The use of f, the so-called Darcy-Weisbach Coefficient, was incorporated by Moody (7) in his widely used curves.

Pepersack's (2) data presented as the variation of f with Reynolds number indicates the previously mentioned sharp transition to greatly increased friction factors at Reynolds numbers of approximately 10^5 as shown in figures 1-7. Initial speculation by several parties followed the idea that this transition phenomena was due to vortex formation within the convolutions. The energy dissipation by the vortices was assumed to produce the increased resistance to flow.

Such vortex formation produced by flow over a cavity have in fact been observed and photographed extensively by Wieghardt (8) who also reported an increased drag coefficient for a flat plate with recesses in it.

Thus, the initial assumption of vortex flow within the convolutions which was used in the physical reasoning developing the correlation equation was not pure speculation, but had basis in observed fact. It was felt, however, that in many applications where flexible connectors were longitudinally compressed or bent that some, perhaps most, of the convolutions would be so isolated from the flow that it would be unreason-

able to expect either the formation of vortices or, if formed, their participation in the mainstream flow. It was this conviction which led to the investigation of the establishment of resonance in situations of flow over cavities. The theory of the Helmholtz resonator, as reviewed by Kinsler and Frey (9), predicts the oscillations of fluid in the neck, or entrance, of a cavity at the condition of resonance. It was along this line of reasoning that calculations were carried out to predict the resonant frequency in a typical one inch diameter flexible connector. This frequency was found to be in the neighborhood of 100,000 cycles/sec. Attempts at correlating Helmholtz resonator theory with the phenomena at hand were unsuccessful.

Further literature searching produced several instances in which drastically increased flow resistance became manifest under fully turbulent duct flow in which convolutions or ripples were present on the walls. Seiferth's (10) data show a 57% decrease in the mass flow rate through a water duct from 500 to 700 mm in diameter with convolutions only 1 mm high. These convolutions were formed of deposits of Al_2O_3 on the walls of the duct, and the increased resistance returned to normal once the duct was cleared of these deposits. Although the friction factors in this case are not as high as for Pepersack's data a significant increase does exist. Some flat plate experiments giving velocity and temperature profiles for flow over both protrusions and cavities were reported by Doenecke (11). In the case reported by Seiferth (10), one would hardly suspect either vortex formation or cavity resonance in such small and shallow ripples. Doenecke reports vortex formation in only a few cases of corrugation size.

It thus became apparent that although the vortex action and

cavity resonance could contribute to the total flow resistance, they were perhaps not directly responsible for the sudden increase noted previously.

A most interesting publication concerning flow through artificially roughened tubes was presented by Nunner (12). Rings with a semicircular crossection were placed in a tube to give a corrugated wall geometry similar to flexible couplings. His results for a single ring size and four different spacings are shown in the figure below where the maximum Reynolds number shown is 8×10^4. It is interesting to note that the

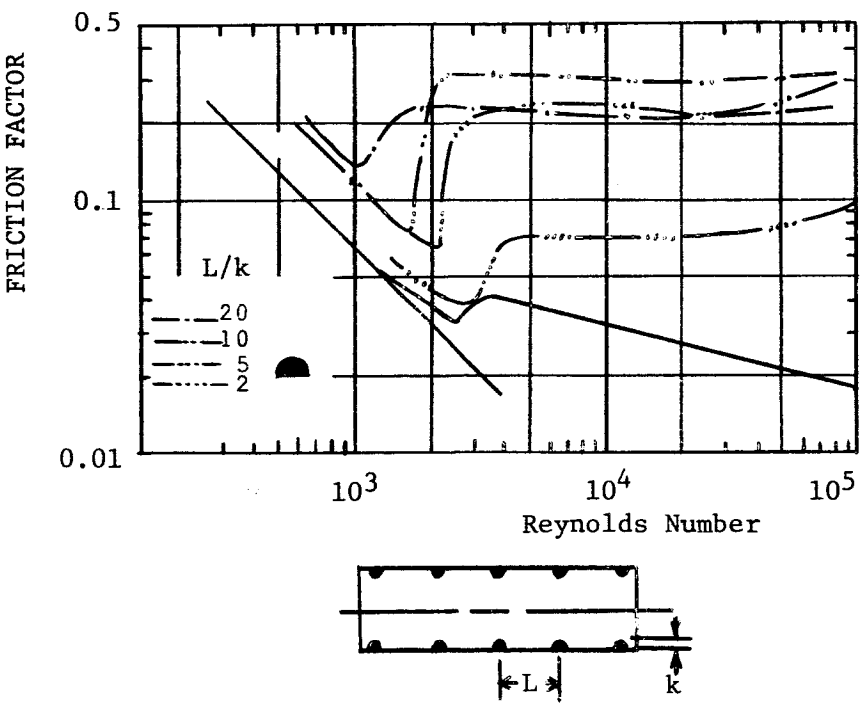

Nunner's Data For Friction Factor For Artificially Roughened Pipes.

curves indicate an increasing friction factor near a Reynolds number of 10^5 in a manner similar to the data of Pepersack (2). Nunner's data for the 4 mm diameter semicircular ring show four points all with the

same S/D ratio (or ε/D, relative roughness ratio) which have drastically different friction factors due only to the longitudinal spacing. Of particular interest is the last set of data with the rings pushed completely together producing a corrugated wall which has no cavities or convolutions. This configuration produced as great a tendency toward suddenly increased friction factors as did those configurations which more closely resemble convoluted tubing. Similar experiments with artifically corrugated tubes have been reported by Mobius (13) and Wiederhold (14).

As a result of the above information, a crude test was attempted during one of the experimental runs of the present research effort. While air flow through a flexible coupling was producing a Reynolds number of about 10^5, the coupling was longitudinally compressed. This compression changed the configuration of the convolution cavities with respect to the main flow stream but no significant change in the pressure drop across the coupling was detected.

In view of the above discussion and reasoning, attention was turned to a study of the mechanism of turbulence production. Several aspects of this problem were studied, including;

(a) The contribution to turbulence production of the wall configuration.

(b) The effect on and contribution to the flow characteristics of flexible walls.

(c) Applicability of recent experimental studies of turbulent skin friction over compliant surfaces.

(d) The Coanda effect.

In order to gain more insight into the problem, the general area

of flow over rough surfaces was studied. The flow phenomena which produces this increased friction factor is rather obviously connected with the geometry of the flow tube. Any search for an explanation of this phenomena must start with postulates concerning the effects of variation in geometry. Reasonable postulates are most easily obtained by careful study of the literature concerning flow through ducts of various geometries and flow over surfaces of different configurations. Toward this end a study of the literature reveals several previous experimental efforts in which a flow phenomena occurred which was similar to the one of interest here.

Perhaps the earliest such work is that of Fromm (15) who, in 1923, conducted some experiments on flow in a two dimensional channel with saw-tooth walls in which friction factors as high as 0.2 were achieved. Similar work was performed in 1928 by Fritsch (16). Extensive work has also been performed with pipes of non-uniform roughnesses. Some of the earliest of these showed friction factors as high as 0.4 for water flow through pipe with quite irregular internal geometry due to a galvanizing process. These tests conducted by Feely and Riggle (17) on 1/8 inch standard galvanized pipe are shown in the paper by Kemler (18). The results of two experimental efforts were published in 1958, one by Koch (19) and the other by Nunner (12), both of which reported friction factors for flow tubes with artificial uniform roughnesses. Koch made use of thin orfice-like ring-shaped discs inside of smooth pipe, whereas, Nunner installed rubber rings of semi-circular cross sections. Both authors presented friction factor versus Reynolds Number results which indicate much higher friction factors than for typical rough pipe. For instance,

friction factors as high as 4 were reported by Koch and as high as 0.3 were reported by Nunner. Both these results indicate a tendency toward increased friction factors in the neighborhood of Reynolds Numbers of 10^5. These increases occurring as a change from an otherwise constant value following the laminar to turbulent transition. A somewhat similar experiment was carried out in 1940 by Mobius (20) in which he investigated flow through artificially roughened pipes, roughnesses being produced by small rings of square cross sections in which he reported friction factors as high as 0.1.

In 1953 Wieghardt (21) conducted some interesting experiments for flow over rectangular ribs placed at right angles to the flow stream and also flow over circular cavities. Both situations produced an increase in the drag coefficient of the plate to which the ribs were attached or in which the holes were drilled and in some cases vortex patterns were observed within the holes. Photographs of these patterns are shown accompanying his article. Wieghardt also presents some interesting nomogramms for determining pressure drops and drag coefficients over such flow obstructions. Wieghardt's work receives some discussion in Schlichting's Boundary Layer Theory (4th edition) on pages 554 and 555. A very interesting example of the increased friction factor due to internal regular roughnesses was reported in 1949 by Wiederhold (14) and also in 1950 by Seiferth and Druger (10). Both these papers report a water duct in which a mass flow decreased by 57% during a long period of usage. It was found that this increase in friction factor which was of the order of 0.06 was due to a rib-like deposit of aluminum oxide on the walls of the duct. This work is mentioned briefly in Schlichting's text on page 529. These

results are of particular interest because of the geometrical similarity to the convoluted tubing which are the subject of this investigation.

With heat transfer being his main interest, Doenecke (11) presented some heat transfer and friction studies of turbulent forced convection over rough plates. This work took place in 1963.

Naval architects and Marine engineers for some time have studied flow over rough surfaces. An article entitled "Boundary Layer Characteristics For Smooth and Rough Surfaces" by F. R. Hama (22) presents a rather good bibliography of the literature in this area. Specifically, there are two references which deserve mention, both being dissertations from the State University of Iowa. The first by W. D. Baines (23), the second by W. F. Moore (24) concerning investigation of Boundary Layer Development Along A Rough Surface.

The most recent article of interest is one which appeared in the February, 1965 issue of The Journal of the Royal Aeronautical Society. This article by R. D. Mills (25), entitled "On The Closed Motion of Fluid in a Square Cavity" presents a two dimensional incompressible solution for the vortex motion of a fluid in such a cavity. In his work, Mills references the photographic results of Wieghardt (21) and Baturin (26) who have photographed this vortex flow in rectangular cavities as well as the experimental results of Roshko (27), Mills (28), and Linke (29). Mills approaches the problem from the standpoint of a periodic solution to the boundary layer equations. His analysis yields an infinite series expression for the velocity distribution in the cavity which he compares with the work of Roshko and others.

An article which has come to our attention very recently is that of V. K. Migay (30), entitled "The Aerodynamic Effectiveness of a Discontinuous Surface". Migay's work is concerned with delay of the separation point in a diffuser by means of supplying the diffuser wall with convolutions placed normal to the flow stream. In an auxiliary experiment, using water and sawdust, he found vortex formations within the convolutions or cavities. But more interesting, he found that "at high speeds, intense ultrasonic radiation was registered". He goes on to discuss the concept, previously considered in this work, of a Helmholtz resonator.

Another interesting area of investigation is that of cross flow over cylinders at high Reynolds number. Roshko (31) presents some results of very high Reynolds number flow over cylinders in which the drag coefficient first decreases and then again increases this phenomena being due to boundary layer separation and motion of the separation point along the surface of the cylinder. A striking variation in the drag coefficient of the cylinder is produced by the motion of this separation point. It is felt that this phenomena could also be part of the friction factor increase of the subject investigation.

"The Study of Flow Over a Corrugated Surface" is the subject of a NACA technical note by Corrsin and Kistler (32) in 1954. They reported the results of a wind tunnel flow in which one wall was corrugated sinusoidally. Velocity profiles and friction coefficients were reported for the turbulent boundary layer which was formed. The main subject of the paper, however, was the propagation of the turbulence produced in the boundary layer into the potential flow in the main stream of the wind

tunnel.

It was stated by Clauser (33) that "the customary zero velocity point is located at the variable height minus $\sqrt{\frac{2}{c_f}}$ ", where c_f is the local skin friction coefficient. Be adjusting the boundary condition in this manner such that the zero velocity occurs not at the wall but at some midway point between the top of the protrusion and the bottom, he found that data for rough pipes could be fitted more reasonably.

A similar effect was noted by Moore (24). He showed that

> "When plotted in terms of the parameters normally used for pipe flow, $\frac{U_o - U}{U^*}$ and y/δ, the velocity profiles differ systematically from the one for smooth plates, but when the origin for y is adjusted by adding 2/3 k to all the y values, the rough-plate profiles are brought into fair agreement with the smooth plate profile."

In Moore's nomenclature U* is the shear velocity, $\sqrt{\tau wall/\rho}$.

Another quite pertinent report is NACA Report 1174, entitled "The Structure of Turbulence and Fully Developed Pipe Flow" by John Laufer (34). This work makes up the primary reference on turbulent flow in ducts as discussed in the text book, TURBULENCE, by Hinze (35). It is quite pertinent to quote from page 486 of Hinze's book. "We conclude, therefore, that at present, determination of the velocity distribution close to a rough wall is still in the purely empirical stage and that there is no way to predict this distribution for an arbitrary roughness pattern; at any rate, it is not possible to express the effect of such a roughness pattern in terms of one single roughness parameter". The general description of turbulent pipe flow as given by Laufer and repeated by Hinze, is

flow under the assumption of rotational symmetry in the time mean properties and steady mean flow the equation becomes

$$\frac{1}{\rho}\frac{\partial \overline{P}}{\partial r} = -\frac{1}{r}\frac{d}{dr}(r\,\overline{u_r^2}) + \frac{\overline{u_\phi^2}}{r} .$$

Using the notation shown below

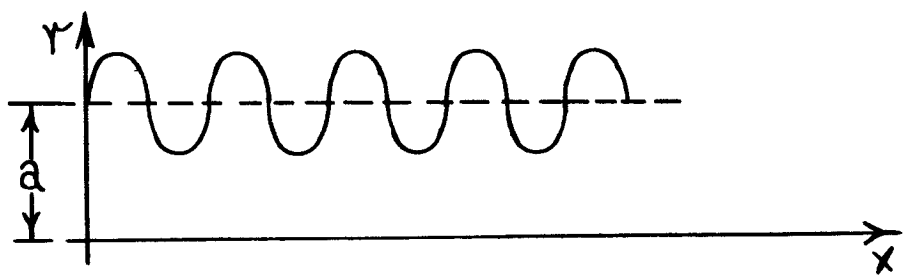

and assuming a sinusoidal shape for the convoluted tube, a quadrature can be indicated yielding

$$\frac{1}{\rho}\int_{r=0}^{r=a+\sin x}\frac{\partial \overline{P}}{\partial r}\,dr + \int_{r=0}^{r=a+\sin x}\frac{1}{r}\,d\,(r\,\overline{u_r^2}) = \int_{r=0}^{r=a+\sin x}\frac{\overline{u_\phi^2}}{r}\,dr .$$

The properties and predictions of this equation were investigated and no results were immediately found to indicate the validity of the approach.

Before extensive investigation of the usefullness of this technique could be completed, a publication was discovered which made use of momentum integral methods. Konobeev and Zhavoronkov (37) investigated experimentally and analytically the flow of a gas through a tube with wavy roughness. They used momentum integral methods coupled with a sinusoidal tube boundary

as follows: The flow adjacent to the wall is responsible for the production of small eddies of great energy intensity. This energy is dissipated in the form of a diffusion of eddy energy toward the center of the tube where there exists large elongated eddies. It is felt that a possible explanation for the increased friction factor of the subject research could lie in the existence of large eddies at the wall, that is, in the convolutions rather than the small high intensity eddies as described by Laufer.

The experimental results of Knudsen and Katz (36) describe the observation of eddy patterns in the area between fins on a transverse helical finned tube. The fact that these eddies were observed for all turbulent flows (even at very low Reynolds numbers) supports the contention that the mere existance of an eddy or vortex in the convolution is not in itself responsible for the sudden increase in friction factor. If the eddy phenomena plays a significant roll it must be due to a sudden change in character of the eddy flow in the cavity. It is doubtful that flow visualization will be possible at such high Reynolds numbers to detect any such suspected changes in the character of the eddies at the onset of this increase in friction factor.

Due to the uncertainty about the phenomena responsible for the sudden increase in friction factor, it was felt that a method of analysis might be used which did not rely on any of the above postulates. This led to consideration of the use of momentum integral techniques. The question posed was whether or not such techniques applied to a flow with a convoluted boundary might predict the increase in friction factor which has been found. If one writes the r-momentum equation for turbulent pipe

as described above. Their results, however, failed to predict any sudden increase in friction factor. Their analytical results agreed with their experimental data, which surprisingly does not show any sudden change of friction factor for Reynolds number as high as 10^6. It is noted, however, that the convolution heights used were quite shallow, having E/D ratios below 0.05. It is appropriate to quote their conclusion. "Therefore, we conclude that the coefficient of friction in tubes with long-wave roughness is the same function of Re number as the coefficient of friction for smooth tubes ....." They did however acknowledge a heavy dependence of the friction coefficient on the "form of the crest of the wave".

A thorough study was made of a recent Ph. D. dissertation on the subject of "Flow over a Rough Surface" by H. W. Townes (45). Townes made extensive measurements of velocity distributions of the flow of water over transverse square cavities. Although the flow was of the open channel type, the results were applicable here especially for the many photographs of the flow. Excellent results of a dye method of flow visualization were of value since the study concentrated on the region of interaction between the cavity flow and mainstream flow. This study coupled with further study of Laufer's work (34) prompted consideration of the significant dimensionless groups involved in the problem. It was felt that the characteristic length dimension to describe the surface roughness should be reconsidered. The average roughness height, as used by Nikuradse is not appropriate for convoluting tubing. As another possible characteristic surface dimension, the ratio of the convolutions' volume to surface area, was studied. This parameter may be written as

$$E_{v/a} \simeq \frac{1}{4}\left[\frac{2 + E/D}{1/E + 1/D + 2/5 + E/SD}\right] .$$

Preliminary indications are that this length would be satisfactory but no significant advantage would be gained by its use.

Possibly a more reasonable choice of a non-dimensional quantity to characterize the surface roughness is to be found with dimensional analysis. Assuming the pertinent variables to be T_w, ρ, ν, and some geometric length such an analysis will predict the following significant dimensionless number

$$E^* = \frac{EV_T}{\nu} ,$$

where V_T is the shear velocity defined by $V_T = \frac{Tw}{\rho}$, or $V_T = -\nu \frac{\partial V}{\partial r}$ wall. The detailed experiments performed by Laufer led him to the conclusion that in the close proximity of the wall "using the similarity parameters V_T and ν/V_T flow field in this region was shown to be independent of the Reynolds number" (34). In this case the characteristic length is the ratio ν/V_T.

It seems only reasonable, however, that the quantity used to characterize the roughness elements be in some way related to some characteristic dimension of the mainstream turbulent flow. Such a quantity is to be found in what Hinze (35) calls the micro scale or dissipation scale of turbulence.

Efforts toward achieving positive identification of the phenomena responsible for the sudden increase in friction factor have not been successful. It is felt that the literature reviewed and the possibilities

considered have been sufficient but that without internal measurements or flow visualization, further efforts would prove to be fruitless. Furthermore, it has become apparent from several sources, among them some in-house NASA experiments, that flow visualization of the subject phenomena at Reynolds numbers of 10^5 and higher is impossible at the present state of the art.

In an effort toward completeness an investigation was initiated to study the entrance region in a convoluted pipe.

In that the flow of a compressible fluid through a conduit generates the problem of entrance effects and exit effects, it became apparent that some consideration must be made for the separation of the entrance effects, the fully developed flow regime, and the exit effects.

The analytical prediction of the entrance effects and the exit effects are not feasible at this time because of the lack of information concerning the velocity profile and the wall shearing stress parameter. It was thus concluded that an experimental approach to investigate these three regions would be necessary.

(2) Flow Through Arbitrary Systems

The determination of pressure drop characteristics for complex piping systems is of primary importance in many engineering applications. The object of this study was to present a method whereby the pressure drop in an arbitrary flow system can be determined as a function of the mass flow rate.

The analysis considers a compressible fluid flowing at subsonic velocities through an arbitrary pipe system which contains components normally found in typical flow installations. These components are

1) straight pipe
2) elbows and bends
3) abrupt expansions
4) abrupt contractions
5) parallel pipes
6) flexible metal hoses

In addition to these components, a portion of the analysis considers arbitrary configurations where the loss coefficients pertinent to additional components are known.

Pressure losses are classically determined by means of the Darcy equation

$$\Delta P = \frac{K\rho_2 \bar{V}_2^2}{2g_c}, \qquad (9)$$

where K is a loss coefficient determined by experimentation. For systems utilizing an incompressible fluid, Benedict (38) shows that the pressure drop for a pipe system may be determined by considering a loss coefficient, K, for the individual components of the system. He concluded that an overall loss coefficient could be obtained by adjusting the individual

loss coefficients to a common reference area and then summing the results. Thus:

$$K_{o,n} = K_{o,1}\left(\frac{An}{A_1}\right)^2 + K_{1,2}\left(\frac{An}{A_2}\right)^2 + \text{---}K_{n-1,n}. \qquad (10)$$

In addition, Benedict found that the compressible loss coefficients could be combined in a somewhat similar manner. However, the procedure is a considerably more difficult one than that dealing with incompressible flow.

The procedure presented here utilizes numerical techniques to solve the system of equations relating the pressure drop in each component to the flow parameters for the system.

The analysis of the flow system to determine the pressure drop is based upon the assumption that the flow is:

1) steady
2) isothermal
3) subsonic

The flow system was analyzed by breaking the system into individual components and by proceeding upstream from the exit, computing the pressure drop in each component for a given mass flow rate. The pressure drop was summed with the pressure from the preceding component so that density changes, due to the increase in pressure, would be considered. In this manner the pressure drop for the entire system may be determined. The analysis was then repeated for another mass flow rate so that the end result of the program was a set of points determining a curve of pressure drop as a function of mass flow rate.

As was stated previously, the system to be analyzed was broken into individual components. In this study, the following components were incorporated into a computer program which solved the equations for the system. These components, which are normally found in most flow systems,

were:

(a) abrupt expansion losses
(b) abrupt contraction losses
(c) viscous losses in straight pipes
(d) bend losses
(e) arbitrary losses, valves, tees, etc.
(f) flexible hose losses
(g) losses in parallel flow

These losses will be described in detail later.

An additional section of the analysis was peculiar only to the test system under consideration. This section computes the pressure drop in the turbine flow meter. The flow measuring equipment automatically switches the flow at a specified volumetric flow from a one inch turbine type flow meter to a two and one-half inch turbine type flow meter.

In the analysis, the components above may be arranged or combined in any order so that any given system may be simulated. Thus a plenum chamber may be represented by a sudden expansion, a straight section and a sudden contraction.

The losses for the individual components of the system are:

(a) Abrupt Expansion Losses

Flow losses occur in piping systems when the flow area abruptly increases. Benedict, Carlucci, and Swetz (38) analyzed these losses for a compressible fluid. They determined that the pressure losses could best be predicted by a relation based on a pressure ratio, either total or static, rather than on a loss coefficient. For abrupt expansion losses, where the fluid suddenly emerges from a small flow area to a larger flow area, this relation was

$$\frac{P_2}{P_1} = 1 + \left(\frac{1-\bar{R}_1}{\bar{R}_1}\right) (2\beta^2) \quad (1 - \beta^2), \tag{11}$$

where $\frac{P_2}{P_1}$ is the static pressure ratio, $\bar{R}_1$ is the static to total pressure ratio, and β is the ratio of upstream diameter to downstream diameter. The subscripts 1 and 2 denote upstream and downstream conditions respectively.

Although, strictly speaking, this relation was derived for a constant density fluid, in reference (38) it is seen that equation (11) may be used for any fluid with little appreciable error.

(b) Abrupt Contraction Losses

In systems where the fluid encounters an abrupt decrease in the area of its system boundaries, a pressure loss, somewhat similar to that for abrupt enlargements, is found. Again, Benedict, Carlucci and Swetz (38) use the pressure ratio concept to predict these losses. Unlike the abrupt enlargement relationship previously discussed, it is not possible to obtain an explicit analytic expression. However, an analytic expression based on experimentally determined coefficients may be determined. This expression was

$$\frac{P_{t2}}{P_{t1}} = \frac{1}{1 + (1-\bar{R}_2)\ (K_{1,2})_2}\ , \qquad (12)$$

where P_{t2}/P_{t1} is the total pressure ratio, $\bar{R}_2$ is the static to total pressure ratio. $(K_{1,2})_2$ is an experimentally determined coefficient given by

$$(K_{1,2})_2 = \frac{1}{(C_c)^2\ (C_v)^2} - \frac{2}{C_v} + 1 \qquad (13)$$

where C_v is an experimentally determined coefficient and C_c is a function of the diameter ratio β.

From the data taken by Weisbach (39), a least-squares equation was obtained expressing C_c as a function of β. This was given by reference

(38) as

$$C_c = 0.16375 + 0.13318\beta^2 - 0.26095\beta^4 + 0.51146\beta^6 \ , \quad (14)$$

where β is the ratio of upstream diameter to downstream diameter.

(c) Viscous Losses in Straight Pipe

Pressure losses in straight pipes are due primarily to the viscous effects of the fluid. In this analysis, the pressure drop was found from the Darcy-Weisbach equation

$$\Delta P = f\frac{L}{D}\rho\frac{\overline{V}^2}{2g_c} \quad (15)$$

where ΔP is the pressure drop, f is the Darcy-Weisbach friction factor, L is the pipe length, D is the hydraulic diameter, $\overline{V}$ is the mean downstream velocity, and ρ is the fluid density. The friction factor f in equation (15) has been shown by Nikuradse (40) and others to be a function of the Reynolds number, and a relative roughness term. The Reynolds number is defined by

$$Re = \frac{\rho\,\overline{V}D}{\mu} \ , \quad (16)$$

where ρ is the density of the fluid, $\overline{V}$ is the mean velocity of the fluid, D is the inside diameter, μ is the dynamic viscosity. The relative roughness, k_s/r, is defined by the ratio of the height of grain protrusion, k_s, to the hydraulic radius of the pipe, r.

The relation used in this analysis to predict the Darcy-Weisbach friction factor for turbulent flow was developed by C. F. Colebrook (41). This equation is given by

$$\frac{1}{\sqrt{f}} = 1.74 - 0.868 \log_e \left(\frac{k_s}{r} + \frac{18.7}{Re_D\sqrt{f}} \right), \quad (17)$$

where k_s is the equivalent sand roughness of the pipe and Re_D is the Reynolds number based on the inside pipe diameter. Because of its transcendental nature, equation (17) required an iterative type solution.

For laminar flow, i. e., Re_D less than approximately 2300, the Darcy-Weisbach friction factor is found to be

$$f = \frac{64}{Re_D} \quad . \tag{18}$$

(d) Bend Losses

Pressure losses due to bends are the result of viscous losses in the main flow plus losses in the secondary flow caused by the bend. These losses are a function of the radius of the bend and the bend angle. The loss coefficient, C, for bends and elbows of 90° was obtained from data by K. H. Beij (42) as presented by V. L. Streeter (43). For bends other than 90°, the loss coefficient was assumed to be proportional to the ratio of the bend angle of the pipe to a bend angle of 90°. For angles less than 90°, Smith (44) shows that this is very nearly true. However, for bend angles greater than 90° the analysis is conservative. In addition to the loss due to the bend, the loss due to the viscous effects must also be included so that the equation used was

$$\Delta P = \left(\frac{C\theta}{\pi/2} + f\ \theta\ \frac{r}{D} \right) \frac{\rho\ \overline{V}}{2g_c} \tag{19}$$

where ΔP is the pressure drop, C is the loss coefficient due to the bend, θ is the bend angle, f is the Darcy-Weisbach friction factor as determined by equation (12), r is the bend radius, D is the inside pipe diameter, ρ is the fluid density and $\overline{V}$ is the downstream mean fluid velocity.

(e) Arbitrary Losses

Frequently data is available or can be experimentally determined whereby a loss coefficient to be used in equation (9) can be found. This section was added to the study so that the analysis would be as general as possible. The pressure drop was computed by equation (9) where the loss coefficient K was determined by one of three general equations as a function of one of three variables. These variables were:

1. Reynolds number based on diameter
2. Mass flow rate
3. Cross section area

The particular equations for the loss coefficient K were:

1. $K = AX^B$
2. $K = A + B \ln X$
3. $K = A + BX + DX^2 + GX^3$

where K is the loss coefficient, A, B, D, and G are arbitrary constants obtained from a curve fit of loss coefficient data and X is one of the variables listed above.

With this analysis, components such as valves, where the loss coefficient as a function of flow area or Reynolds number, may be incorporated into the system.

(f) Flexible Hose Losses

Frequently dynamic flow systems utilize flexible metal hoses as components in the system. Equation (6) was used to determine these losses.

(g) Losses in Parallel Lines

Flow in parallel lines is characterized by the fact that the pressure drop across the lines must be the same. However, due to

possible different configurations and properties of the lines, the flow rates through the respective pipes may be considerably different.

In the analysis of this flow, two different geometries were considered with an arbitrary number of lines in each geometry.

The method of solution consisted of assuming that a fraction of the total flow went through the pipes of one geometry and the remainder of the flow went through the pipes of the other geometry. The pressure drop across each was then calculated according to equations (15) and (17). The fraction of flow through the respective pipes was then adjusted until the pressure drop across each was equal.

The relationships for pressure drop discussed previously were programmed for solution on a digital computer. This program is presented in Appendix B.

The analysis of a given system was accomplished in the following manner. The individual components in the system were numbered in sequence beginning with the exit of the system. A code was provided to relate the pressure drop relations with the order of solution of the components. Beginning at the exit of the system, and specifying a constant mass flow rate, the static pressure drop across the first component was computed according to the appropriate relation presented above. This pressure drop was then summed with the downstream pressure to obtain the pressure upstream of the component. From this pressure, a density and hence a velocity can be computed for use in determining the pressure drop in the next component. For components where the pressure drop is based upon an upstream velocity and density, such as the flexible hose, an iterative procedure was employed to determine the upstream conditions.

By adjusting the density of the fluid as the analysis progresses up the system, compressibility effects of the gas were included. For example, in long pipes, where the pressure drop is large, the pipe would be broken into a series of short sections so that the compressibility effects could be accounted for more accurately.

After analyzing each component, the static pressure at that point in the system, the pressure drop across that component, and the component number were printed. After analyzing the entire system for a given flow rate, the pressure drop across the system and the mass flow rate were printed. In addition, comments were printed when an iterative procedure within the program did not converge.

A schematic of the system that was studied is shown in Figure 16. This system was selected as a model for two reasons. It was readily available for testing with very little modification, and it possessed most of the components found in flow systems. These components are listed below in order of their occurrence in the system.

1) abrupt expansion
2) straight section
3) abrupt contraction
4) straight section
5) abrupt expansion
6) straight section
7) arbitrary configuration (valve)
8) straight section
9) flexible metal hose
10) straight section
11) abrupt contraction
12) abrupt contraction
13) parallel flow
14) abrupt expansion
15) straight section
16) arbitrary configuration (valve)
17) arbitrary configuration ("T")
18) flow meter
19) arbitrary configuration (valve)

20) arbitrary configuration ("T")
21) arbitrary configuration ("T")
22) straight section
23) arbitrary configuration (pressure regulator)
24) straight section
25) elbow
26) straight section
27) elbow
28) straight section
29) elbow
30) straight section
31) elbow
32) straight section
33) arbitrary configuration (valve)
34) arbitrary configuration ("T")
35) straight section
36) elbow
37) straight section
38) elbow
39) straight section
40) elbow
41) straight section
42) elbow
43) straight section
44) arbitrary configuration (valve)
45) straight section
46) elbow
47) straight section
48) elbow
49) straight section
50) abrupt contraction

Loss coefficients and relative roughness factors for the above components were taken from standard literature sources when available. However, the loss coefficient for the flow meter and the pressure regulator required experimental evaluation.

In addition to the analysis just described, a subsidiary analysis was performed on the pressure vessel supplying air to the system by predicting the pressure history of the tank as it vented through the test line. The purpose of this analysis was two-fold. It served to validate the predicted pressure drop through the system and tested the applicability of using the steady state pressure drop prediction for some

transient conditions.

The differential equation relating the pressure in the tank with time was derived by considering the equation of state of the gas,

$$P\tilde{V} = M\tilde{R}T, \tag{20}$$

where P is the tank pressure, $\tilde{V}$ is the tank volume, M is the mass of the gas in the tank, $\tilde{R}$ is the gas constant, and T is the gas temperature.

It was assumed that the expansion of the gas followed a polytropic process such that the pressure temperature relation was

$$\frac{T}{T_o} = \left(\frac{P}{P_o}\right)^{\frac{n-1}{n}}, \tag{21}$$

where T is the temperature of the gas, P is the gas pressure and n is the polytropic exponent. The zero subscript indicated initial conditions.

From equations (20) and (21), the following relation was derived:

$$\frac{dP}{dt} = n\left(\frac{\tilde{R}T_o}{\tilde{V}}\right)^{n}\left(\frac{\tilde{V}}{\tilde{R}T}\right)^{n-1}\left(\frac{P}{P_o}\right)^{n-1}\dot{m}, \tag{22}$$

where $\frac{dP}{dt}$ is the pressure change with time and $\dot{m}$ is the mass flow rate. The derivation of equation (22) is presented in Appendix C.

In order to solve equation (22), a relationship expressing the mass flow rate, $\dot{m}$, as a function of tank pressure, P, was obtained by curve fitting the pressure drop versus mass flow rate prediction determined by the preceding analysis.

The polytropic exponent, n, is a function of the heat transfer to the gas and had to be determined experimentally. In a preliminary blow-down of the tank, it was found that polytropic exponent was approxi-

mately 1.06. However, since n is basically a function of the heat transfer to the gas from the tank, it was reasoned that for a short period of time after venting began, the process was essentially adiabatic, due to the fact that temperature difference between the gas and the tank would initially be small. As venting continued, this temperature difference would become greater, increasing the heat transfer, and thus decreasing n to the value obtained experimentally.

It was decided, therefore, to approximate n, as a function of time, by the equation

$$n = 1.06\ (1 + 0.34e^{-0.1t}). \tag{23}$$

Equation (22) was solved numerically by using a Runga-Kutta method of solving differential equations.

III. EXPERIMENTAL

A. Selection of Equipment

The guiding philosophy in the selection of the instrumentation was founded on the premise that it should be capable of handling both static and medium transient flow conditions, that it should be compatible with the equipment owned by the Department to expedite maintenance, that it should accommodate the range of pressures, flow rates, etc., that were anticipated during the course of this study.

The selection procedure led to procurement of a four channel Sanborn 150 series recorder with three carrier and one DC preamplifiers; a Cox Instrument system consisting of two turbine type flow meters, a manifolding system, and a mass flow rate meter with pressure correction adjustments; a digital voltmeter; a frequency meter owned by the Department; and three Pace Engineering pressure transducer kits. This equipment was then integrated into the data acquisition system described in greater detail in the section on data acquisition and reduction in this report.

B. Description of Experimental Facility

In order to implement phase three of this research effort a flow system was constructed to provide a means of obtaining data on flow through flexible tubing and through tubing-fitting systems of various configurations.

The flow system was divided, for convenience, into two sections, a supply section and a measurement section. The air compressors, dryer, storage tanks, surge tanks and associated piping form the supply section while the plenums, test length, instrumentation, and pressure regulator comprise the measurement section. The layout and details of both sections

are shown in Figures 9-13. The primary component of the supply section is the 2000 cubic foot supply tank. The compressors, surge tanks, dryers and associated equipment exist to furnish dry air at about 120 psia to the supply tank which has a pressure rating of 150 psia. The measurement section's main components are the pressure regulator, flow meter, recording instrumentation, transducers, and test section. Important in the design of the measurement section is the provision of inlet lengths of smooth pipe prior to the convoluted test section. These sections of pipe were chosen to have an L/D ratio of 40 for each diameter of the flexible coupling to be tested in order to insure that fully developed flow exists at the entrance to the test section. This choice of inlet lengths is in accordance with the findings of Nikuradse as discussed by Schlicting (3). By the provision of entrance lengths any pressure drop which might be ascribed to the developing flow in the test section is eliminated.

There was enough flexibility designed and built into the system to allow measurements to be made conveniently on a variety of tubing and tubing-fitting configurations. A special capability is the ability of the measurement section to accommodate tubing sections under various degrees of lateral bending.

C. Procedures for Data Acquisition and Processing

(1) Flexible Tubing

The improved correlation equation (6) was used to calculate the lengths of flexible connectors that would be required for a comprehensive experimental effort. In order to insure the availability of data covering the full range of the phenomena involved, the non-dimensional parameters FN1 and FN2 were used as experimental independent

variables in the selection of test sections. These geometrical parameters, as well as Reynolds numbers and pressure drops, were calculated for flexible connectors of several manufacturers and for diameters from 1/4 inch to 2 1/2 inches, using equation (6). Twelve sections were chosen on this basis and were ordered directly from the manufacturers. Each of these sections were provided with pressure taps as shown in Figure 13. As indicated in Figure 11, the data recorded for each section were:

(a) Length, manufacturer and geometrical characteristics of the section.

(b) Pressure and temperature at the flow meter.

(c) Flow meter indication.

(d) Pressure at entrance to the section.

(e) Pressure difference between the ends of the section.

(f) Ambient pressure and temperature.

The dimensions of each section are taken from manufacturer's information and from laboratory measurements.

All pressures are measured with water and mercury manometers and with Pace transducers whose output, along with that of the flow meter, was directed to the Sanborn 150 Series four channel pre-amplifier and recorder console. It was found necessary, for reasons of accuracy, to also read the flowmeter output directly with a CMC Model 200B frequency counter. This information is converted to a volumetric flow rate by a special calibration curve provided by the manufacturer. The air stream temperature was measured by a thermocouple and recorded manually.

A typical data sheet is shown as Appendix B. This raw data was

reduced entirely by digital computer operations. At the start of each series of test runs a set of data called "The Calibration Run" is obtained. Analysis of this data generated a pressure-voltage output relationship for the pressure transducers. After the calibration run was made, general test runs were made on various test sections and with various flow rates.

By use of the pressure-voltage relation obtained from the calibration run, the voltage readings from each of the transducers were converted directly to psi values. Using a relationship developed from information obtained from the flow meter manufacturer, the flow meter frequently readings were converted directly to volumetric flow rate.

The product of density and volume flow rate produces mass flow rate. The mean velocity of the stream is obtained by dividing the mass flow rate by the product of the density and the cross-sectional area of the test section. Knowing the velocity density, and temperature of the flow enables the calculation of the Reynolds number. This is accomplished by means of a temperature dependent viscosity relationship for air developed from standard references.

Friction factor is calculated by the formula:

$$f = \frac{D}{L} \quad \frac{\Delta P}{\rho V^2/2g_c} \quad .$$

An entrance section study was initiated to determine the effects and characteristics of the developing velocity profile in a section of flexible tubing. Pressure taps were spaced logarithmically down the length of a tube as shown in Figure 14 and data were recorded with the apparatus indicated in Figure 15.

(2) Arbitrary Flow Systems

In order to substantiate the procedure for predicting the pressure drop in arbitrary flow systems, the results of the analysis required verification by experimentation.

A schematic of the apparatus used for this experimentation is presented in Figure 16. The components making up this system were; two plenum chambers, one globe valve, four gate valves, two tees, a turbine flow meter, a pressure regulator, a section of flexible metal hose, ten elbows, and twenty straight sections. This system was supplied with air, at a maximum pressure of 150 psig, from a 2000 cubic feet storage vessel.

The experimental phase of the study was broken down into three areas. The first phase consisted of obtaining pressure drop data on those components of the system where the information was not available in the literature. The second and third phases dealt with verifying the predicted pressure drop.

Phase I.

Although pressure drop coefficients can be found in the literature for most components in the system, this information was not available for the flow meter or the pressure regulator. Therefore, in order to perform the analysis, these coefficients had to be determined experimentally.

As mentioned previously, the flow measuring equipment consisted of a one inch turbine type flow meter, Model number GL16, and a two and one-half inch turbine flow meter, Model number GL40, furnished by Cox Instrument Company. Depending on the volumetric flow rate, the flow was diverted from one flow meter to the other by a solenoid controlled,

pressure operated, gate valve.

For low volumetric flow rates, less than 44 cfm, the air flowed through the one inch flow meter. At greater flow rates, it went through the two and one-half inch meter.

In order to obtain the required loss coefficients, the following data was required:

1) pressure drop across the flow meter
2) absolute pressure downstream of the flow meter
3) volumetric flow rate
4) air temperature

The required pressures were obtained from either a thirty inch water manometer or a ten foot mercury manometer, depending on the pressure range. Volumetric flow rates were obtained from the flow meter in the form of turbine speed. This speed, in cycles per second, was converted to volumetric flow rate by a calibration curve furnished by the flow meter manufacturer. A copper-constantan thermocouple was used to determine the temperature of the gas stream.

The data were reduced by a computer program in order to obtain an effective Darcy-Weisbach friction factor, f, for the flow meter.

The determination of the pressure drop characteristics of the pressure regulator presented a problem in that the pressure drop was not only flow dependent but also was a function of the regulator setting. This problem was eliminated by adjusting the pressure regulator at its maximum setting which was higher than the supply pressure. At this condition, the regulator acted only as a flow constriction and did not regulate the pressure.

As in the case of the flow meter previously discussed, the re-

quired measurements were the pressure drop across the regulator, the downstream pressure, the volumetric flow rate, and the temperature. The density, ρ, of the fluid was found from the pressure and temperature, using the perfect gas equation of state. From the density of the gas, the volumetric flow rate, and the cross sectional area of the pipe, an average velocity was determined. These were used to determine the loss coefficient for the regulator.

Phase II.

The second phase of experimentation on the system was concerned with validating the predicted pressure drop. Only part of the total piping system was used in this test; that portion from the flow meter to the exit. There were two reasons for this choice of test section; existing pressure taps were available at the flow meter and the major pressure drop in the system occurred in this section.

The information sought in this test was the pressure drop through the test section as a function of the mass flow rate of air. This would be compared with the predicted pressure drop in order to ascertain the accuracy of the analysis.

The pressure immediately upstream of the flow meter was determined with the use of the ten foot mercury manometer previously discussed. This gage pressure represented the pressure drop through the system since the test section was exhausting into the surrounding atmosphere.

The volumetric flow rate was determined in a manner previously discussed, measuring the speed of the turbine and converting to flow rate by the use of calibration curves. The mass flow rate was obtained by

multiplying the volumetric flow rate by the density of the air. This density was calculated from the perfect gas equation of state.

Phase III.

The final phase of testing was that of validating the pressure history prediction of the supply tank during venting. The information required from this test was the pressure in the supply tank, and the temperature of the air as a function of time.

The pressure in the tank was measured with a 0-100 psig diaphram type pressure transducer with an error of less than 1 psi. The output from the transducer was recorded on a Sanborn, two channel, strip chart recorder as a function of time.

The temperature of the air in the tank was required in order to estimate the polytropic exponent of the expansion process. This temperature was measured with a copper-constantan thermocouple inserted in the exhaust line six inches from the supply tank. The output voltage from the thermocouple was amplified and then recorded on the strip chart recorder. This was then converted to temperature with the use of calibration charts.

After calibrating the various measurement devices in the system, the test was initiated by suddenly opening a valve and allowing the tank to vent to atmosphere. During venting, the test variables discussed above were continuously recorded on the strip charts.

IV. RESULTS

A. Empirical Equation

The results of the research study may be summarily expressed as the development of an empirical equation which makes an approximation to the friction factor variation as a function of Reynolds number for various cross-sectional geometries of flexible corrugated connectors. The generalized nature of this equation - equation (6) - makes extension to various commercially available hoses a relatively simple matter. The comparison of the equation with experimental observations for hoses of various manufacturers indicates the validity of extending the equation to other geometries.

B. Experimental Results

(1) Flow Through Convoluted Tubing

The experimental data collected in this study for flow through flexible tubing were plotted on logarithmic coordinates and are presented in Figures 17 through 22. The data are arranged according to the diameter of each section tested and the values of the dimensionless parameters FN1 and FN2 are given for each diameter. The ranges of the parameters, FN1 and FN2, and Reynolds number covered in this study were:

$$0.0133 \leq FN1 \leq 0.0448$$

$$0.0568 \leq FN2 \leq 0.1250$$

$$1.84 \times 10^4 \leq Re \leq 9.83 \times 10^5$$

Three separate test runs were made on each section of hose and the data from all three runs are plotted in the figures.

The data collected show an increase in friction factor similar to the data of Pepersack. This increase began at a Reynolds number of

about 1 x 10^5 which also supports Pepersack's findings. In Figures 23 through 25, Pepersack's curves and the data of this study are plotted for flexible hose having approximately the same values of the parameters, FN1 and FN2, and for flexible hose of the same diameter and manufacturer. It is seen that, in all cases, Pepersack's curves level off at a lower value of friction factor than does the data of this study. It is also noted that the data of this study compare more favorably with Pepersack's curves having approximately the same values of the parameters FN1 and FN2 than with Pepersack's curve of the sections having the same inside diameter and manufacturer as the sections tested in this study. It can be concluded from this that, even though the data of this study differs somewhat from Pepersack's data, the parameters FN1 and FN2 are significant dimensionless quantities forming a worthy basis for comparison of data on pressure drop in flexible metal hose.

It is significant to note in comparing the data of this study with Pepersack's curves that not only were higher values of friction factor obtained after transition, but also a wider range of Reynolds numbers is involved in the transition. In most cases Pepersack's transition occurs from Reynolds numbers of about 1 x 10^5 to 2.5 x 10^5 while the transition indicated by this study takes place from Reynolds numbers from about 1 x 10^5 to 7 x 10^5.

An informal series of tests were made on several of the test sections in which temperatures were measured. Thermocouples were inserted into the convolutions from the outside and the tube was wrapped with masking tape. These preliminary, random results are shown in Figures 26 through 30. The unusual longitudinal temperature distributions are dis-

turbing. The flow should be closely approximated by Fanno type flow in which the stagnation (total) temperature is constant. No explanation is immediately apparent for this phenomena.

(2) Flow Through Arbitrary Systems

Flow Meter Loss Coefficient

At flow rates less than 44 cfm, where the flow was diverted through the one inch diameter flow meter, the Darcy-Weisbach friction factor, f, was found to be approximately 6.0. With the system operating with the two and one-half inch diameter flow meter, flow rates greater than 44 cfm, the friction factor was approximately 0.01. These values were found to be somewhat flow dependent but the variation was relatively small. Therefore, they were taken to be constant.

Pressure Regulator Loss Coefficient

The loss coefficient, K, for the pressure regulator is shown in Figure 31. Here the loss coefficient is plotted on logarithmic co-ordinants as a function of Reynolds number, Re_D. From the figure it is seen that the loss coefficient is very large and is highly flow dependent.

In order to use these results in the analysis, a functional relationship for K was required. It was noted that on the logarithmic co-ordinants, K was approximately a linear function of the Reynolds number. Therefore, a first degree exponential function would approximate the data. This relationship was found to be

$$K = 3.65 \times 10^{11} \, Re_D^{-1.84}, \text{ for } 2 \times 10^4 \leq Re_D \leq 2 \times 10^5. \qquad (24)$$

System Pressure Drop

The pressure drop in the portion of the system from

the flow meter downstream to the exit is presented in Figure 32. The pressure drop is plotted as a function of the mass rate of flow. Also shown in Figure 32 for comparison purposes is the predicted pressure drop described in the previous section. As can be seen from the Figure 4, the predicted pressure drop agrees closely with the measured pressure drop except at very low flow rates, where the error is approximately 25%. However, it should be noted that the one inch diameter, ten foot long flexible metal hose in the line produces the major pressure drop in the system, and, at the low flow rates, the accuracy of the friction factor equation for the hose is 30%. Thus, the majority of the error in this region could be due to the pressure drop prediction in the hose.

At the higher flow rates, greater than 0.1 lbm/sec, the error is on the order of 4 - 5%. Thus, the pressure drop prediction agrees very closely with the measured pressure drop throughout the major portion of the flow range.

System Blowdown

In the final phase of testing, the storage tank was allowed to vent through the test system. The pressure history of the tank during blowdown and the predicted pressure history obtained from the analysis discussed are shown in Figure 33. As can be seen in Figure 33, very good agreement was obtained between the predicted and the actual pressure drop with a maximum deviation of less than 2%. At the end of the 600 seconds the deviation was 0.8% which was less than the 1% accuracy of the pressure transducer.

In testing, it was found that the pressure drop through the test line was dependent on the fluid temperature. This presented a

problem in that the temperature was constantly changing during venting and the analysis of the pressure drop prediction was based on an isothermal assumption. Although a mean temperature of the fluid during venting was used in the prediction, some error would be introduced. The longer the blowdown period, the greater would be the temperature drop and hence the greater this error would become.

Based upon the close agreement that was found between the predicted and experimentally determined pressure drop, it is concluded that the pressure drop of a compressible fluid in an arbitrary flow system may be adequately determined by the method presented in this study. In addition to being used for the steady state case, on which the analysis was based, the results indicated that the method could also be applied to slow transient or quasi-steady conditions, such as a tank blowdown, which are characterized by relatively slow pressure changes on the order of 3 psi per minute.

V. Conclusions and Recommendations

A. Conclusions

The following conclusions may be drawn from the results of this study:

1. A reasonable approximation to the friction factor for convoluted flexible metal hoses of various geometries may be obtained from the correlation equation (equation 6) generated during the course of this work. The equation does have physical limitations but appears valid for diameters greater than 3/4" with conventional shaped convolutions.

2. A method of analyzing the steady state and quasi-steady state flow characteristics of a system of tubing and fittings has been generated which includes flexible metal hoses.

3. Observation of the significant increase in friction factor at a Reynolds number of the order of 10^5 indicates that some type of secondary flow transition may occur in cavity wall type flow.

4. Significant entrance and exit effects have been noted.

B. Recommendations

1. Further consideration should be given to obtaining velocity distributions in flows of the type encountered in cavity wall flow.

2. Further investigation of the development of a better correlation equation should be undertaken.

3. Unsteady flow in a system incorporating flexible metal hoses should be undertaken.

4. Attention should be given to techniques of instantaneous velocity measurement without introducing probes into the stream.

LIST OF REFERENCES CITED

1. Belcher, J. G. 1964. Pressure drop in Flexible Metal Hoses, Bellows, and Gimbal Joints. - An Annotated Bibliography. Brown Engineering Company Report No. ER - 1174. (Prepared under Contract NAS8-11166.)

2. Pepersack, F. J. 1960. Pressure Losses in Flexible Metal Hose Utilized in Propulsion Fluid Systems of XSM - 68B and SM - 68B. Technical Memorandum Baltimore 25-10, Martin - Baltimore.

3. Schlicting, H. 1960. Boundary Layer Theory. Fourth Edition. McGraw-Hill, New York. Page 502.

4. Colebrook , C. F. 1939. Turbulent flow in Pipes with Particular Reference to the Transition Region Between Smooth and Rough Pipe Laws. Journal of the Institution of Civil Engineers. 133-156, Paper No. 5204.

5. Pai, S. 1956. Viscous Flow Theory, Vol. 1-Laminar Flow. D. Van Nostrand Company, Princeton, New Jersey.

6. Sparrow, E. M., S. H. Lin, and T. S. Lundgren. 1964. Flow Development in the Hydrodynamic Entrance Region of Tubes and Ducts. Physics of Fluids 7:338-347.

7. Moody, L. F. 1944. Friction Factors for Pipe Flow. ASME Transactions 66.671 -678.

8. Wieghardt, K. 1953. Erhöhung Des Turbulenten Reibungswiderstandes Durch Oberflachenstorungen. Forschungshefte Für Schiffstechnik 1, 65-81.

9. Kinsler, L. E. and A. R. Frey. 1962. Fundamentals of Acoustics. Second Edition. John Wiley and Sons, New York. 186-213

10. Seiferth, R. and W. Krüger. 1950. Überraschend hohe Reibungsziffer einer Fernwasserleitung. Zeitschrift V. D. I. 92:189-191.

11. Doenecke, J. 1964. Contribution À L' Étude de la Convection Forcée Turbulent le Long de Plaques Rugueuses. International Journal of Heat and Mass Transfer 7:133-142.

12. Nunner, W. 1958. Wärmeübergang und Druckabfall in Rauhen Rohren. VDI Forschungsheft 455.

13. Mobius, v. H. 1940. Experimentelle Untersuchung des Widerstandes und der Geschwindigkeitsverteilung in Rohren mit regelmässig angeordneten Rauhigkeiten bei turbulenter Strömung. Physik Zeitschrift 41:202-225.

14. Wiederhold, v. W. 1949. Uber den Einfluss von Rohrablagerungen auf den Hydraulischen Druckabfall. Gas - und Wasserfach 90:634-641.

15. Fromm 1923. Flow in rough pipes. Zeit. für Angew. Math. und Mech. 3, 339-358.

16. Fritsch 1928. Turbulent flow in pipes. Zeit. für Angew. Math. und Mech. 8, 199-216.

17. Feely and Riggle. Flow of fluids in small pipes. unpublished thesis, University of Pittsburg.

18. Kemler, E. 1933. A study of the data on the flow of fluid in pipes. ASME Transactions, 55.

19. Koch, R. 1958. Pressure drop and heat transfer for flow through empty, baffled, and packed tubes. VDI Forschungsheft 469.

20. Mobius, v. H. 1940. Experimentelle Untersuchung des Widerstandes und der Geschwindigkeitsverteilung in Rohren mit regelmässig angeordneten Rauhigkeiten bei turbulenter Strömung. Physik Zeitschrift 41:202-225.

21. Wieghardt, K. 1953. Erhöhung Des Turbulenten Reibungswiderstandes Durch Oberflachenstorungen. Forschungshefte Für Schiffstechnik 1. 65-81.

22. Hama, F. R. 1954. Boundary-layer characteristics for smooth and rough surfaces. Society of Naval Arch. and Marine Engineers. 62.333-358.

23. Baines, W. D. 1950. An exploratory investigation of boundary-layer development on smooth and rough surfaces. Ph. D. dissertation, State University of Iowa.

24. Moore, W. F. 1951. An experimental investigation of the boundary-layer development along a rough surface. Ph. D. dissertation, State University of Iowa.

25. Mills, R. D. 1965. On the closed motion of a fluid in a square cavity. Journal Royal Aero. Society 69,116-120.

26. Baturin, W. W. 1959. Lüftungsanlagen für Industriebauten. 2nd ed. Veb Verlag Technik, Berlin p. 187.

27. Roshko, A. 1955. Some measurements of flow in a rectangular cut-out. NACA TN 3488.

28. Mills, R. D. 1961. Flow in rectangular cavities, Ph. D. thesis, London University.

29. Linke, W. 1957. Stromungsvorgänge in Zwangsbelufteten Raumen. VDI Berichte 21.

30. Migay, V. K. 1962. The aerodynamic effectiveness of a discontinuous surface. Inzhenerno-Fizicheskiy Zhurnal, 5, 20-24. (AD602564)

31. Roshko, A. 1961. Experiments on the flow past a circular cylinder at very high Reynolds number. Journal of Fluid Mechanics, 10, 345-356.

32. Corrsin, S. and Kistler, A. 1954. The free-stream boundaries of turbulent flows. NACA TN 3133.

33. Clauser, F. H. 1954. Turbulent boundary layers in adverse pressure gradients. Journal Aero. Sci. 21, 91.

34. Laufer, J. 1954. The structure of turbulence in fully developed pipe flow. NACA Tr 1174.

35. Hinze, J. O. 1959. Turbulence. McGraw-Hill, New York.

36. Knudsen, J. G. and D. L. Katz 1958. Fluid Dynamics and Heat Transfer. pages 192-197, McGraw-Hill Book Co., Inc., New York.

37. Kono Beev, V. I. and Zhavoronkov, N. M., 1962, "Hydraulic Resistances in Tubes with Wavy Roughness", International Chemical Engineering, Vol. 2, No. 3.

38. Benedict, R. P., Carlucci, N. A., and Swetz, S. C., "Flow Losses in Abrupt Enlargements and Contractions" Journal of Engineering for Power, Trans. ASME, Vol 88, January 1966, p. 73.

39. Weisbach, "Mechanics of Engineering", Trans. E. B. Coxe, Van Nostrand Book Company, New York, N. Y., 1872, p. 821.

40. Nikuradse, J., Stromungsgesetze in Rauhen Rohren, V.D.I. Forschungsheft 361, Berlin, (1933).

41. Colebrook, C. F. "Turbulent Flow in Pipes, with Particular Reference To The Transition Region Between The Smooth and Rough Pipe Laws", Journal of the Institute of Civil Engineers, Vol. 11, (1938-1939).

42. Beij, K. H., "Pressure Losses for Fluid Flow in 90° Pipe Bends, J. Research Natl. Bur. Standards, Vol. 21, 1938.

43. Streeter, V. L., ed. "Head Losses Other Than Those of Boundary Resistance", Handbook of Fluid Dynamics, New York: McGraw-Hill Book Company, Inc.

44. Smith, A. J. W., "The Flow and Pressure Losses in Smooth Pipe Bends of Constant Cross Section", Royal Aeronautical Society Journal, Vol. 63, July 1963, p. 437-447.

45. Townes, H. W. 1965. Flow Over a Rough Surface. Ph. D. Dissertation - California Institute of Technology.

LIST OF OTHER REFERENCES

1. Haines, F. D. 1963. Comparison of the stability of Poiseuille Flow and the Blasius Profile for Flexible walls. Boeing Scientific Research Laboratories Report D1-82-0264.

2. Ritter, H. and L. T. Messum. Water tunnel Measurements of Turbulent Skin Friction on Six different compliant surfaces of 1 ft. length. Admiralty Research Laboratory Report ARL/N4/G/HY/9/7.

3. Benner, S. D. and G. K. Korbacher. 1964. The Coanda effect at deflection surfaces widely separated from the jet nozzle. University of Toronto UTIAS Tech. Note No. 78.

4. Kraichnan, R. H. 1963. Studies of the Direct - Interaction Approximation for turbulence. Contract Nonr-3999(00).

5. Powell, A. 1964. Fluid Motion and Sound. UCLA Engineering Department Report No. 64-61. Contract Nonr-233(62).

6. Weinbaum, S. 1965. Entropy Boundary Layers. Avco Corp. Research Report 207. Contract AF04(694)-414.

7. Mills, R. D. 1964. On the transfer of heat in a cavity at high and low speeds. Aeronautical Research Council Report 26049.

8. Plate, E. J. and V. A. Sandborn. 1964. An Experimental Study of Turbulent boundary layer structure. Final report on U. S. Army Research Grant DA-SIG-36-039-62-G24.

9. Laufer, J. 1954. The Structure of Turbulence in Fully Developed Pipe Flow. NACA TR 1174.

10. Hinze, J. O. 1959. Turbulence. An Introduction to its Mechanism and Theory. McGraw-Hill, New York.

11. Laster, M. L., "A Theoretical and Experimental Analysis of Length-wise Pressure Gradient for Flow of Air in Small Bore Tubing Considering the Effect of Elevated Temperature," MS thesis, Georgia Institute of Technology, Atlanta, Georgia, August, 1957.

12. Hall, Newman A., "Thermodynamics of Fluid Flow," Prentice Hall, Inc., New York, New York, 1951, p. 101.

13. Langhaar, H. L., "Steady Flow in Transition Length of Straight Tubes," Trans. ASME, vol. 64, 1942, p. A55.

14. Hearon, R. C., "Pressure Loss Measurements in Flexible Hose", Master's Thesis, Mississippi State University, 1965.

15. Rosenhan, A. K., "Correlation of Friction Factors for Flexible Metal Hose", Master's Thesis, Mississippi State University, 1965.

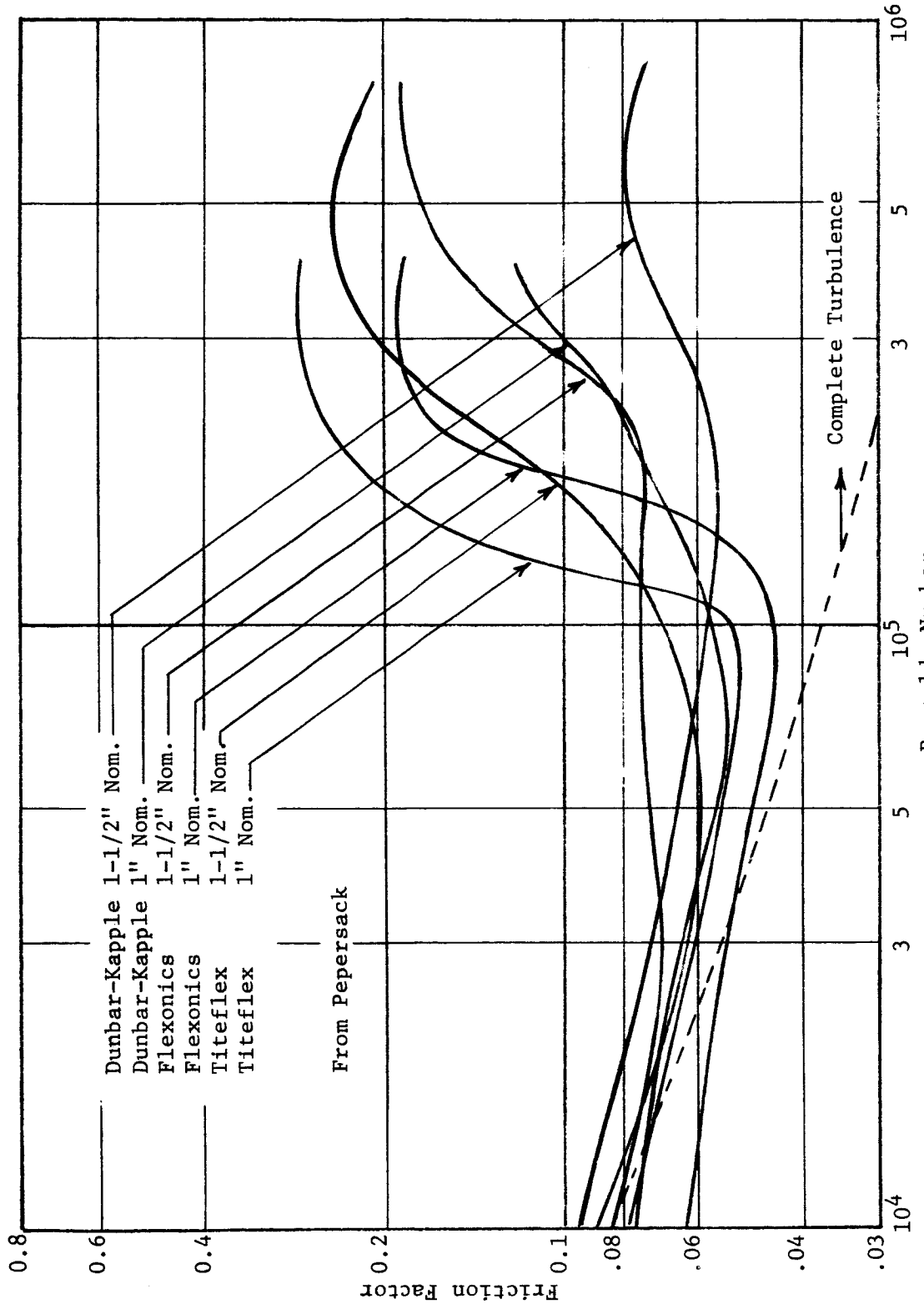

Figure 1. Friction Factors for Flow in Flexible Metal Hose According to Pepersack.

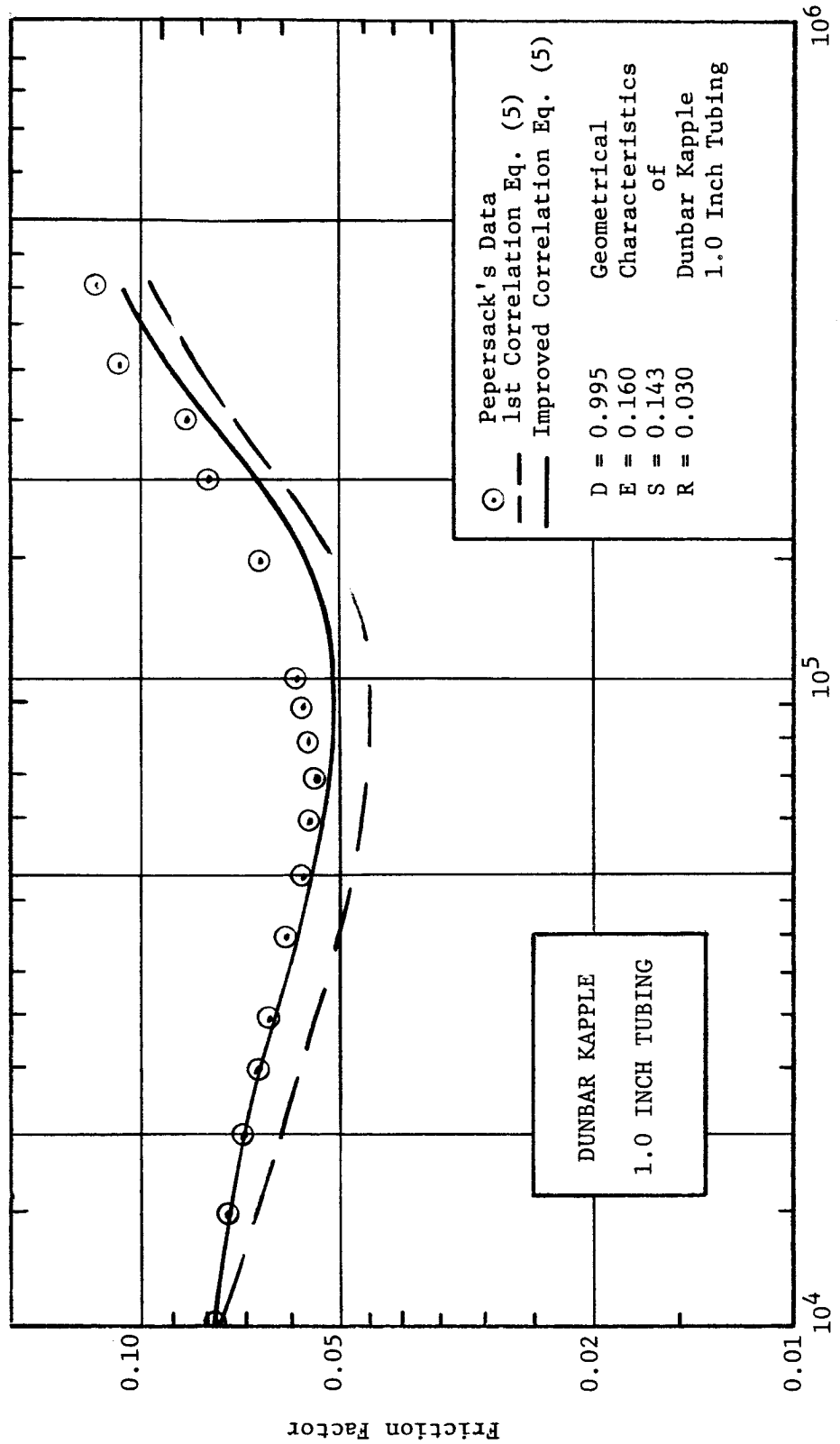

Figure 2. Comparison of Correlation Equations with Experimental Data.

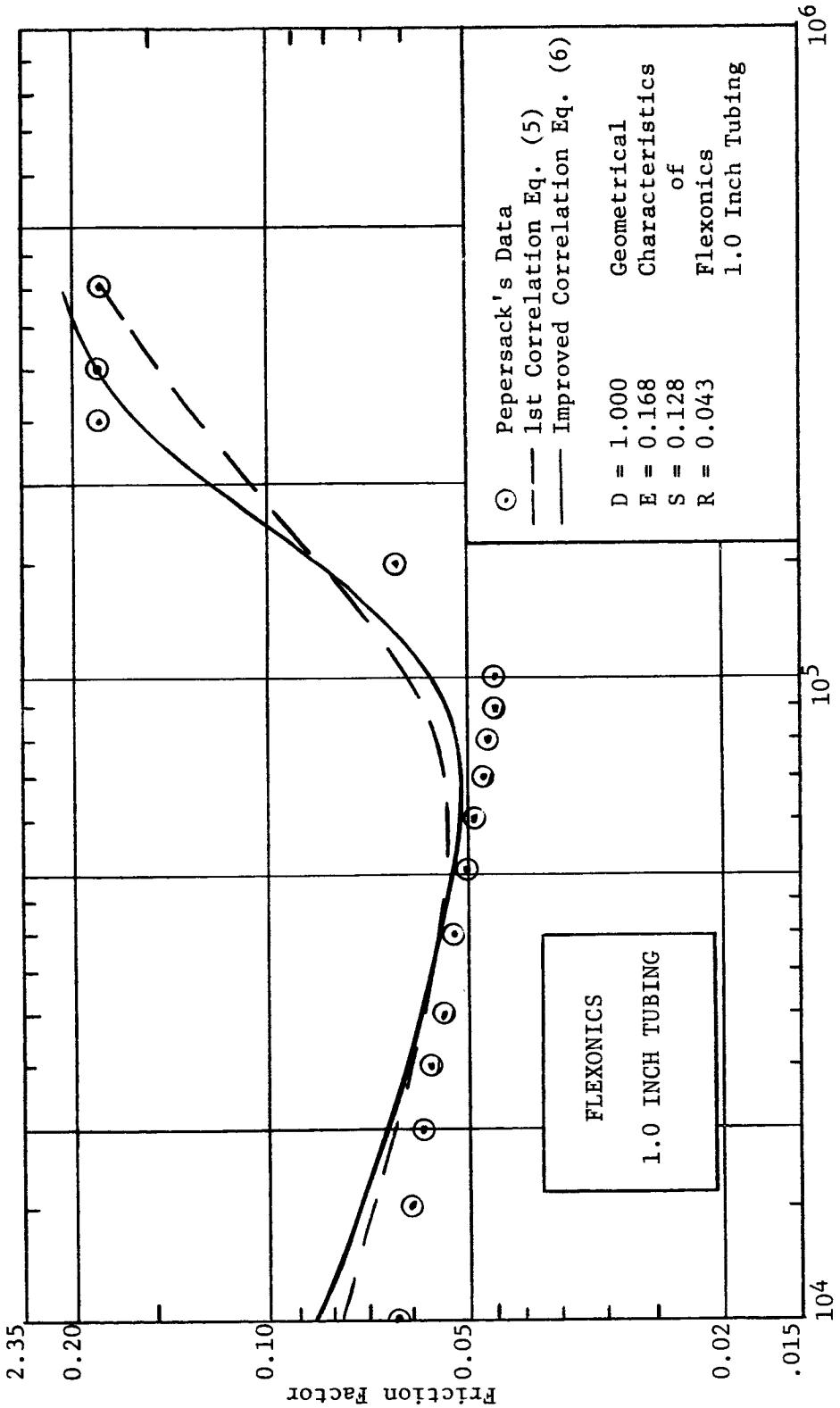

Figure 3. Comparison of Correlation Equations with Experimental Data

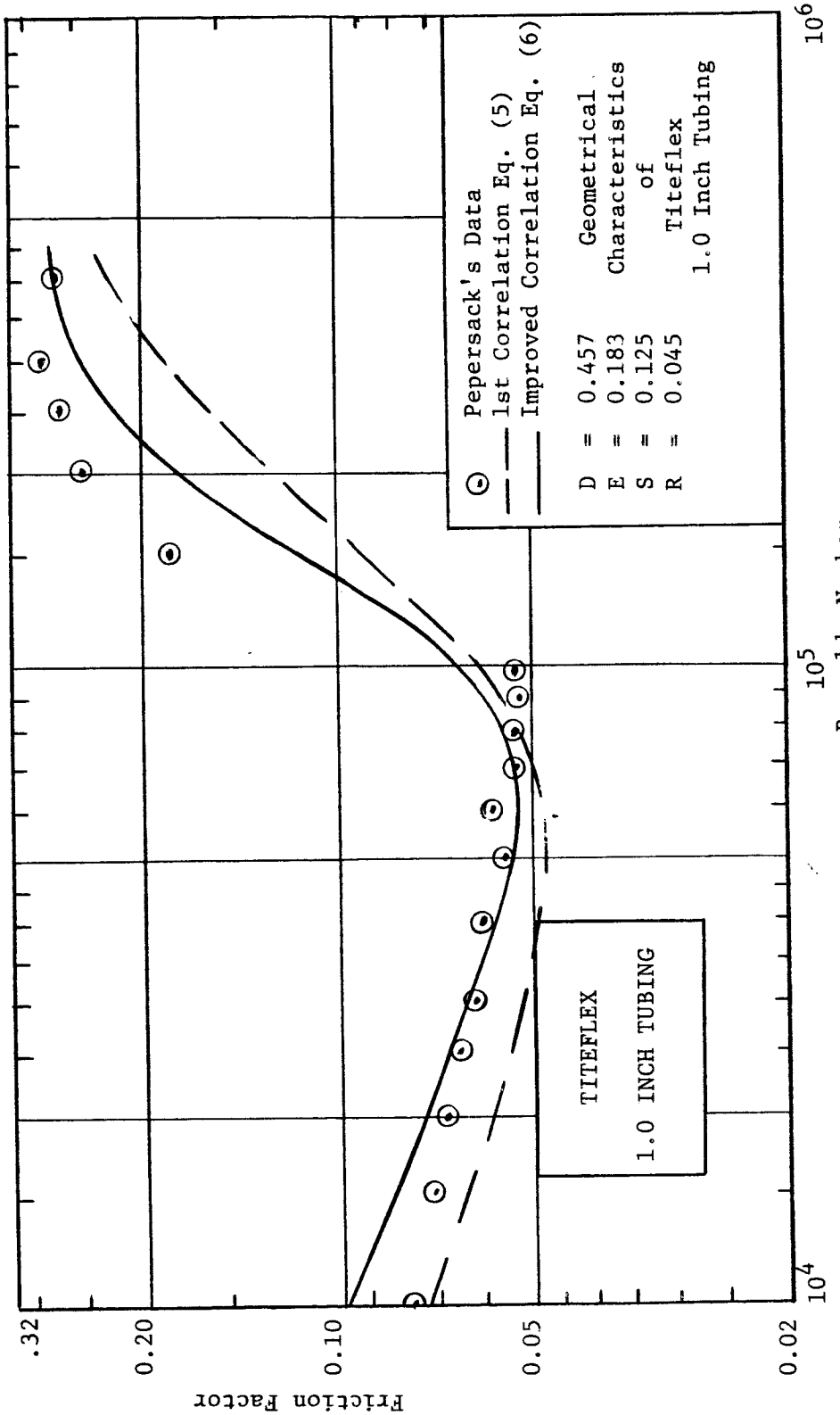

Figure 4. Comparison of Correlation Equations with Experimental Data

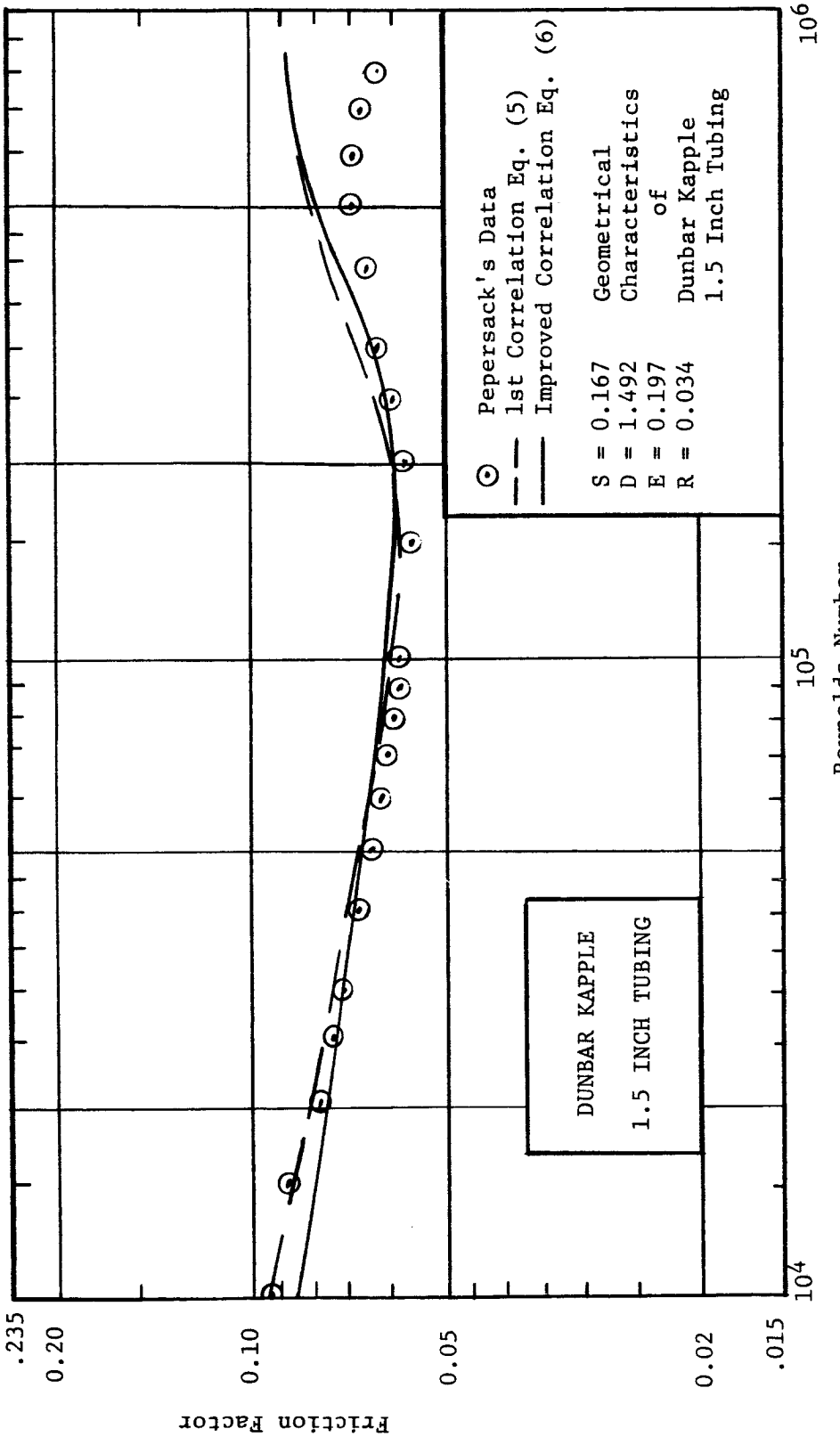

Figure 5. Comparison of Correlation Equations with Experimental Data

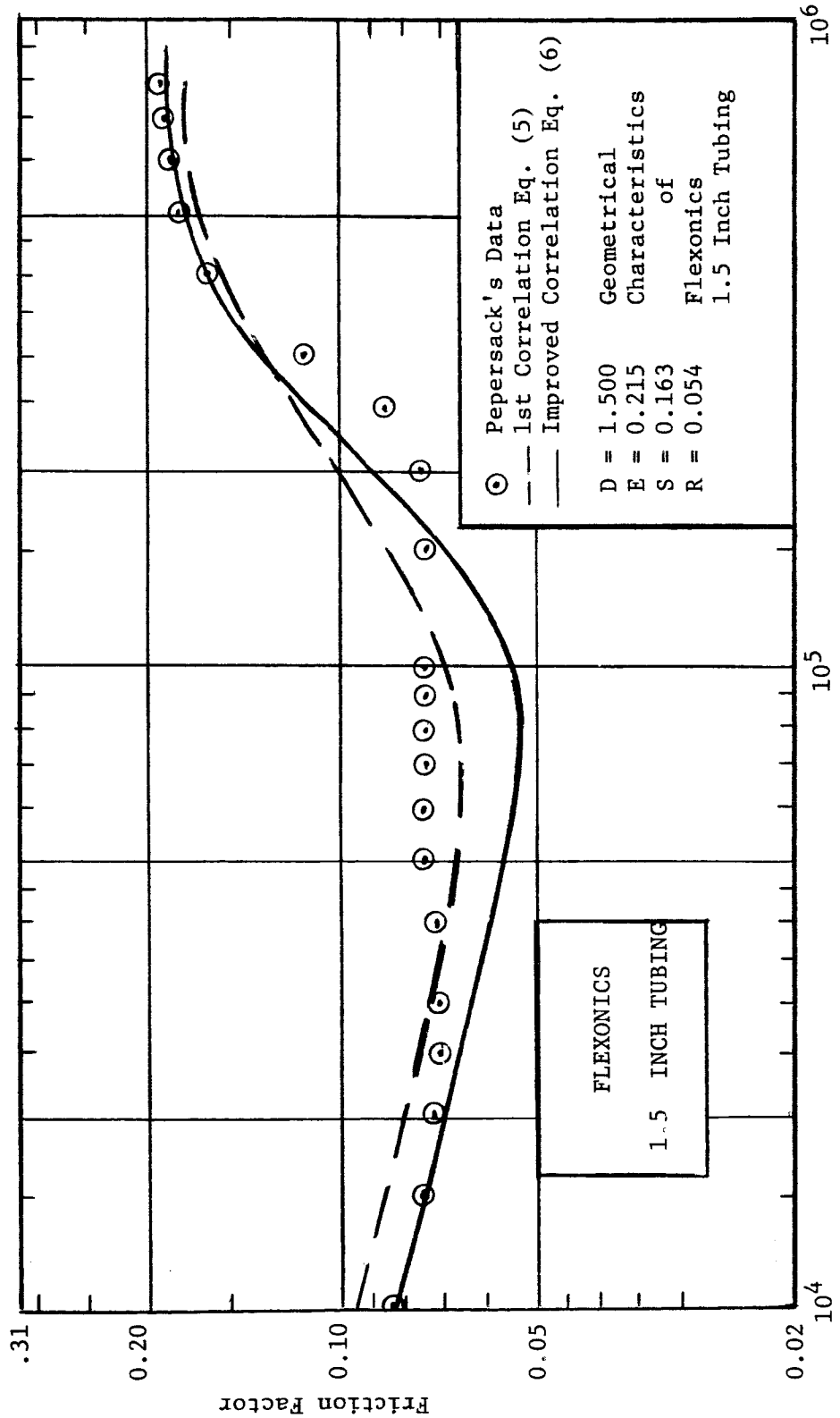

Figure 6. Comparison of Correlation Equations with Experimental Data

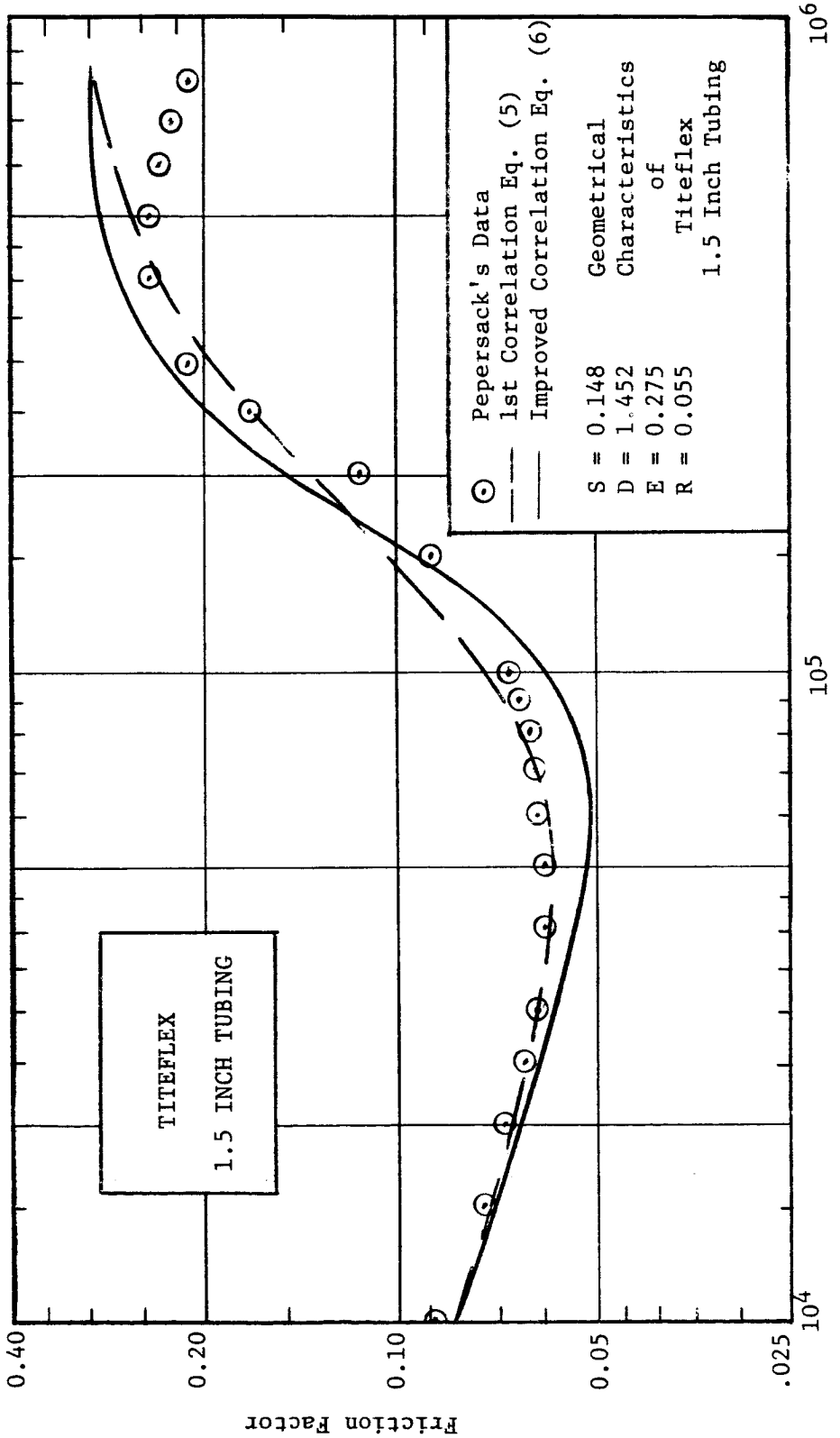

Figure 7. Comparison of Correlation Equations with Experimental Results

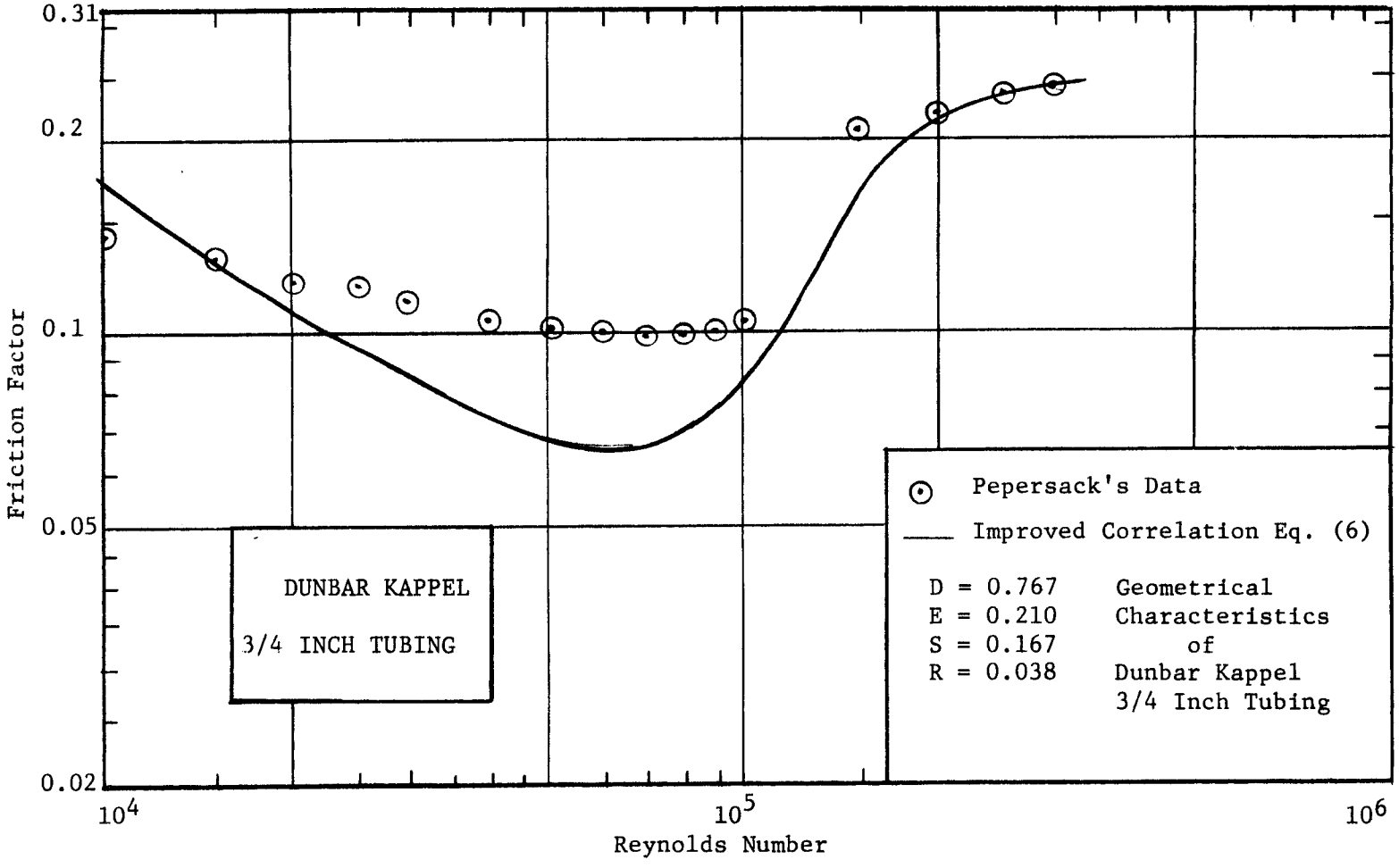

Figure 8. Comparison of Correlation Equation with Experimental Results

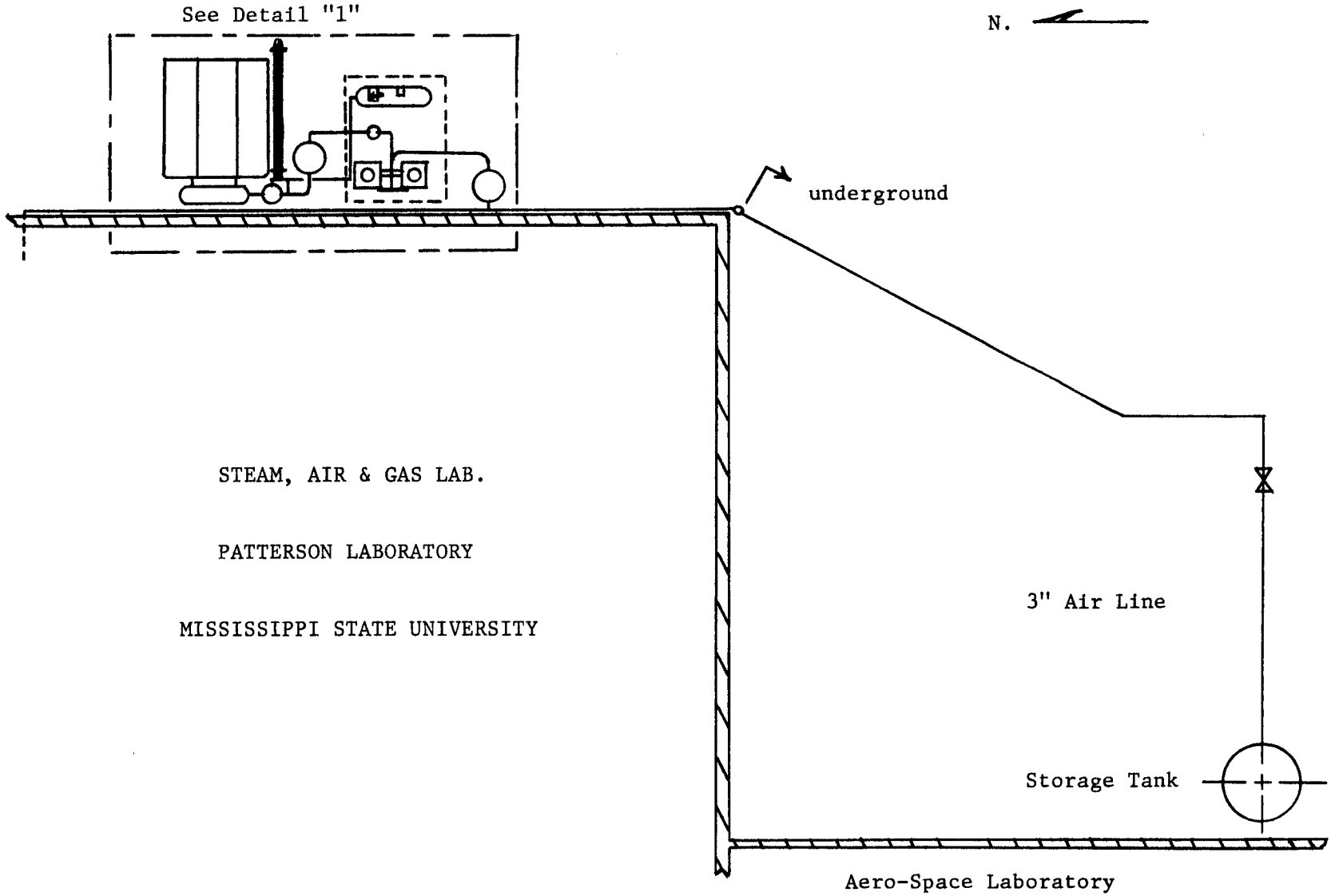

Figure 9. Supply Section

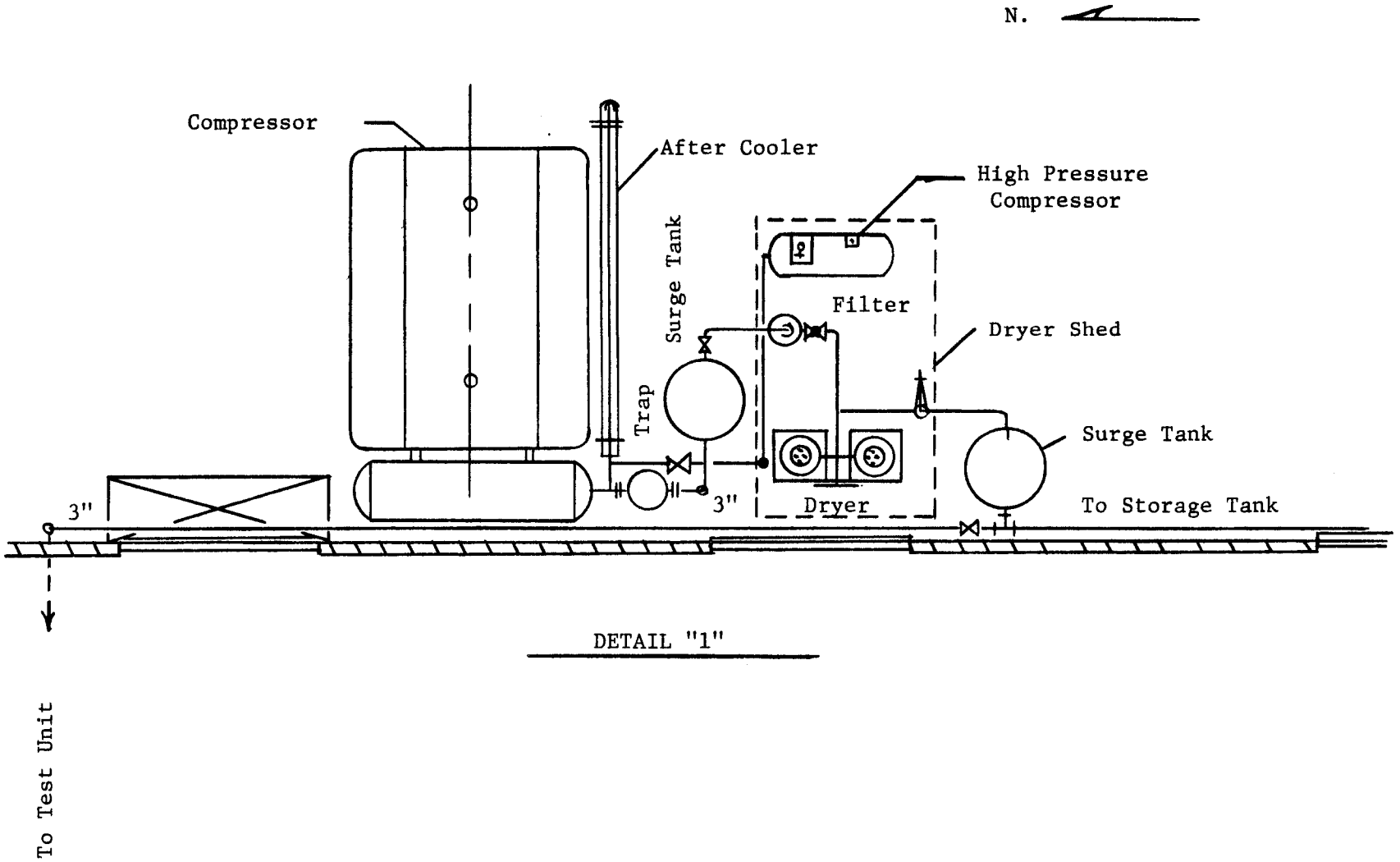

Figure 10. Supply Section Details

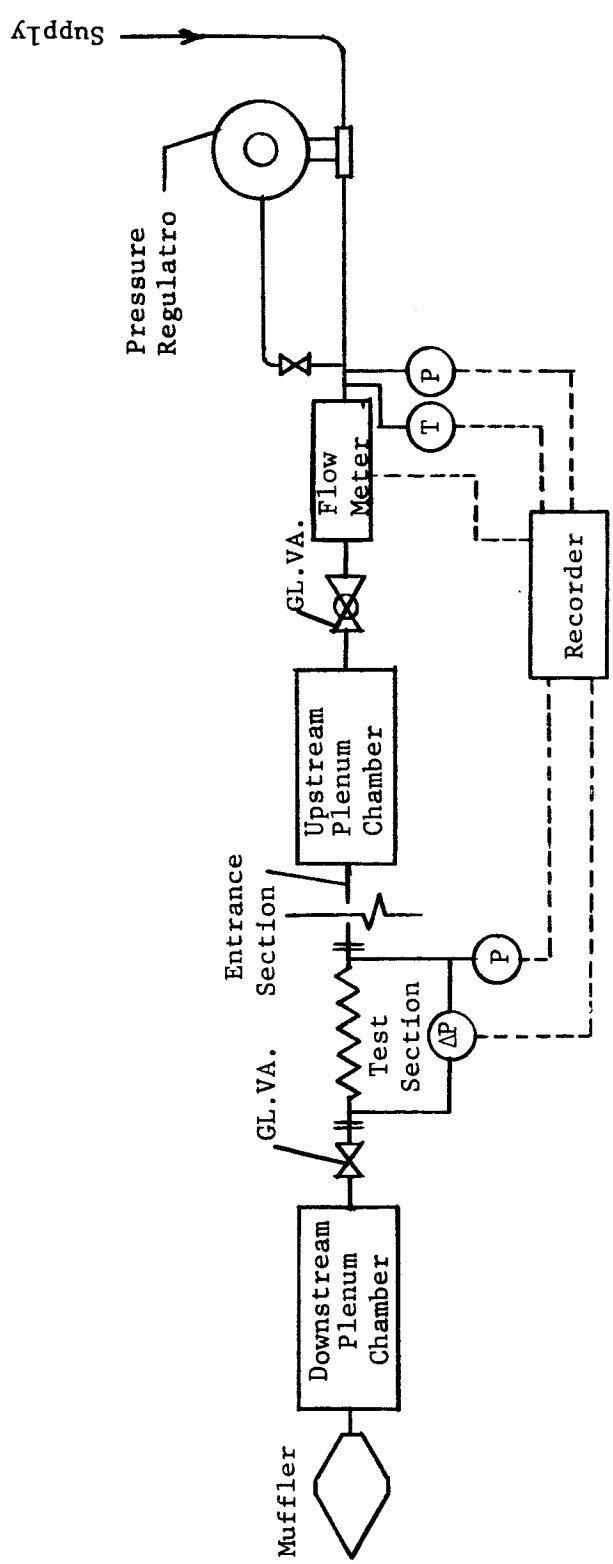

Figure 11. Measurement Section

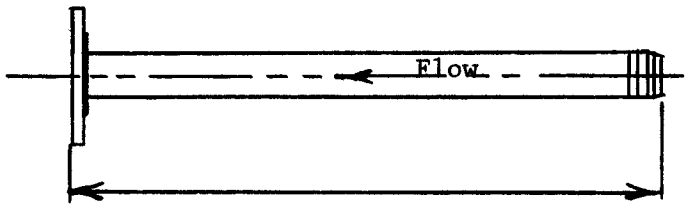

Upstream Entrance Section

Dimensions

Nom. Pipe Size	L
1/4 "	12"
3/8"	15"
3/4"	2' - 6"
1"	3' - 4"
1 1/2"	5' - 0"
2"	6' - 8"
2 1/2"	8' - 4"

ENTRANCE SECTION SCHEDULE

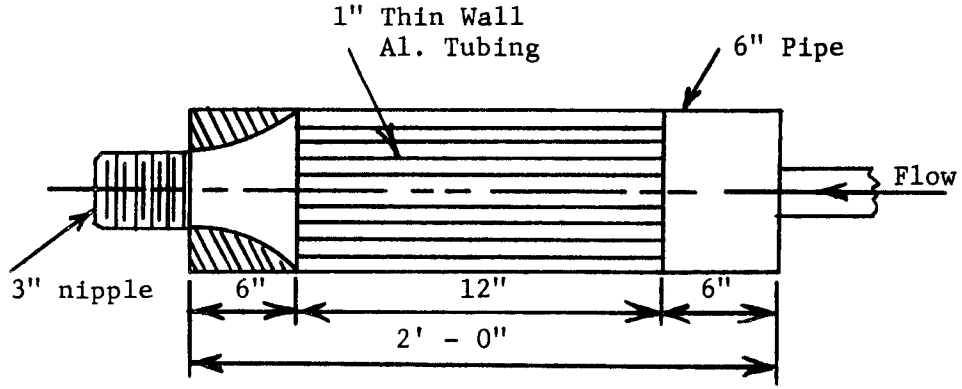

UPSTREAM PLENUM CHAMBER

X - SECTION

Figure 12. Measurement Section Details

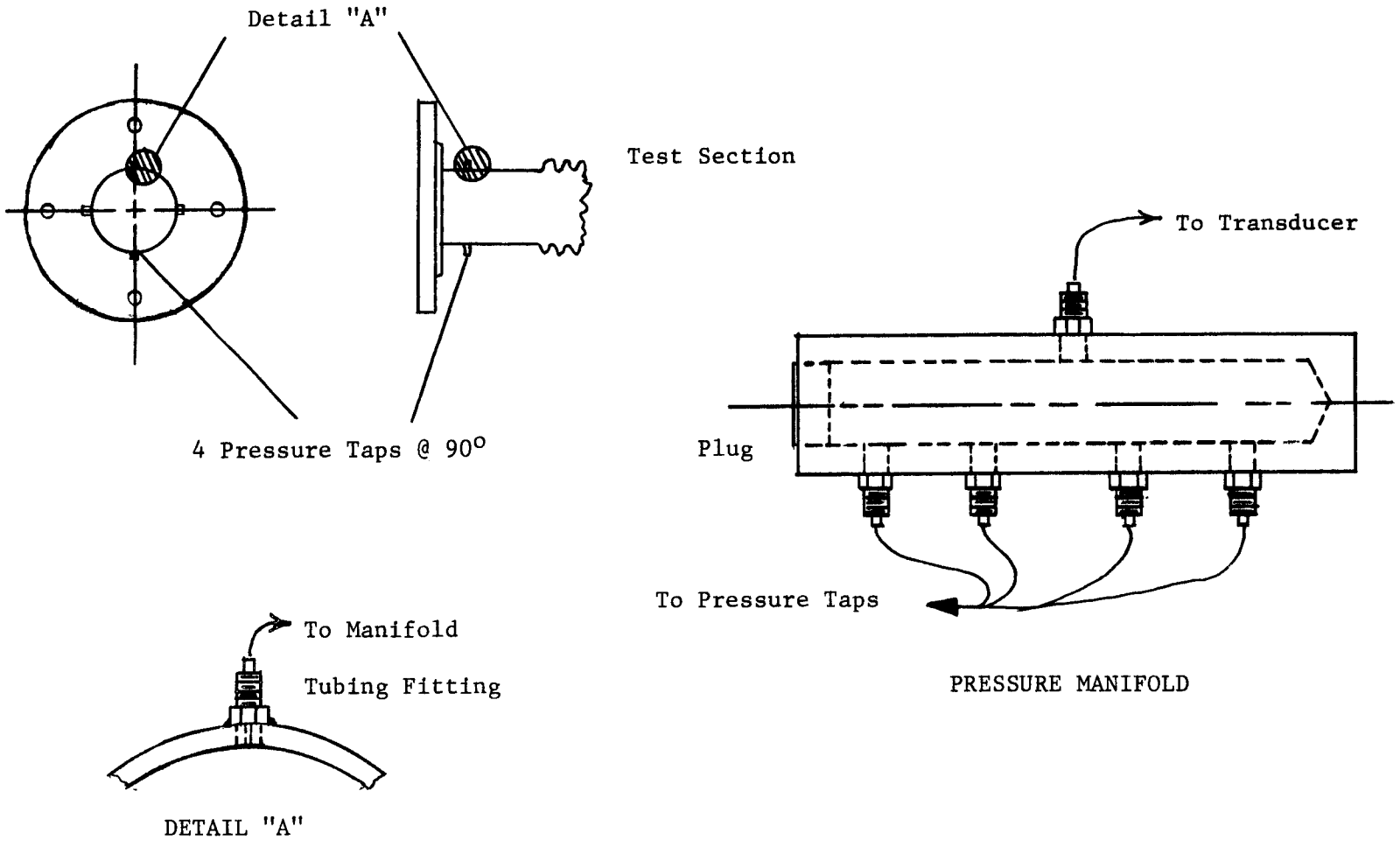

Figure 13. Pressure Measurement Connections

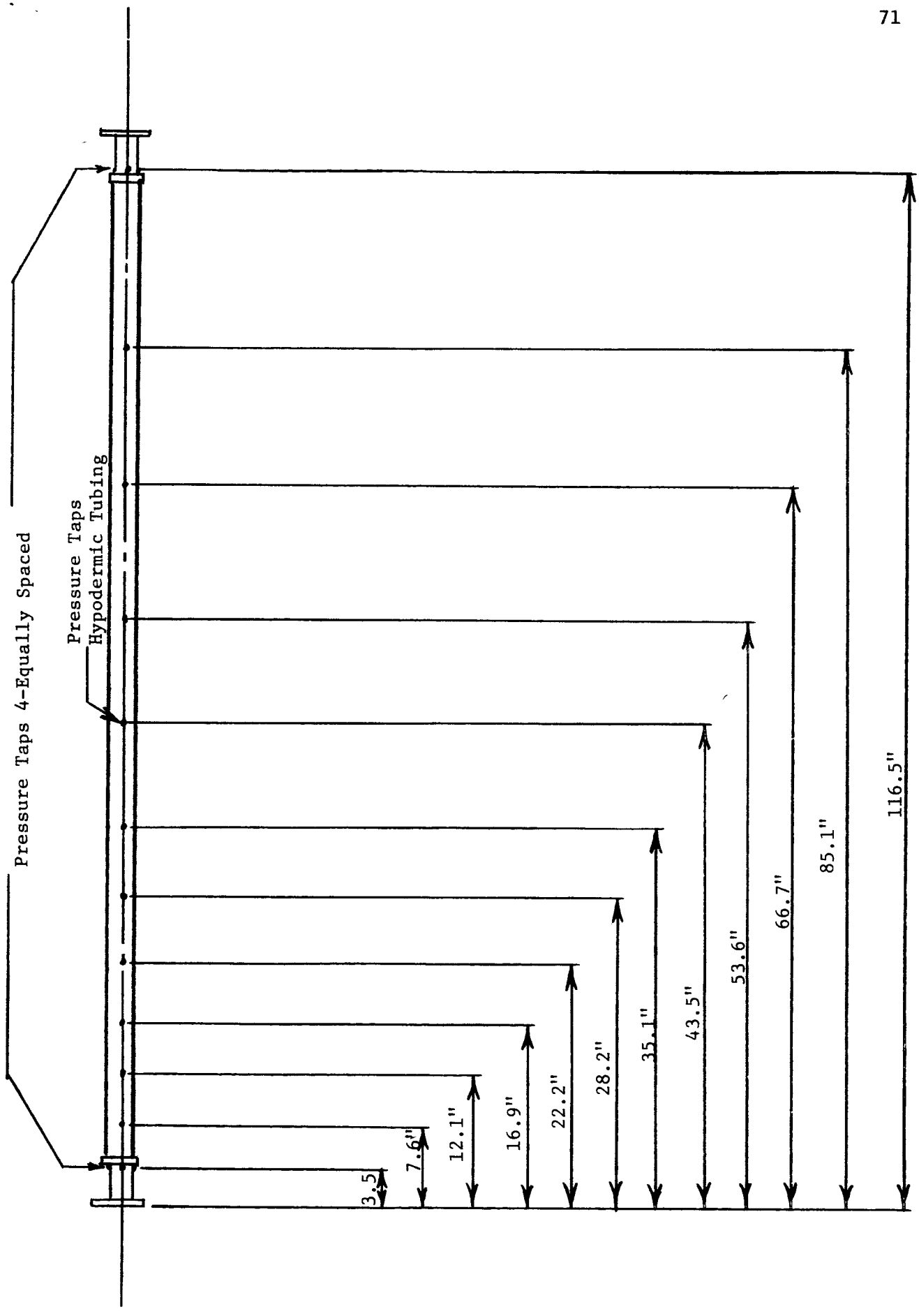

Figure 14. Schematic Diagram of Test Section for Entrance Effects

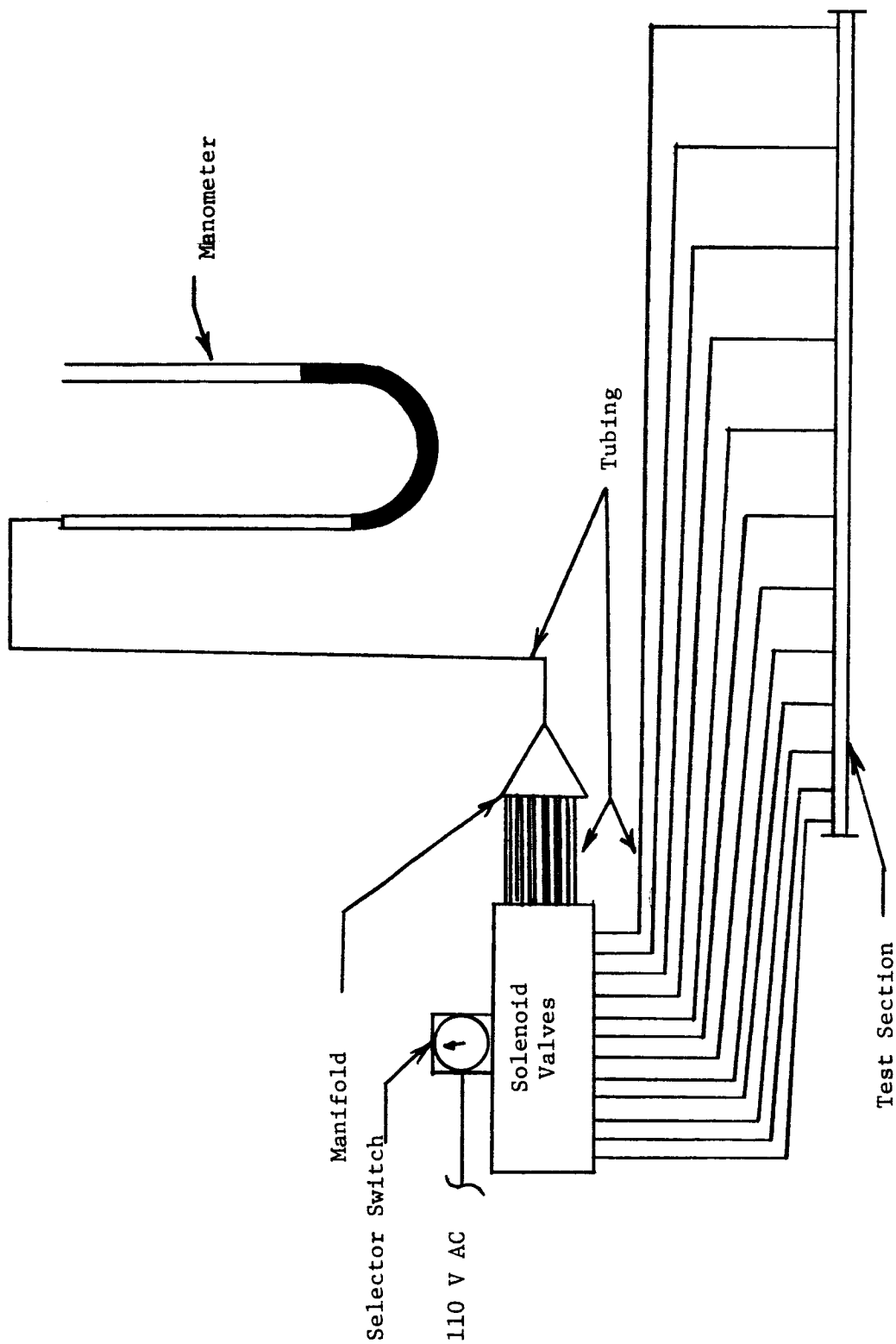

Figure 15. Schematic Diagram of Test Apparatus for Entrance Effects

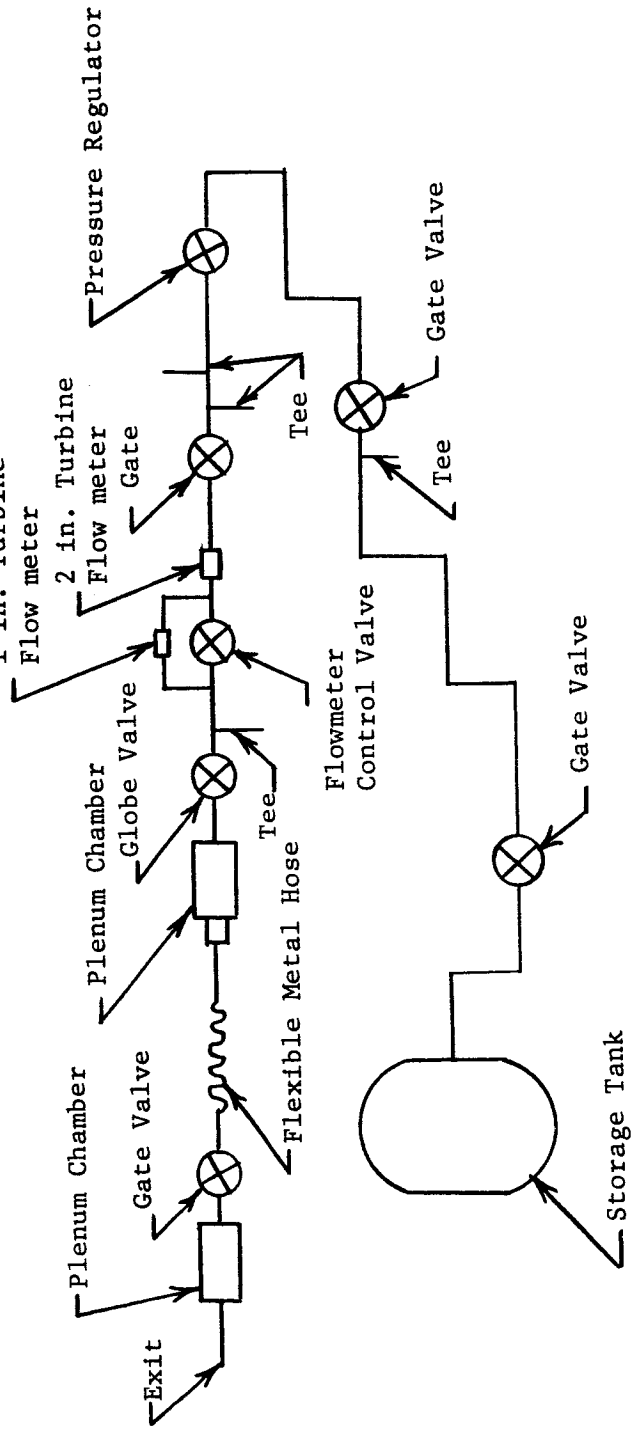

Figure 16. Schematic of Test Apparatus for Arbitrary Flow System.

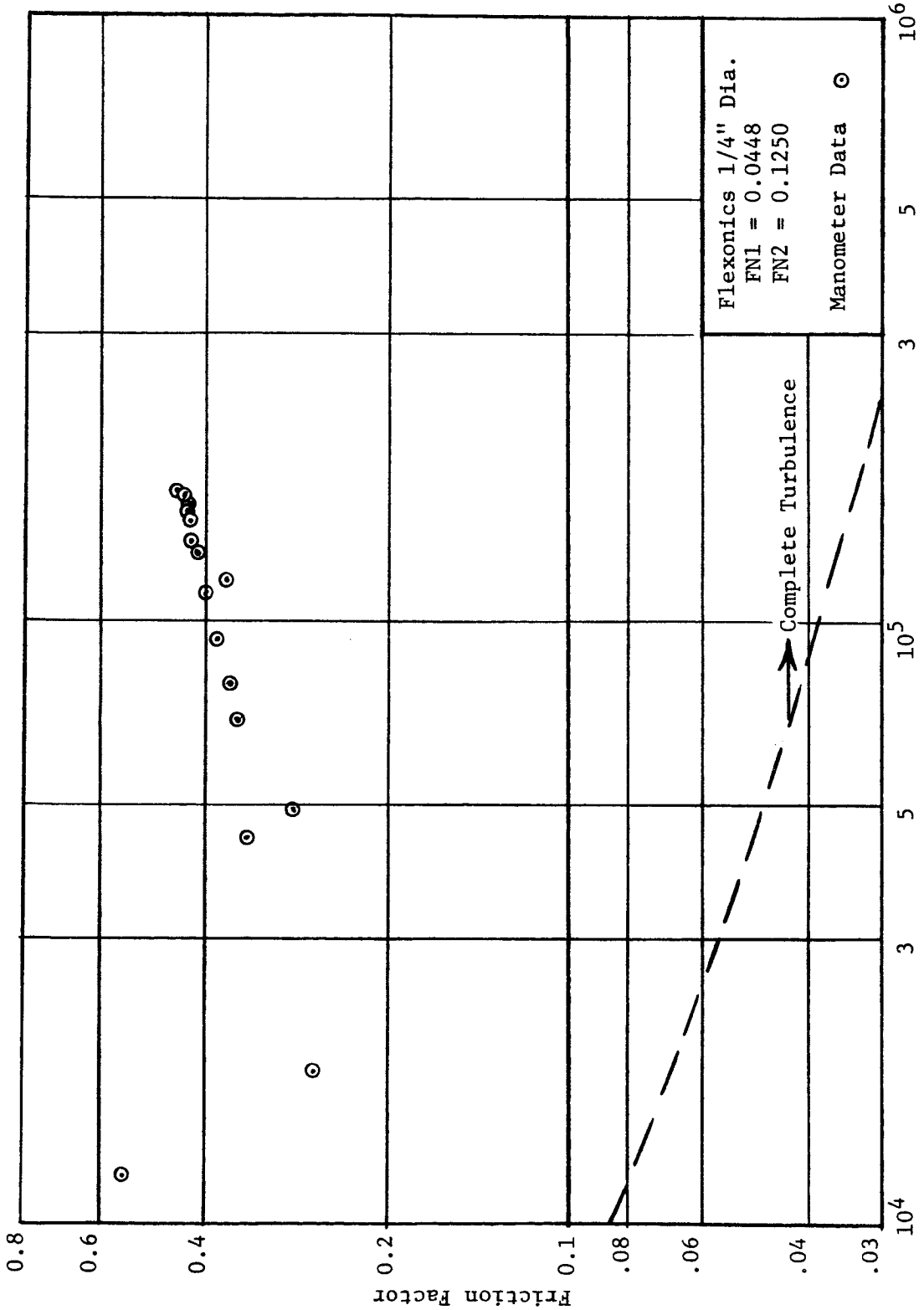

Figure 17. Friction Factor vs Reynolds Number for 1/4" Dia. Hose

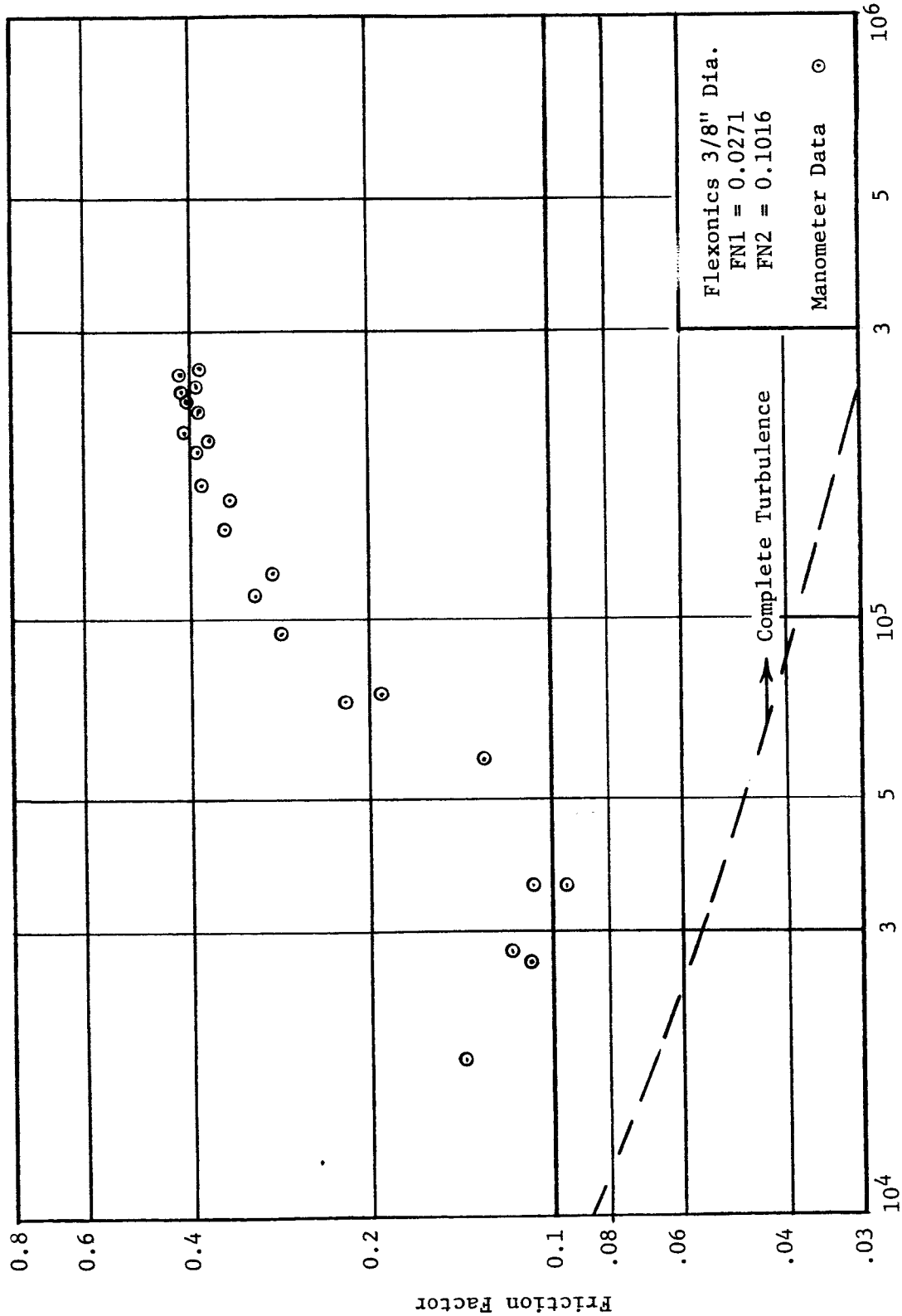

Figure 18. Friction Factor vs Reynolds Number for 3/8" Dia. Hose

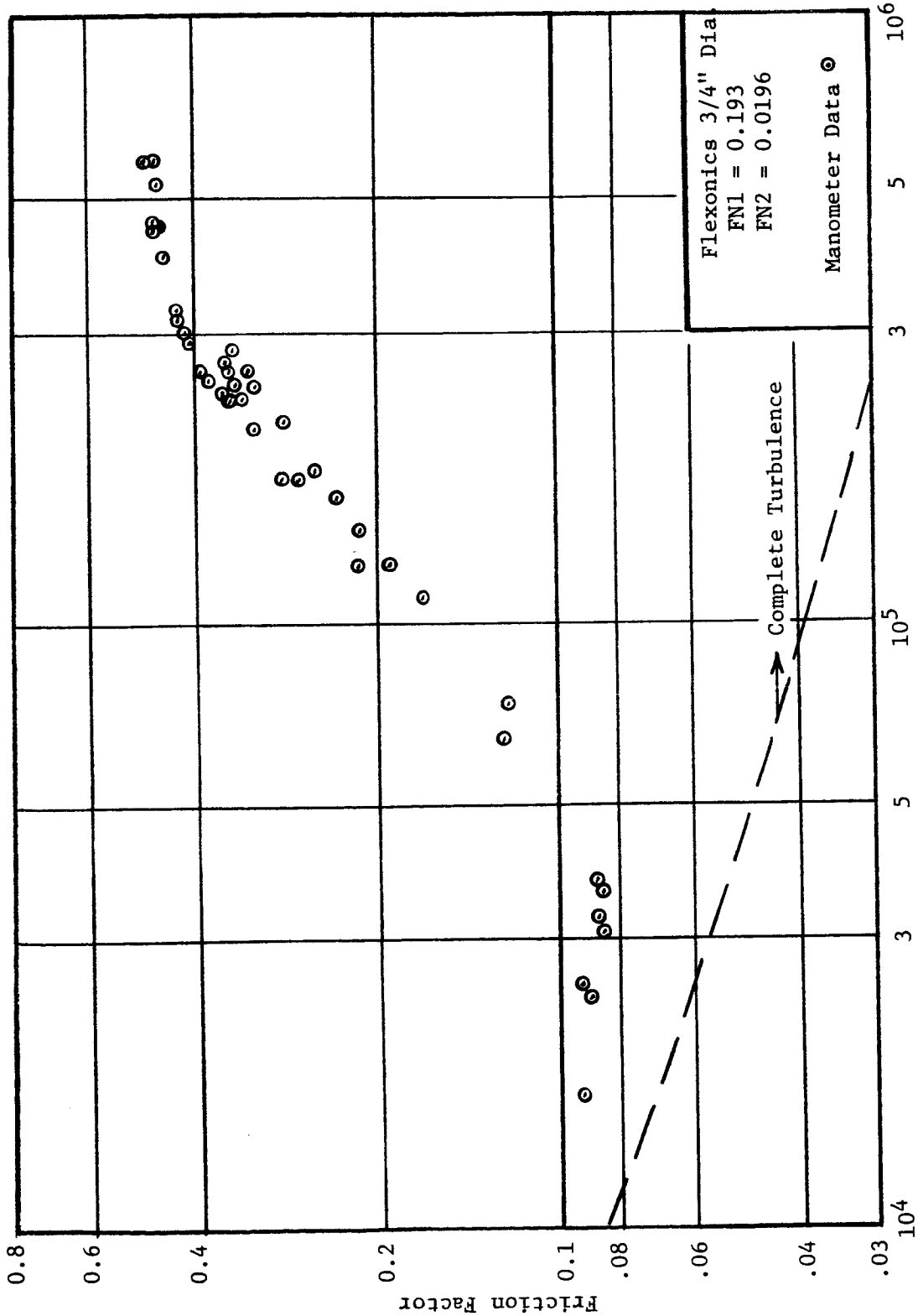

Figure 19. Friction Factor vs Reynolds Number for 3/4" Dia. Hose

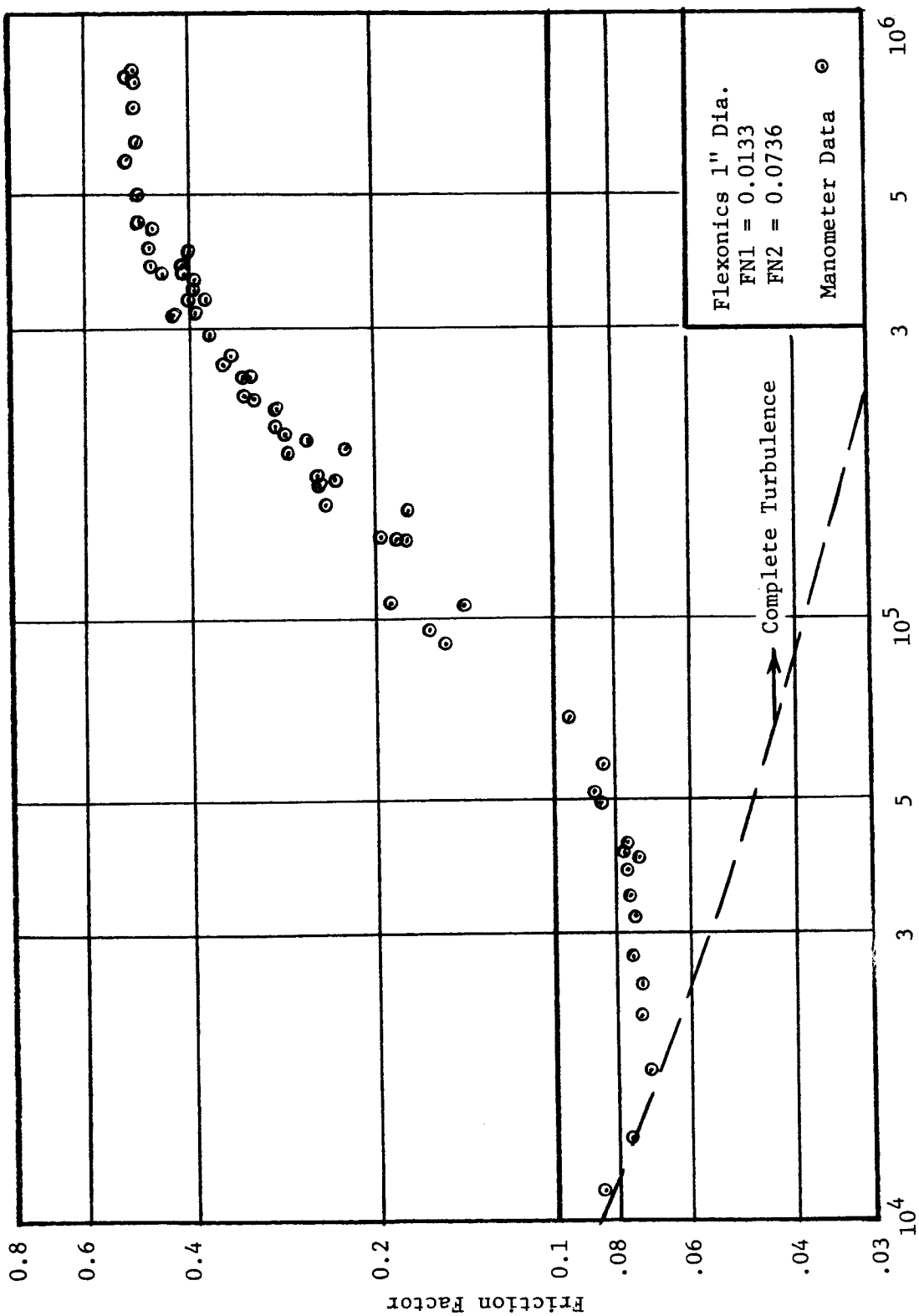

Figure 20. Friction Factor vs Reynolds Number for 1" Dia. Hose

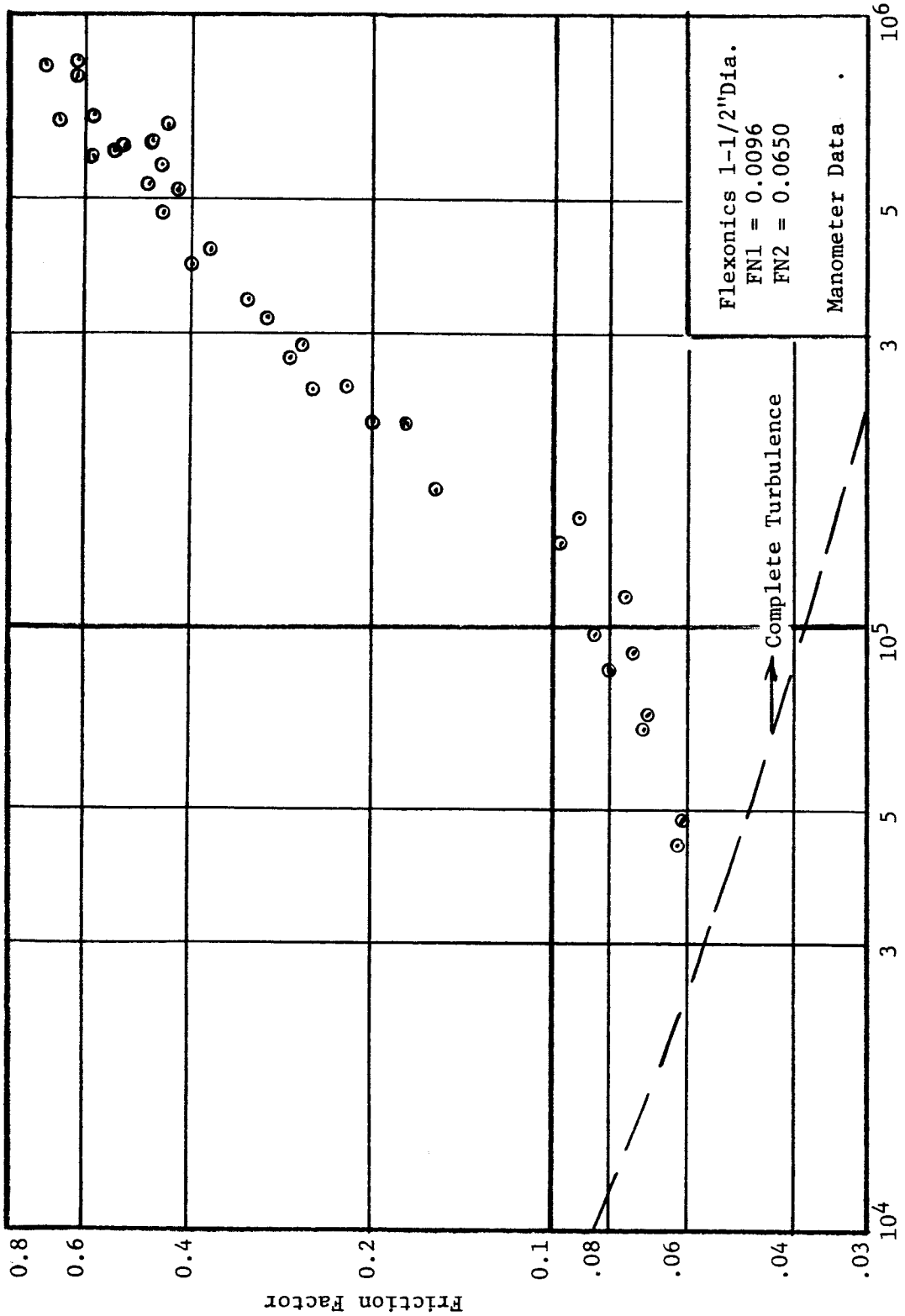

Figure 21. Friction Factor vs Reynolds Number for 1-1/2" Dia. Hose

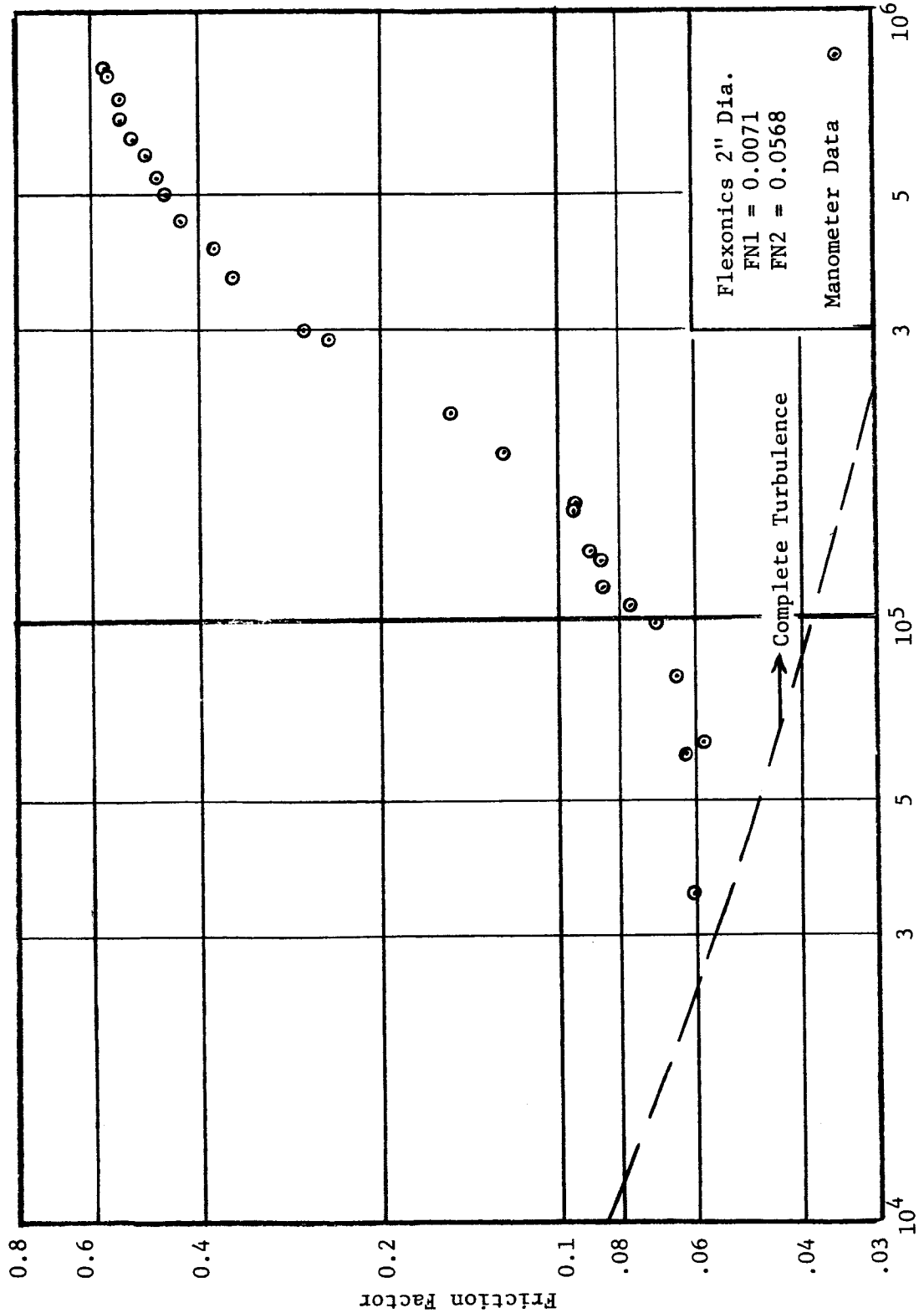

Figure 22. Friction Factor vs Reynolds Number for 2" Dia. Hose

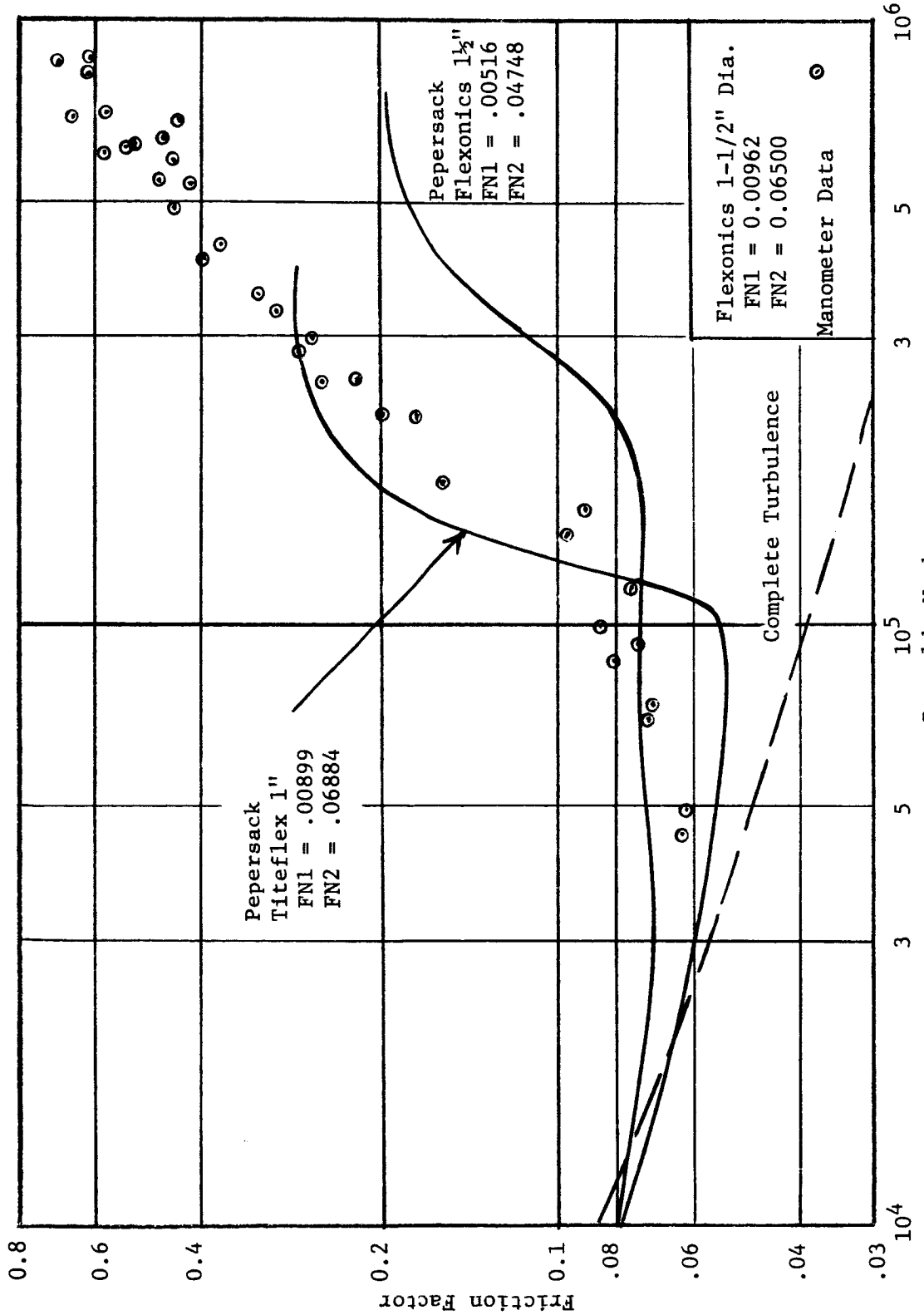

Figure 23. Comparison of Data

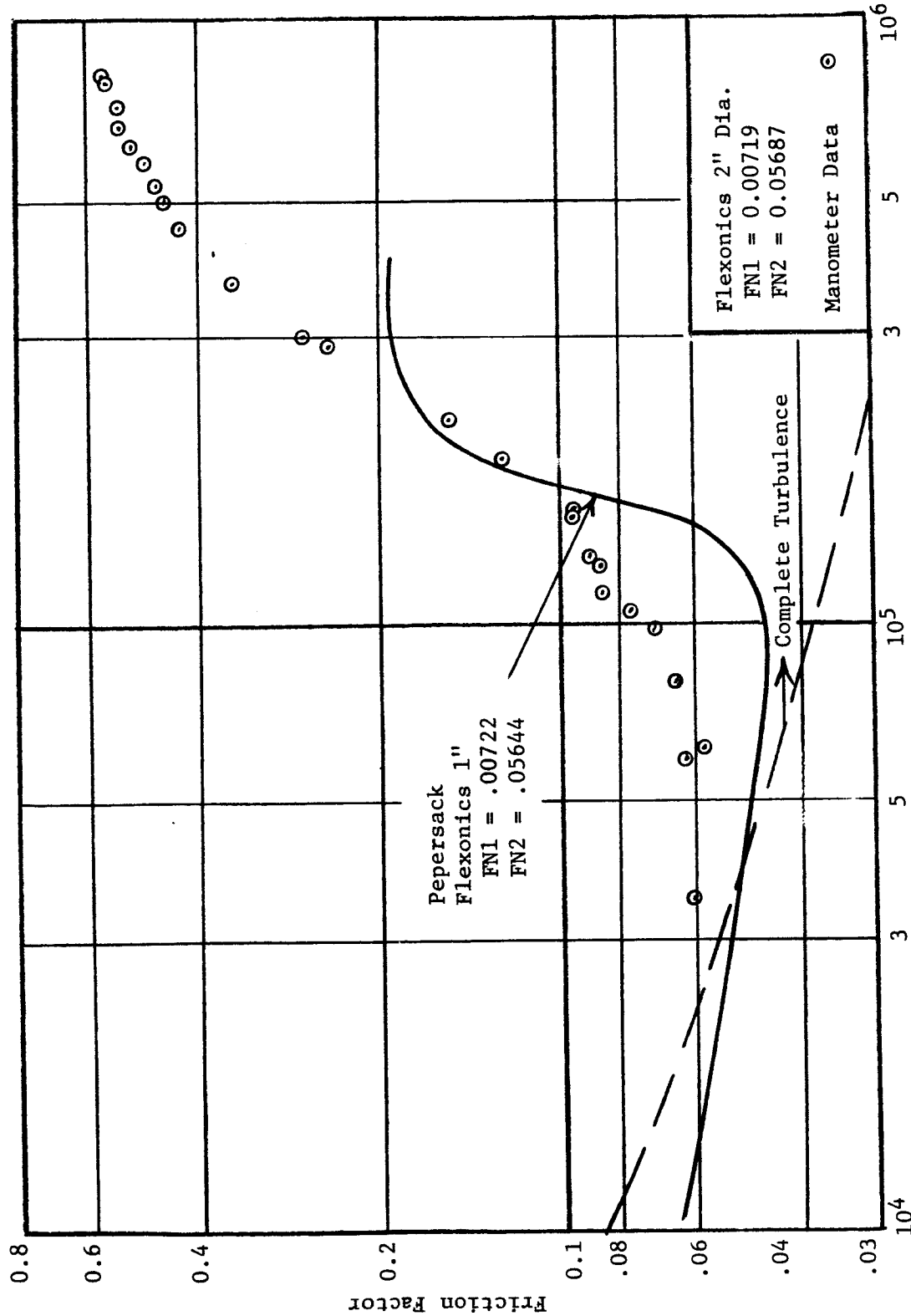

Figure 24. Comparison of Data

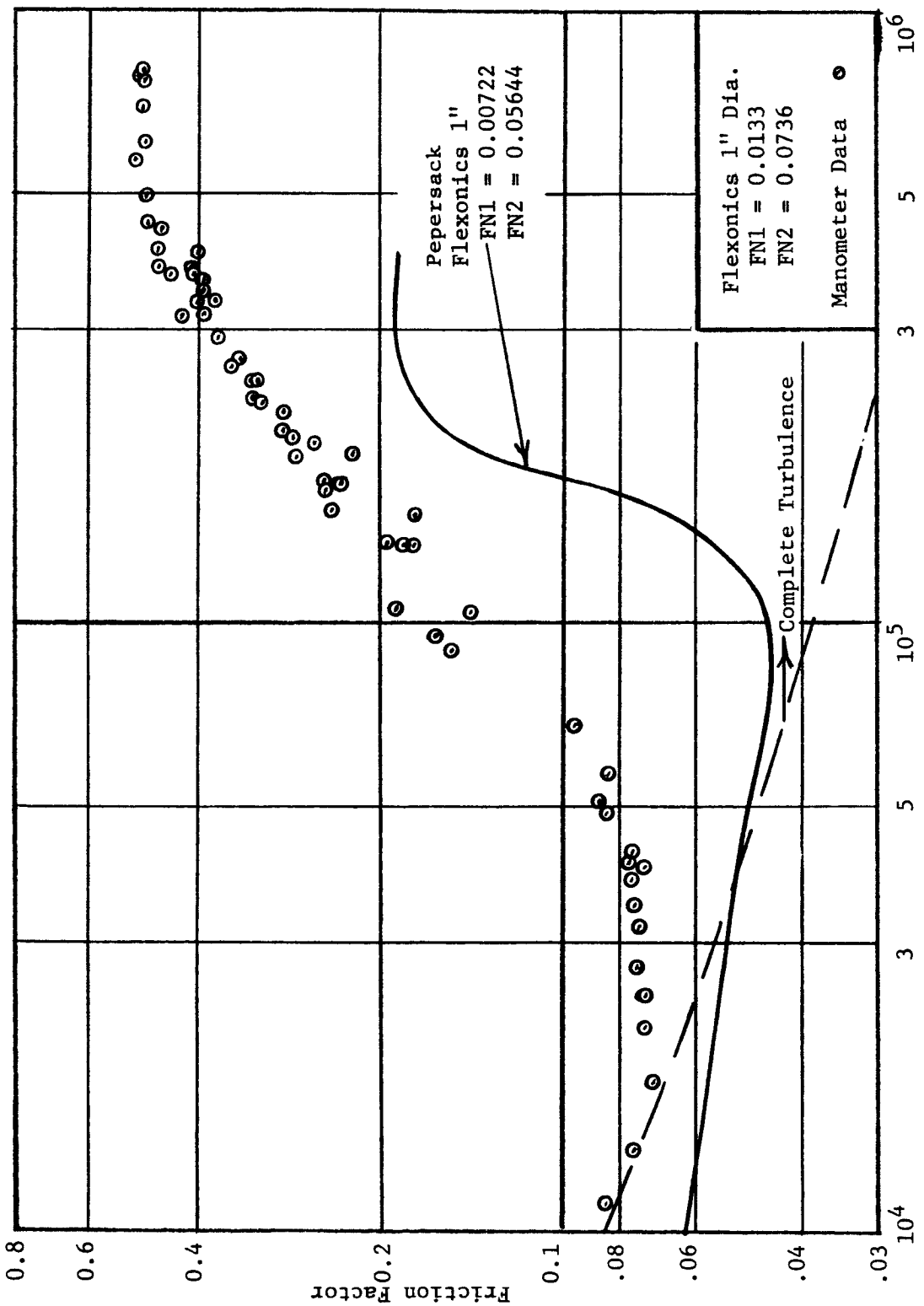

Figure 25. Comparison of Data

Series 79: Section F8 1" x 10'

Thermocouple Number	Run A	Run B	Run C
26	89.5	89	89.25
27	89.5	89	89.25
28	89.5	89.5	89.5
29	89.5	89.5	89.5
30	89.5	89.5	89.5
31	89.5	89.5	89.5
32	90.5	90.5	90.5
33	90.0	90	90
34	90.5	91	91
35	94	93.5	93.5
36	103.5	103.5	103.25

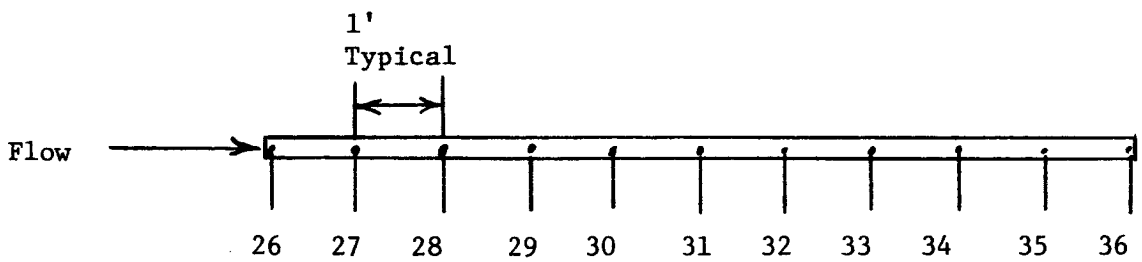

Figure 26. Longitudinal Temperature Distribution (Temperatures given in ^{o}F)

Series 80: Section F-3: 3/8" x 1'

Thermocouple Number	Run A	Run B	Run C	Run D	Run E
26	93	98	103.7	109.1	110.5
27	92.9	99	100.7	118.2	124.5
28	92.2	100.5	105.5	109.9	109.8
29	92.4	97	101.1	105.6	106.2
30	93	140	153.5	169	178
31	94	98	110	114.2	114.5
33	92.8	95.2	98.7	102.5	103
34	93.2	100.5	98.5	100.8	101.5
35	92.5	101.5	103.8	106.7	107.5

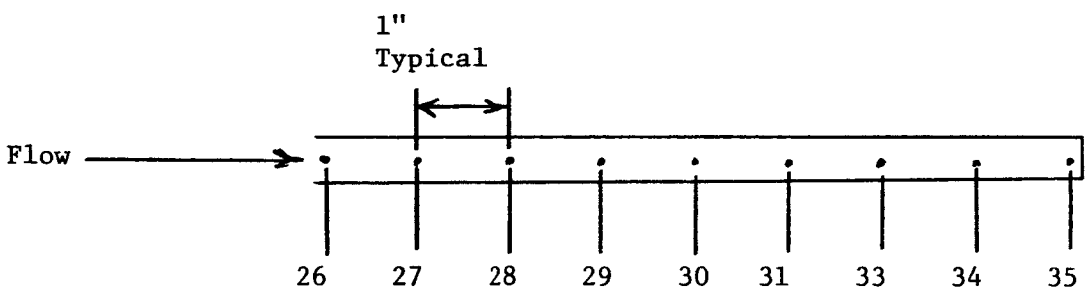

Figure 27. Longitudinal Temperature Distribution (Temperatures in ^{o}F)

Series 81: Section F-3: 3/8" x 1'

Thermocouple Number	Run A	Run B	Run C	Run D	Run E
26	98.8	104.9	109	113.2	118.8
27	105.9	123.6	137.8	148	158
28	97	99.2	101.1	102.6	104
29	105.9	112.1	120	128.4	133
30	102.7	105.6	109.8	112.6	115.4
31	96	98	100	102.2	104
33	99.7	103.5	108.7	115.1	118
34	99	101.3	103.1	106	107
35	102	103.8	104.4	107	107

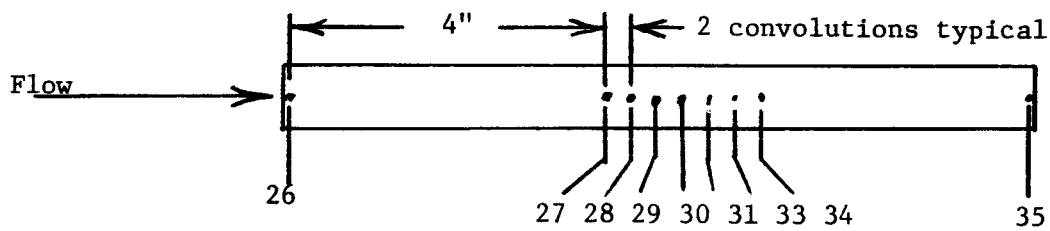

Figure 28. Longitudinal Temperature Distribution (Temperatures in ^{o}F)

Series 82: Section F1: 1/4" x 1'

Thermocouple Number	Run A	Run B	Run C	Run D
26	88.7	88.9	89.8	89.8
27	89	89.1	90.2	90
28	89.1	89.1	90	90
29	88.3	88.7	89.6	89.9
30	88	88.2	89.1	88.5
31	90.1	91.4	91.8	92
33	89	91	91.8	92.2
34	91	91.8	92	92.2
35	91.3	93.5	93.8	93.8
36	92.8	99.2	102	109.3

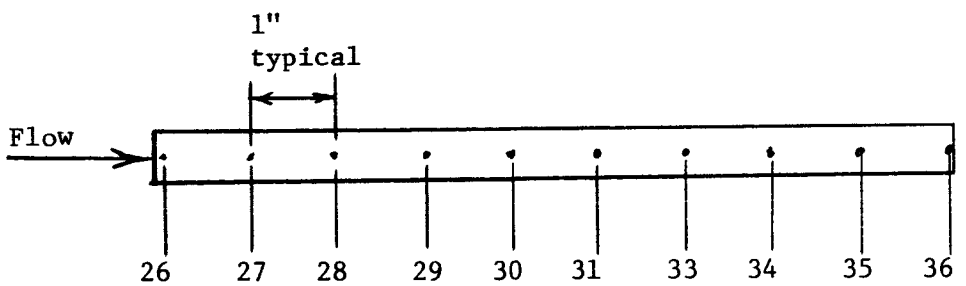

Figure 29. Longitudinal Temperature Distribution (Temperatures in ^{o}F)

Series 35: Section F8: 1" x 10'

(Mid-Point Temperature)

Reynolds Number	f	Temperature ^{o}F	ΔP psi
1.14×10^5	0.042	94.5	0.41
1.32×10^5	0.072	94.5	0.90
1.45×10^5	0.158	95.0	2.26
1.64×10^5	0.188	98.0	3.12
1.82×10^5	0.224	98.7	4.35
2.04×10^5	0.272	100.0	5.96
2.41×10^5	0.325	102.5	8.67
2.69×10^5	0.361	105.0	10.77
3.02×10^5	0.389	108.0	12.99
3.47×10^5	0.406	111.0	15.70
3.88×10^5	---	115.0	---
4.98×10^5	0.436	119.0	23.9
5.51×10^5	0.445	119.0	26.9
5.98×10^5	0.443	119.5	29.4
6.29×10^5	0.433	121.0	30.5

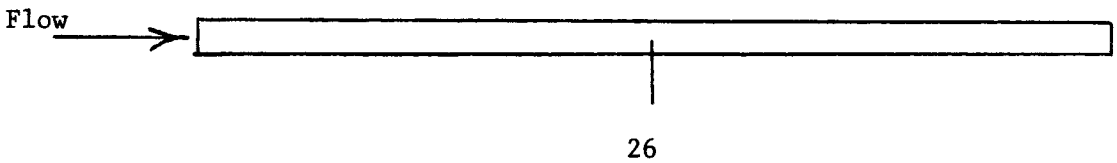

Figure 30. Variation of Midpoint Temperature with Reynolds number.

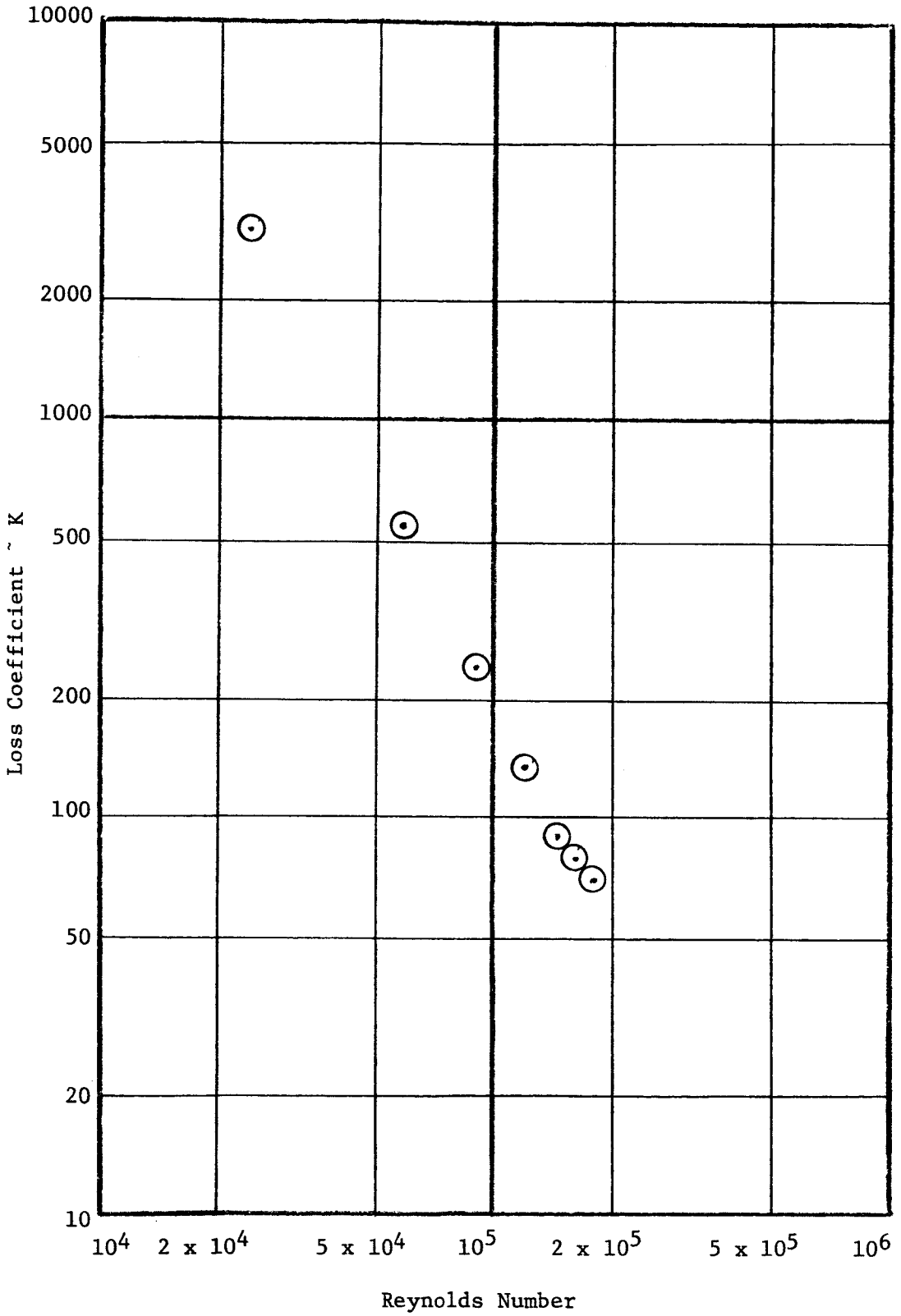

Figure 31. Loss Coefficient vs. Reynolds Number for Pressure Regulator

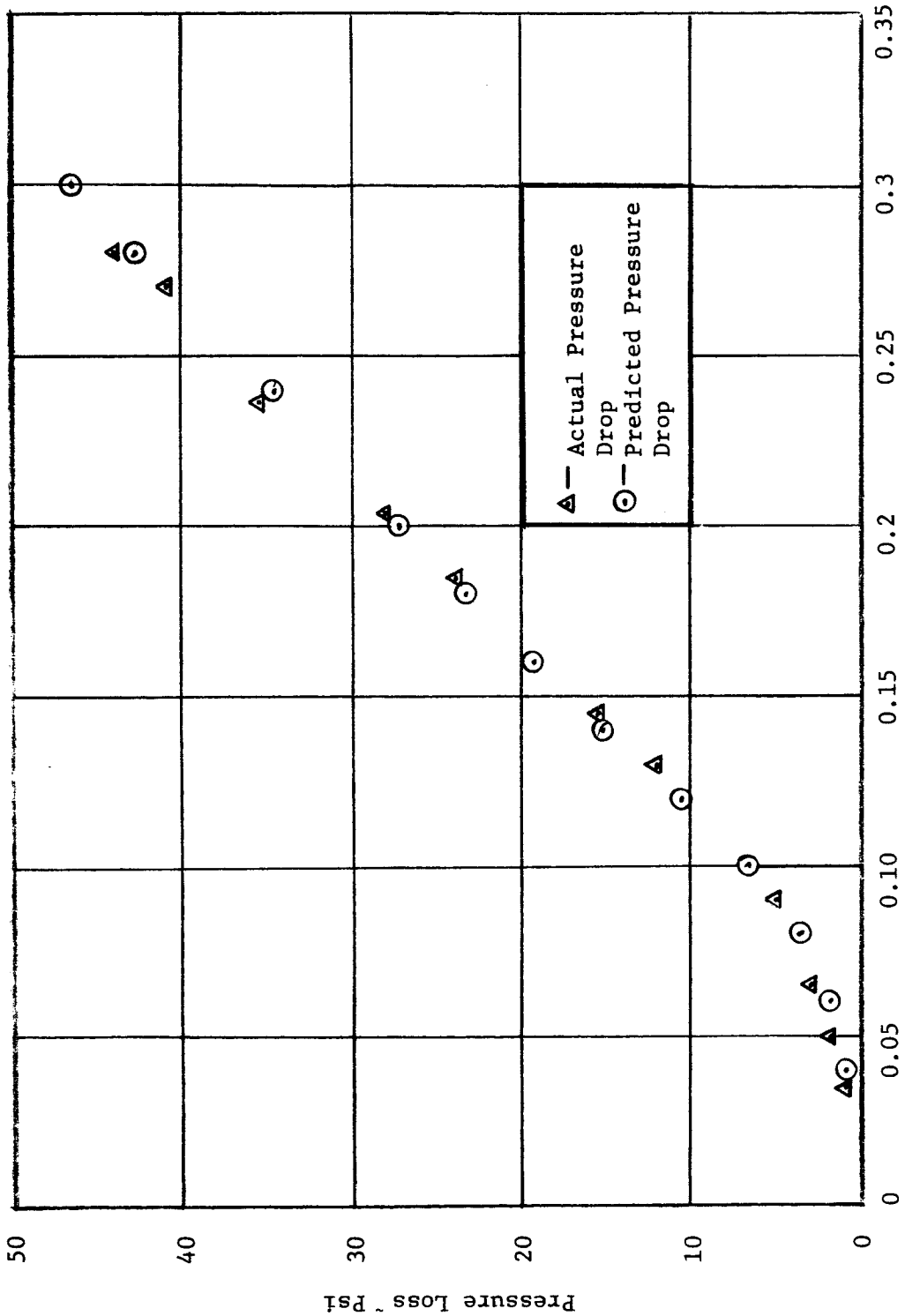

Figure 32. Comparison of Predicted Pressure Drop and Actual Pressure Drop.

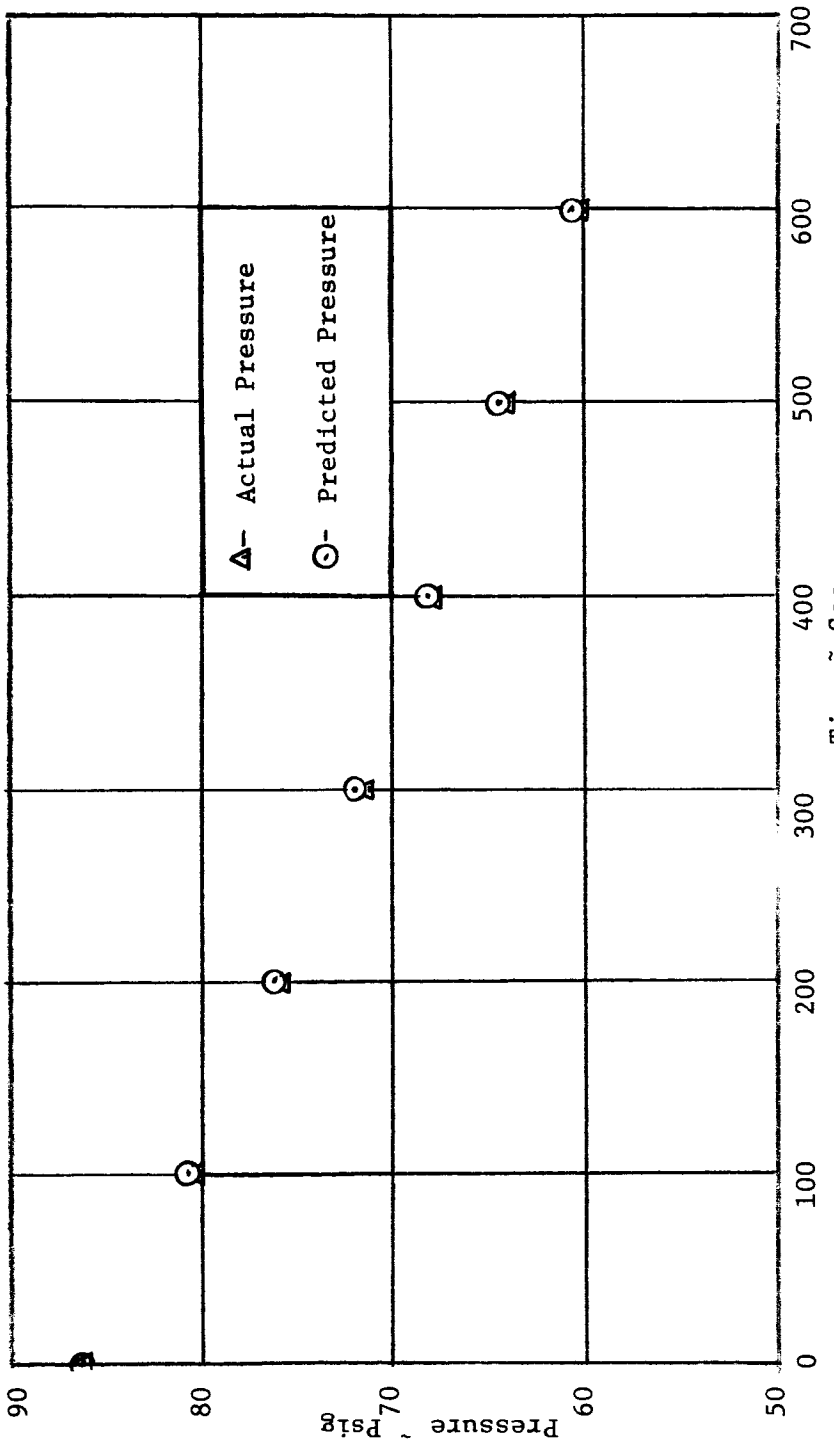

Figure 33. Comparison of Predicted Pressure History and Actual Pressure History.

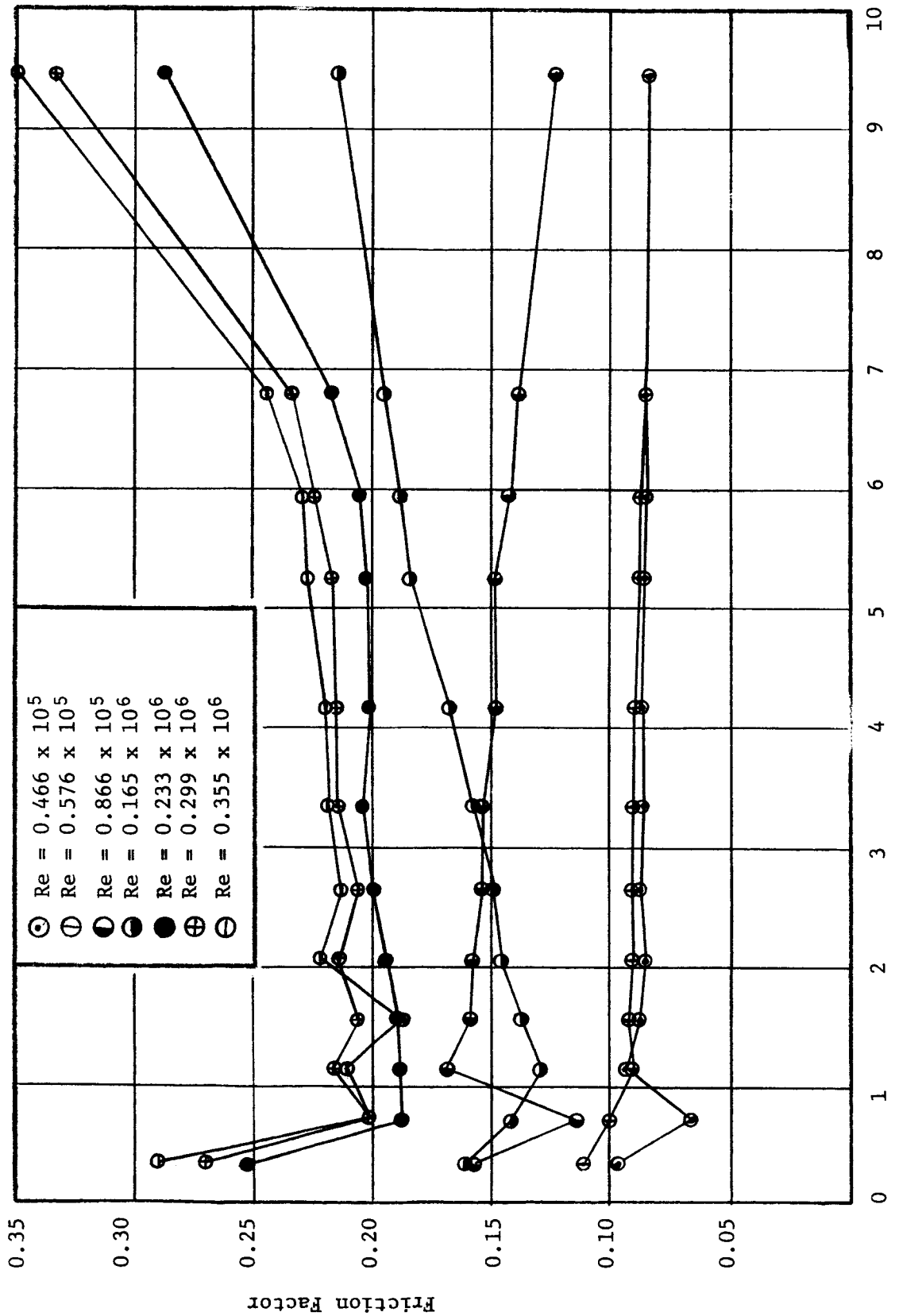

Figure 34. Entrance Effects Study on Flexonics 1 inch Diameter Hose

Appendix A

FRICTION FACTORS

Consider the flow tube shown below.

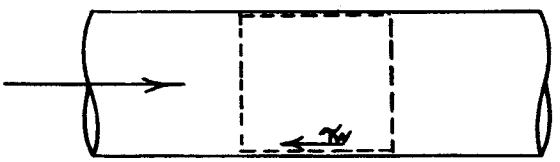

A momentum balance on the control volume yields, for steady flow:

$$-AdP - \tau_w \, dA_w = \dot{m}dV \qquad (1)$$

Where: A = cross section area

A_w = surface area of the wall

τ_w = shear stress in the fluid at the wall

$\dot{m}$ = mass rate of flow

dP = pressure difference across the length of the control volume

dV = velocity change across the length of the control volume

The usual definition of friction factor is

$$f' = \frac{\tau_w}{(1/2)\,\rho V^2} \qquad (2)$$

where ρ is the fluid density.

Substitution into (1) yields

$$- AdP - f' \frac{\rho V^2}{2} dAw = \dot{m}dV. \qquad (3)$$

The characteristic (hydraulic) diameter may be written as

$$D \equiv \frac{4A}{dAw/dx} \qquad (4)$$

where x is the axial coordinate.

Appendix A (continued)

Thus; $-AdP - f' \rho V^2/2 \frac{4 A dx}{D} = \dot{m}dV$

or: $$4f' = - \frac{dp}{(\rho V^2/2)d(X/D)} - \frac{2 dV}{V d (X/D)} \qquad (5)$$

Then using the Darcy-Weisbach friction factor,

$$f \equiv \frac{- dP}{(\rho V^2/2) d(X/D)} \qquad (6)$$

one has

$$4f' = + f - \frac{2 dV}{Vd(X/D)} \qquad (7)$$

It then is apparent that defining a friction factor as

$$\frac{dP}{(\rho V^2/2) d(X/D)} \quad \text{or} \quad \frac{P}{(\rho V^2/2) (L/D)}$$

neglects the momentum change of the stream due to any modification of the mean velocity. The velocity and density are related however through the continuity equation $\dot{m} = \rho AV$. For a constant area duct and steady flow conditions

$$\dot{m}/A = \rho V = \text{constant.}$$

Thus $$d(\rho V) = 0 \qquad (8)$$

Therefore for incompressible fluids either friction factor is valid, and

$$4f' = f \qquad (9)$$

APPENDIX B

Computer Program for Pressure Drop in Flow System

```
      DIMENSIOND(100),PRESS(100),F(50),XL(50),A1(25),
     3    ,E(10),R1(10),S(10),XL1(10),XMDOT(25)
     1    ,A4(25),N1(25),N(25),R(25),THETA(25),DT(10),
     2    ,CN(10),XLT(10),XLH(10),FT(10),FH(10),FB(25),
     4A2,25),A3(25),DH(10),BN(10),IDO(100)
        READ220,TEMP,GAMMA,PRESSX,RC
        READ224,IX,KX,LX,MX,NX,JX,II,J1X
          READ219,(XMDOT(I1),I1=1,II)
      READ225,(D(I),I=1,IX)
  300 IF(JX-1)302,301,301
  301 READ212,(F(J),J=1,JX)
      READ213,(XL(J),J=1,JX)
  302 IF(KX-1)304,303,303
  303 READ214,(N(K),N1(K),K=1,KX)
      READ215,(A1(K),A2(K),A3(K),A4(K),K=1,KX)
  304 IF(LX-1)306,305,305
  305 READ216,(R(L),THETA(L),FB(L),L=1,LX)
  306 IF(MX-1)309,307,307
  307 READ217,(DT(M),DH(M),XLT(M),XLH(M),FT(M),FH(M),
     1M=1,MX)
      READ232,(BN(M),CN(M),M=1,MX)
      READ218,(IDO(I),I=1,IX)
  309 IF(J1X-1)400,310,310
  310 READ223,(E(J1),R1(J1),S(J1),J1=1,J1X)
      READ234,(XL1(J1),J1=1,J1X)
  400 DO401I1=1,II
  308      I=1
           J=1
           K=1
           L=1
           M=1
           J1=1
          PRESS(I)=PRESSX
  320      XMU=EXPF(-11.4227+.0014979*TEMP)
  321      TEMPR=TEMP+460.
           SS=49.1*(TEMPR)**.5
           CON=1./(RC*TEMPR)
  100     IDOX=IDO(I)
           IF(I-IX)402,402,403
  402 GO TO(1,2,3,4,5,6,7,8,9),IDOX
C     PRESSURE LOSS IN STRAIGHT SECTIONS
    1     D(I)=D(I)/12.
          RHO=PRESS(I)*144.*CON
          A=3.14159*D(I)*D(I)/4.
          VEL=XMDOT(I1)/(A*RHO)
          K1=1
          XMACH=VEL/SS
```

Appendix B (continued)

```
            Y=4.0
            RE=RHO*VEL*D(I)/XMU
        IF(RE-2300.)55,55,51
   55       XF1=64./RE
        GO TO 53
   51       AC=(18.7*Y)/RE
            AB=2.*F(J)/D(I)
            XLOG=LOGF(AB+AC)
            Y1=1.74-.863*XLOG
            XF1=1./(Y1*Y1)
            XF=1./(Y*Y)
            ERRO=ABSF(XF1-XF)
        IF(K1-200)50,53,53
   50   IF(ERRO-.001)53,53,52
   52       Y=Y1
        GOTO51
   53       FR=XF1*XL(J)/D(I)
            VSQ=VEL*VEL*RHO/9270.
            DELP=FR*VSQ
            PRESS(I+1)=PRESS(I)+DELP
        IF(SENSE SWITCH 2)520,530
  530   CONTINUE
        IF(SENSE SWITCH 1)500,501
  500   CONTINUE
        PUNCH203
        PUNCH201
        PUNCH200,PRESS(I+1),DELP,I
        GO TO 520
  501   CONTINUE
        PRINT203
        PRINT201
        PRINT200,PRESS(I+1),DELP,I
  520   CONTINUE
            I=I+1
            J=J+1
        GOTO100
    54  PRINT202,ERRO
        GOTO53
C       EXIT LOSS
    2       RHO=PRESS(I)*144.*CON
            K1=1
            D(I)=D(I)/12.
            A=3.1459*D(I)*D(I)/4.
           VEL=XMDOT(I1)/(A*RHO)
            DELP=VEL*VEL*RHO/9270.
```

Appendix B (Continued)

```
            PRESS2=PRESS(I)+DELP
     25     RHO2=PRESS2*144.*CON
            VEL2=XMDOT(I1)/(A*RHO2)
            XMACH=VEL2/SS
        IF(XMACH-.3)21,22,22
     22 PRINT211,XMACH
     21     DELP2=VEL2*VEL2*RHO/9270.
            PRESS3=PRESS(I)+DELP2
            ERRO=ABSF(PRESS3-PRESS2)
        IF(K1-200)27,26,26
     27 IF(ERRO-.001)23,24,24
     24     PRESS2=PRESS3
            K1=K1+1
        GO TO 25
     26 PRINT202,ERRO
        GO TO 23
     23 PRESS(I+1)=PRESS3
            DELP=DELP2
        IF(SENSE SWITCH 2)521,531
    531 CONTINUE
        IF(SENSE SWITCH 1)503,504
    503 CONTINUE
         PUNCH204
        PUNCH201
        PUNCH200,PRESS(I+1),DELP,I
        GO TO 521
    504 CONTINUE
        PRINT204
        PRINT201
        PRINT200,PRESS(I+1),DELP,I
    521 CONTINUE
            I=I+1
        GOTO100
C       SUDDEN CONTRACTION LOSS
      3     RHO=PRESS(I)*144.*CON
            K1=1
            D(I)=D(I)/12.
            A=3.14159*D(I-1)*D(I-1)/4.
           VEL=XMDOT(I1)/(A*RHO)
           XMACH =VEL/SS
        IF(XMACH-.3)31,32,32
     32 PRINT211,XMACH
     31     RATIO=D(I-1)/D(I)
            CV =.975*.975
            B = RATIO *RATIO
```

Appendix B (continued)

```
            CC = .61375 + (.13318+(-.26095 +.51146*B)*B)*B
            DA=1./(CV*CC*CC)
            EA=2./CC
            XK1=DA-EA+1.
            PV = RHO * VEL*VEL/9270.
            PT = PRESS(I)+PV
            RP = PRESS(I)/ PT
            PT3=(1.+(1.-RP)*XK1)*PT
            PS = PRESS(I)+ 1.
   36       RHO = PS*144.*CON
            AA=3.14159*D(I)*D(I)/4.
            VEL=XMDOT(I1)/(AA*RHO)
            PS1= PT3- RHO* VEL*VEL/9270.
      IF(K1-200) 34,33,33
   34       ERRO= ABSF(PS1-PS)
      IF(ERRO-.001)33,33,35
   35       PS=PS1
            K1=K1+2
      GO TO 36
   33      PRESS(I+1)=PS1
           DELP =PRESS(I+1)-PRESS(I)
            PRESS(I+1)=PRESS(I)+DELP
      IF(SENSE SWITCH 2)522,532
  532 CONTINUE
      IF(SENSE SWITCH 1)505,506
  505 CONTINUE
      PUNCH205
      PUNCH201
      PUNCH200,PRESS(I+1),DELP,I
      GO TO 522
  506 CONTINUE
      PRINT205
      PRINT201
      PRINT200,PRESS(I+1),DELP,I
  522 CONTINUE
            I=I+1
      GO TO 100
C     ARBITRARY CONFIGURATION
    4       RHO=PRESS(I)*144.*CON
            D(I)=D(I)/12.
            A=3.14159*D(I)*D(I)/4.
            VEL=XMDOT(I1)/(A*RHO)
           XMACH =VEL/SS
      IF(XMACH-.3)41,42,42
   42 PRINT211,XMACH
```

Appendix B (continued)

```
   41     RE=RHO*VEL*D(I)/XMU
      IF(N1(K)-1)60,61,62
   60       X=XMDOT(I1)
      GOTO63
   61       X=RE
      GOTO63
   62       X=A
      GOTO63
   63 IF(N(K)-1)64,65,66
   64       XK=A1(K)+(A2(K)+(A3(K)+A4(K)*X)*X)*X
      GOTO67
   65       XK=A1(K)*X**A2(K)
      GOTO67
   66     XK=A1(K)+A2(K)*LOGF(X)
      GOTO67
   67       DELP=XK*VEL*VEL*RHO/9270.
            PRESS(I+1)=PRESS(I)+DELP
      IF(SENSE SWITCH 2)523,533
  533 CONTINUE
      IF(SENSE SWITCH 1)507,508
  507 CONTINUE
      PUNCH206
      PUNCH201
      PUNCH200,PRESS(I+1),DELP,I
      GO TO 523
  508 CONTINUE
      PRINT206
      PRINT201
      PRINT200,PRESS(I+1),DELP,I
  523 CONTINUE
            I=I+1
            K=K+1
      GOTO100
C     LOSS IN ELBOWS
    5       RHO=PRESS(I)*144.*CON
            K2=1
            D(I)=D(I)/12.
            A=3.14159*D(I)*D(I)/4.
            Y=4.0
            VEL=XMDOT(I1)/(A*RHO)
            RE=RHO*D(I)*VEL/XMU
      IF(RE-2300.)74,74,70
   74       XF1=64./RE
      GO TO 73
   70       AC=(18.7*Y)/RE
```

Appendix B (continued)

```
            AB=2.*FB(L)/D(I)
            XLOG=LOGF(AB+AC)
            Y1=1.74-.863*XLOG
            XF1=1.0/(Y1*Y1)
            XF=1./(Y*Y)
            ERRO=ABSF(XF1-XF)
        IF(K2-200)71,71,93
     71 IF(ERRO-.001)72,72,73
     72     Y=Y1
            K2=K2+1
        GOTO70
     73     RATIO=R(L)/D(I)
            XLOG=LOGF(RATIO)
            XK1=.4118776*XLOG*.4343
            XK2=.40510085*XLOG*XLOG*.4343*.4343
            XK=.27555202-XK1+XK2
        AD=(XK/90.*THETA(L)+XF1*THETA(L)*RATIO*.01745)/9270.
            DELP=AD*VEL*VEL*RHO
            PRESS(I+1)=PRESS(I)+DELP
        IF(SENSE SWITCH 2)524,534
    534 CONTINUE
        IF(SENSE SWITCH 1)509,510
    509 CONTINUE
        PUNCH207
        PUNCH201
        PUNCH200,PRESS(I+1),DELP,I
        GO TO 524
    510 CONTINUE
        PRINT207
        PRINT201
        PRINT200,PRESS(I+1),DELP,I
    524 CONTINUE
            I=I+1
            L=L+1
        GOTO100
     93 PRINT202,ERRO
        GO TO 73
  C     PRESSURE LOSS IN TUBE BUNDLES
      6 CONTINUE
            DELH=.05
            H=.09
        AT=3.14159*DT(M)*DT(M)/4.
        AH=3.14159*DH(M)*DH(M)/4.
        YT=4.
        YH=4.
```

Appendix B (continued)

```
      RHO =PRESS(I)*144.*CON
      K5=1
  800 XMT=(1.-H)*XMDOT(I1)/BN(M)
      XMH=H*XMDOT(I1)/CN(M)
      VELT=XMT/(AT*RHO)
      VELH=XMH/(AH*RHO)
      RET=RHO *VELT*DT(M)/XMU
      REH=RHO *VELH*DH(M)/XMU
      AB=2.*FT(M)/DT(M)
      K1=1
      K2=1
  801 AC=(18.7*YT)/RET
      YT1=1.74-.863*LOGF(AB+AC)
      XFT1=1./(YT1*YT1)
      XFT=1./(YT*YT)
      ERRO=ABSF(XFT1-XFT)
      IF(K1-200)804,804,823
  804 IF(ERRO-.0001)803,803,802
  802 YT=YT1
      K1=K1+1
      GOTO801
  803 AD=2.0*FH(M)/DH(M)
      AE=18.7*YH/REH
      YH1=1.14-.863*LOGF(AD+AE)
      XFH1=1./(YH1*YH1)
      XFH=1./(YH*YH)
      ERROH=ABSF(XFH1-XFH)
      IF(K2-200)805,805,825
  825 PRINT202,ERROH
      GO TO 807
  805 IF(ERROH-.001)807,807,806
  806 YH=YH1
          K2=K2+1
      GOTO803
  807     DELPT =(XFT1*XLT(M)/DT(M)+1.5)*VELT*VELT*RHO
     1/9270.
          DELPH =(XFH1*XLH(M) /DH(M)+1.5) *VELH*VELH*RHO
     1/9270.
  816 DDP=DELPT-DELPH
      DDDP=ABSF(DDP)
      IF(K5-100)817,817,821
  817 IF(DDDP-.03)822,822,818
  818 IF(DDP)819,822,820
  819 H=H-DELH
      DELH=DELH/2.
```

Appendix B (continued)

```
      K5=K5+1
      GOTO800
  820 H=H+DELH
      K5=K5+1
      GOTO800
  821 PRINT208,DDDP
  822 PRESS(I+1)=PRESS(I)+DELPT
      IF(SENSE SWITCH 2)525,535
  535 CONTINUE
      IF(SENSE SWITCH 1)511,512
  511 CONTINUE
      PUNCH209
      PUNCH201
      PUNCH200,PRESS(I+1),DELP,I
      GO TO 525
  512 CONTINUE
      PRINT209
      PRINT201
      PRINT200,PRESS(I+1),DELP,I
  525 CONTINUE
          D(I)=D(I)/12.
      I=I+1
          M=M+1
      GOTO100
  824 PRINT202,ERROH
      GOTO807
  823 PRINT202,ERRO
      GOTO803
C     PRESSURE LOSS IN FL OW METER
    7     RHO=PRESS(I)*144.*CON
          K1=1
          D(I)=D(I)/12.
          A=3.14159*D(I)*D(I)/4.
          VEL=XMDOT(I1)/(A*RHO)
          RE=RHO*VEL*D(I)/XMU
          Q=XMDOT(I1)/RHO
      IF(Q-44.)101,101,102
  101     XF=6.
      GOTO103
  102     XF=.01
  103     DELP=XF*5.25*VEL*VEL*RHO/(D(I)*9270.*4.)
          PRES2=PRESS(I)+DELP
  111     RHO2=PRESS2*144.*CON
          VEL2=XMDOT(I1)/(A*RHO2)
          Q=XMDOT(I1)/RHO2
```

Appendix B (continued)

```
      IF(Q-44.)104,104,105
  104     XF=6.
      GOTO106
  105     XF=.01
  106     DELP=XF*5.25*VEL2*VEL2*RHO/(D(I)*9270.)
          PRESS3=PRESS(I)+DELP
          ERRO=ABSF(PRESS3-PRESS2)
      IF(K1-200)107,107,108
  107 IF(ERRO-.001)109,109,110
  110     PRESS2=PRESS3
          K1=K1+1
      GOTO111
  109     PRESS(I+1)=PRESS3
      IF(SENSE SWITCH 2)526,536
  536 CONTINUE
      IF(SENSE SWITCH 1)513,514
  513 CONTINUE
      PUNCH210
      PUNCH201
      PUNCH200,PRESS(I+1),DELP,I
      GO TO 526
  514 CONTINUE
      PRINT210
      PRINT201
      PRINT200,PRESS(I+1),DELP,I
  526 CONTINUE
      I=I+1
      GOTO100
  108 PRINT202,ERRO
      GOTO109
C     LOSS IN FLEX HOSES
    8 CONTINUE
          FN1=E(J1)*R1(J1)/(D(I)*D(I))
          FN2=E(J1)*R1(J1)/(S(J1)*D(I))
           RHO=PRESS(I)*144.*CON
           D(I)=D(I)/12.
           A=3.14159*D(I)*D(I)/4.
           K1=1
           VEL=XMDOT(I1)/(A*RHO)
           XMACH=VEL/SS
      IF(XMACH-.3)133,134,134
  134 PRINT211,XMACH
  133     RE=RHO*VEL*D(I)/XMU
          B1=100.*FN1
           B2=.8681/B1
           E1=.283*((1000.0*FN1)**3.5)
```

Appendix B (continued)

```
            C=17.0*FN2-0.3
            D1=(3.62E+13)*(FN1**(-3.71))
            C1=C**B2
            Z1=1.+D1/(RE**4)
            G1=C1/Z1
           Z2=E1/RE
            Z3=.1
  132       Z4=-B1*LOGF(G1+Z2/Z3)
            XF1=1.0/(Z4+1.74)
            ERRO=ABSF(Z3-XF1)
      IF(ERRO-.0001)131,131,130
  130       Z3=XF1
      GOTO132
  131       XF2=XF1*XF1
      K1=1
            DELP=XF2*XL1(J1)/D(I)*VEL*VEL*RHO/(9270.*4.)
      PRESS(I+1)=PRESS(I)+DELP
  135 RHO2=PRESS(I+1)*144.*CON
      VEL2=XMDOT(I1)/(A*RHO2)
            DELP=XF2*XL1(J1)/D(I)*VEL2*VEL2*RHO2/9270.
      PRES2=PRESS(I)+DELP
      ERRO=ABSF(PRESS(I+1)-PRES2)
      IF(K1-200)137,137,140
  140 PRINT202,ERRO
      GO TO 139
  137 IF(ERRO-.001)139,139,138
  138 PRESS(I+1)=PRES2
      K1=K1+1
      GOTO135
  139 PRESS(I+1)=PRES2
      IF(SENSE SWITCH 2)527,537
  537 CONTINUE
      IF(SENSE SWITCH 1)515,516
  515 CONTINUE
      PUNCH222
      PUNCH201
      PUNCH200,PRESS(I+1),DELP,I
      GO TO 527
  516 CONTINUE
      PRINT222
      PRINT201
      PRINT200,PRESS(I+1),DELP,I
  527 CONTINUE
      I=I+1
            J1=J1+1
```

Appendix B (continued)

```
      GOTO100
C     ABRUPT ENLARGEMENT
    9      PRESS(I+1)=PRESS(I)-.1
           D(I)=D(I)/12.
           A=3.14159*D(I)*D(I)/4.
   45      RHO=PRESS(I+1)*144.*CON
           VEL = XMDOT(I1)/(A*RHO)
           PT1 = RHO*VEL*VEL / 9270.
           DR=D(I+1)/(D(I)*12.)
           B = DR*DR
           C = B*B
           DA=2.*B-2.*C
           PT=PRESS(I+1)+PT1
           FA=PRESS(I+1)/PT
           EA=1.-FA
           GA=1.+EA*DA/FA
           PRES=PRESS(I)/GA
           ERRO=ABSF(PRESS(I+1)-PRES)
      IF(ERRO-.001)43,44,44
   44      PRESS(I+1)=PRES
           K1=K1+1
           GO TO 45
   43      PRESS(I+1)=PRES
           DELP =PRESS(I+1)-PRESS(I)
      IF(SENSE SWITCH 2)542,544
  544 CONTINUE
      IF(SENSE SWITCH 1)540,541
  540 CONTINUE
      PUNCH244
      PUNCH 201
      PUNCH200,PRESS(I+1),DELP,I
      GO TO 542
  541 CONTINUE
      PRINT244
      PRINT201
      PRINT200,PRESS(I+1),DELP,I
  542 CONTINUE
           I=I+1
      GO TO 100
  403 CONTINUE
           PRESST=PRESS(IX)-PRESSX
      IF(SENSE SWITCH 1)517,518
  517 CONTINUE
      PUNCH221,I1
      PUNCH226
```

Appendix B (continued)

```
      PUNCH200,PRESST,XMDOT(I1),I1
      GO TO 528
  518 CONTINUE
      PRINT221,I1
      PRINT226
      PRINT200,PRESST,XMDOT(I1),I1
  528 CONTINUE
      DO404I=1,IX
      D(I)=D(I)*12.
  404 CONTINUE
  401 CONTINUE
  200 FORMAT(E20.6,E20.6,10X,I3)
  201 FORMAT( 6X,14HPRESSURE (PSI),7X,13HDELTA P (PSI),
     112X,1HI)
  202 FORMAT(1H ,34HAFTER 200 ITERATIONS THE ERROR IS.,
     1E20.6,2X,4HIN F)
  203 FORMAT(//,1H ,23HSTRAIGHT SECTION LOSSES)
  204 FORMAT(//,1H ,9HEXIT LOSS)
  205 FORMAT(//,1H ,18HSUDDEN CONTRACTION)
  206 FORMAT(//,1H ,23HARBITRARY CONFIGURATION)
  207 FORMAT(//,1H ,11HBEND LOSSES)
  208 FORMAT(1H ,37HTUBE BUNDLE DIDNT CONVERGE, ERROR
     1IS,,E10.2,3HDDP)
  209 FORMAT(//,1H ,31HPRESSURE LOSSES IN TUBE BUNDLES)
  210 FORMAT(//,1H ,26HPRESSURE LOSS IN FLOWMETER)
  211 FORMAT(1H ,14HMACH NUMBER IS,F5.2,3X,21HDATA MAY
     1BE IN ERROR.)
  212 FORMAT(7F10.5)
  213 FORMAT(7E10.5)
  214 FORMAT(2I5)
  215 FORMAT(4F15.8)
  216 FORMAT(3F20.5)
  217 FORMAT(6F10.5)
  218 FORMAT(14I5)
  219 FORMAT(6F10.5)
  220 FORMAT(4F10.5)
  221 FORMAT(1H ,11HEND OF LOOP,I5)
  222 FORMAT(//,1H ,30HPRESSURE LOSS IN FLEXIBLE HOSE)
  223 FORMAT(3E10.5)
  224 FORMAT(8I5)
  225 FORMAT(7F10.5)
  226 FORMAT(1H , 9X,11HPRESS. DROP,15X,4HMDOT,9X,2HI1)
  227 FORMAT(4F20.5)
  228 FORMAT(18X,2HRE,17X,3HVEL,19X,1HA,17X,3HRHO)
  230 FORMAT(I3)
```

Appendix B (continued)

```
  231 FORMAT(6E12.5)
  232 FORMAT(2F10.5)
  234 FORMAT(F10.5)
  235 FORMAT(1H ,I3)
  240 FORMAT(9E9.2,5X,I3)
  241 FORMAT(3E10.2,5XI3)
  242 FORMAT(E10.2,5X,I3)
  243 FORMAT(E20.5)
  244 FORMAT(//,1H ,21HSUDDEN EXPANSION LOSS)
  250 FORMAT(4F15.5)
  251 FORMAT(1H ,6X,8HREY. NO.,7X,8HVELOCITY,11X,4HAREA
     1,8X,7HDENSITY)
  252 FORMAT(F20.10)
      END
```

APPENDIX C

Derivation of Supply Tank Blowdown Equation

Assumptions:

1) Perfect gas
2) Polytropic expansion

For a perfect gas we have:

1) $$P = \frac{\tilde{M}RT}{V}$$

For a polytropic process we have:

2) $$T = T_o \left(\frac{P}{P_o} \right)^{\frac{n-1}{n}}$$

Substituting this into equation (1) we have

$$P = \frac{\tilde{M}RT_o P^{\frac{n-1}{n}}}{V P_o^{\frac{n-1}{n}}}$$

Let

$$C_1 = \frac{\tilde{R} T_o}{V P_o^{\frac{n-1}{n}}}$$

Then

$$P = C_1 M P^{\frac{n-1}{n}}$$

$$P P^{-\frac{n-1}{n}} = C_1 M$$

$$P P^{\frac{1-n}{n}} = C_1 M$$

$$P^{\frac{1-n}{n} + 1} = C_1 M$$

$$P^{\frac{1-n+n}{n}} = C_1 M$$

Appendix C (continued)

$$P^{\frac{1}{n}} = C_1 M$$

$$P = C_1^n \; M^n$$

Taking the time derivative

$$\frac{dP}{dt} = nC_1^n \; M^{n-1} \; \frac{dM}{dt}$$

$$= nC_1^n \left(\frac{PV}{\tilde{R}T} \right)^{n-1} \frac{dM}{dt}$$

Then

$$\frac{dP}{dt} = n \left(\frac{\tilde{R} \; T_o}{VP_o^{\frac{n-1}{n}}} \right) \left(\frac{VP}{\tilde{R} \; T} \right)^{n-1} \frac{dM}{dt}$$